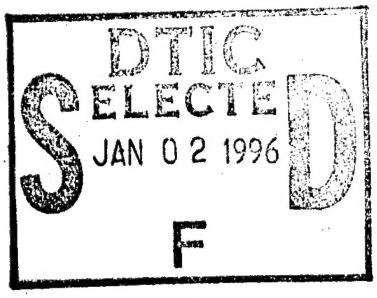

EXPERIMENTAL STUDIES OF GRAPHITE-EPOXY AND BORON-EPOXY ANGLE PLY LAMINATES IN COMPRESSION

T. WELLER

SEPTEMBER 1977

DEPARTMENT OF DEFENSE
PLASTICS TECHNICAL EVALUATION CENTER
ARRADCOM, DOVER, N. J. 07801

03307

הטכניון מכון טכנולוגי לישראל
הפקולטה להנדסה אווירונוטית

TECHNION Israel Institute of Technology
Department of Aeronautical Engineering

September 1977

NASA-CR-145233

Experimental Studies of Graphite-Epoxy and Boron-Epoxy Angle Ply Laminates in Compression

by

T. Weller

Prepared under Grant NSG-7083

for

Langley Research Center

National Aeronautics and Space Administration

September 1977 ERRATA NASA-CR-145233

Page No.		line no.
III	insert '[±75°]'	1
	'[90°]'	2
	'[0°/90°]'	3
	'[0°/±45°/90°]'	4
Fig. 7A	vertical ordinate 'STRESS (psi)'	
Fig. 19AI	insert 'BATCH I'	

NASA-CR-145233

EXPERIMENTAL STUDIES OF GRAPHITE-EPOXY AND BORON-EPOXY ANGLE PLY LAMINATES IN COMPRESSION

By T. Weller

September 1977

Prepared under Grant NSG-7083 BY

TECHNION - ISRAEL INSTITUTE OF TECHNOLOGY
DEPARTMENT OF AERONAUTICAL ENGINEERING
HAIFA 32000 , ISRAEL

for

LANGLEY RESEARCH CENTER

NATIONAL AERONAUTICS AND SPACE ADMINISTRATION

ABSTRACT

The present report describes and presents a test program carried out at NASA Langley Research Center aimed at studying the nonlinear/inelastic response under axial compression across a wide range of angle ply 3M SP-286T3 Graphite-Epoxy and AVCO 5505/5.6MIL. DIA. Boron-Epoxy Laminates. The program is also aimed at defining the strength allowables corresponding to the various laminate configurations and detecting the failure mechanisms which dictate their mode of failure. The program involved two types of specimens for each laminate configuration: compression sandwich coupons (planar specimens) and compression tubes. The test results indicate that the coupons perform better than the tubes, displaying considerably high stress-strain allowables and mechanical properties relative to the tubes. Also it is observed that depending on their dimensions the coupons are susceptible to very pronounced edge effects. This "sensitivity" results in assigning to the laminate "conservative" mechanical properties rather than the actual ones.

TABLE OF CONTENTS

LIST OF SYMBOLS

a	End tabs length, Fig. 1B.
Ex	Young modulus.
$(Ex)_c$	Young modulus in compression.
L	Compression tube lengths, Fig. 1B.
O.D.	Compression tube outside diameter, Fig. 1B.
P	Axial compression load.
$P_{ult.}$	Ultimate axial load.
t	Laminate thickness.
α	Lamina angle.
ϵ_x	Inplane compression strain.
$(\epsilon_x)_{max.}$	Laminate maximum inplane compression strain at failure.
σ_x	Laminate compression stress.
$(\sigma_c)_{ult.}$	Ultimate compression stress.
$(\sigma_{ult.})_{meas.}$	Ultimate compression stress corresponding to laminate measured thickness.
$(\sigma_{ult.})_{nom.}$	Ultimate compression stress corresponding to laminate nominal thickness.

LIST OF FIGURES

APA1	Compression Response of Planar Specimens - GR/E Laminate [0] (Damaged).
APA2	Compression Response of Planar Specimens - GR/E Laminate [±15] (Damaged).
APA3	Compression Response of Planar Specimens - GR/E Laminate [±30] (Damaged).
APA4	Compression Response of Planar Specimens - GR/E Laminate [±45] (Damaged).
APA5	Compression Response of Planar Specimens - GR/E Laminate [±60] (Damaged).
APA6	Compression Response of Planar Specimens - GR/E Laminate [±75] (Damaged).
APA7	Compression Response of Planar Specimens - GR/E Laminate [90] (Damaged).
APA8	Compression Response of Planar Specimens - GR/E Laminate [0/90] (Damaged).
APA9	Compression Response of Planar Specimens - B/E Laminate [±15] (Damaged).
APA10	Compression Response of Planar Specimens - B/E Laminate [0/±45/90] (Damaged).
APB1	Influence of Loading and Unloading on Response of Compression Tubes [±30] GR/E (Test 527 Run 5).
APB2	Influence of Loading and Unloading on Response of Compression Tubes [±45] GR/E (Test 526 Run 5).
APB3I	Influence of Loading and Unloading on Response of Compression Tubes [±75] GR/E (Test 526 Run 6).
APB3II	Influence of Loading and Unloading on Response of Compression Tubes [±75] GR/E (Test 526 Run 7).
APB4I	Influence of Loading and Unloading on Response of Compression Tubes [90] GR/E (Test 609 Run 3).
APB4II	Influence of Loading and Unloading on Response of Compression Tubes [90] GR/E (Test 609 Run 4).
APB5	Influence of Loading and Unloading on Response of Compression Tubes [0/90] GR/E (Test 620 Run 2).
APB6I	Influence of Loading and Unloading on Response of Compression Tubes [0/±45/90] GR/E (Test 609 Run 9).
APB6II	Influence of Loading and Unloading on Response of Compression Tubes [0/±45/90] GR/E (Test 609 Run 10).
APB7I	Influence of Loading and Unloading on Response of Compression Tubes [±15] B/E (Test 527 Run 8).
APB7II	Influence of Loading and Unloading on Response of Compression Tubes [±15] B/E (Test 527 Run 9).

APB8	Influence of Loading and Unloading on Response of Compression Tubes [±45] B/E (Test 526 Run 2).
APB9I	Influence of Loading and Unloading on Response of Compression Tubes [±60] B/E (Test 526 Run 3).
APB9II	Influence of Loading and Unloading on Response of Compression Tubes [±60] B/E (Test 526 Run 8).
APB9III	Influence of Loading and Unloading on Response of Compression Tubes [±60] B/E (Test 526 Run 9).
APB10I	Influence of Loading and Unloading on Response of Compression Tubes [0/90] B/E (Test 609 Run 12).
APB10II	Influence of Loading and Unloading on Response of Compression Tubes [0/90] B/E (Test 609 Runs 13.14).
APB11I	Influence of Loading and Unloading on Response of Compression Tubes [0/±45/90] B/E (Test 537 Run 6).
APB11II	Influence of Loading and Unloading on Response of Compression Tubes [0/±45/90] B/E (Test 537 Run 7).

1. INTRODUCTION

This report represents the test results obtained during the course of a test program carried out at NASA Langley Research Center to study the nonlinear and inelastic compression response of Graphite-Epoxy and Boron-Epoxy laminates across a wide range of laminate configurations.

In spite of their outstanding performance and mechanical characteristics, and consequently increasingly being introduced in the design of new advanced aircraft and space vehicles, the advantageous application of these materials is limited unless we obtain a better physical insight into such phenomena as: nonlinear and inelastic response, failure mechanisms, and loading and unloading characteristics. Better understanding of these phenomena will assess and provide design allowables, and means for defining the offset yield point, which does not exist for these new fabricated materials, to distinguish between the elastic and inelastic regions and their relation to either Max. Stress or Max. Strain.

It is the aim of the present test program to establish and furnish experimentally the information concerned with the abovementioned vital phenomena, as well as to correlate the experimental results with theoretical predictions made by existing analytical tools. Most of these theoretical studies introduce simplifying assumptions when dealing with the nonlinear portion of the response, which can only be made when based on sound experimental evidence which they so lack. The program also undertakes to evaluate better and preferred test techniques and types of specimens, for investigating the objectives of the present program.

In particular, this report details the results obtained for 43 Graphite-Epoxy and 36 Boron-Epoxy compression coupons (planar specimens), and 24 Graphite-Epoxy and 25 Boron-Epoxy compression tubes, all of which were fabricated from prepreg materials. All the specimens were symmetrically laid up and designed to avoid buckling and end failure of the specimens, and to exhibit strength failure of the laminate itself.

2. EXPERIMENTAL INVESTIGATIONS

2.1. TEST SPECIMENS

In the test program nine different types of symmetrical laminate configurations were investigated for each material, see Tables 1 and 2. The program consisted of 43 Graphite-Epoxy and 36 Boron-Epoxy compression coupons, and of 24 Graphite-Epoxy and 25 Boron-Epoxy Compression tubes. For details and dimensions see Figs. 1A and 1B, and Tables 1 and 2.

The laminate facings for the coupons and the laminated walls of the tubes were manufactured from unidirectional prepreg tapes: 3M SP-286T3 Graphite-Epoxy A-S(5.0 Mil), .0052"(.013cm) ply thickness, and Avco 5505/5.6 Mil Dia. Boron-Epoxy, .0067"(.017cm) ply thickness.

The ultimate load capacity for each laminate was predicted with the aid of the SQ5 computer code [1].

2.1.1 Compression Coupons

All the coupons were made of two eight-ply laminate facings bonded to a (3/16)" cell x 5052 x 8.08 #/cu.ft. Al. Honeycomb core (1.000±.005" thickness), which stabilized them against buckling. The load is introduced into the specimens by shearing through steel end doublers bonded to both sides of each laminate facing, see Figs. 1 and 3. To avoid premature end failure of the specimens due to insufficient bonded shearing surface between the end doublers and the laminate, the shearing surfaces required to sustain the abovementioned ultimate loads were calculated with the aid of a computer code developed by the manufacturer, SWRI [2]. These calculations dictated the minimal geometrical dimensions of the doublers.

2.1.2 Compression Tubes

The tubular specimens vary in their wall ply number, see Table 2, to avoid premature failure in a buckling mode. The necessary number of plies was dictated by linear elastic buckling predictions for each laminate configuration, and tube dimensions were calculated with Wu's computer code [3]. An attempt was made to maintain the critical load at buckling, at least twice as high as the ultimate load predicted for the laminate with the SQ5 code. In these specimens the load is again

introduced into the laminate by shearing through steel end tabs split into three segments and bonded to the internal and external surfaces of the tube wall, Fig. 5. Again, to exhibit strength failure of the laminate and avoid premature end failure of the tube, the required shearing surface between the laminated tube wall and the end pieces was calculated with the code of [2] and the geometry of the end tabs designed accordingly. These of course resulted in different end pieces for the variety of laminate configurations tested. See specimens of Fig. 5 for the extremes of design of these doublers.

2.2. TEST SET-UPS AND PROCEDURES

The specimens were loaded in compression between the end platens of tension-compression testing machines, Fig. 2: a 120 kips machine for the compression coupons and a 300 kips machine for the tubes. To avoid introduction of end moments, the lower edge of the specimen was loaded by a swiveling head. The ends of the specimens were ground parallel and flat prior to testing and they were carefully aligned between the lower platen of the swiveling head and the upper platen to assure uniform load-bearing at the edges and axial loading of the specimen. The alignment was guided by the axial strain gages bonded to the laminate surfaces midway between their edges. The specimens were gradually loaded and unloaded and relocated in accordance with the strain gage records, to achieve an almost even strain distribution from the gages.

2.2.1 Compression Coupons

In the first stages of the test program four gages were bonded to the laminated facings of the coupon. Two gages were bonded to each facing. One of them was directed in the axial direction of the specimen, i.e. in the direction of the axial compression loading, to record the axial compression strain response, and the second one was directed transversely to measure Poisson's effect as well as assessing in detecting the transverse failure anticipated by the SQ5 predictions [1] for some of the laminate configurations tested. Elimination of any bending strains whenever introduced into the coupon, due either to initial imperfections or misalignment of the specimen, was achieved by having the gages bonded to both facings and opposite

one another, as well as opposite gages connected in series.

Further studies with the "SNAP" computer code [4] on the effect of coupon dimensions on the nature of stress-strain distribution expected for the coupons have revealed the existence of a very non-uniform stress-strain field, even far away from the loaded boundaries. This behavior is attributed to the combination of high Poisson's ratio values for these particular laminates and restraining of lateral displacements of the loaded edges of the coupons. To observe this Poisson's effect another two gages, one on each facing, were bonded to the very edge of all angle-plied laminates, Fig. 3.

2.2.2 Compression Tubes

Fifteen gages were bonded to the external cylindrical surface of each tube. The developed surface of a tubular specimen as well as gage location and orientation is shown in Fig. 4. Only the gages located midway between the end loading metal pieces of the specimen [(3,4,5);(8,9) and (14,15)], see Fig. 4, served the purpose of obtaining the compression strain response, measuring Poisson's effect and detecting the anticipated transverse failure predicted by preliminary predictions with the SQ5 code as mentioned above for the coupons. All other gages assisted in detecting any irregular behavior like that arising from edge effects and high bending stresses if developed near the bond line of the end tabs of the tubes. Besides measuring the strain response by strain gages, the end-shortening of the tubes was recorded from DCDT's (direct current differential transformers) equally spaced along the circumference of the cylinder, see Figs. 2 and 4. The records obtained from these DCDT's were correlated with the strain gage readings (see Results and Discussion).

It should also be noted that many of the tubes were gradually loaded and unloaded in a cyclic manner to obtain information about the influence of such a procedure on their performance. The results are presented in Appendix B, where it is found that some tubes were slightly affected by increase or reduction of their moduli, whereas some were not influenced at all by this procedure.

3. EXPERIMENTAL RESULTS AND DISCUSSION

In Tables 1 and 2 the results obtained for compression coupons and compression tubes are presented respectively. These tables contain the ultimate values of strength and strain recorded during the course of the tests for all of the tested laminate configurations, as well as the elastic moduli calculated from the reduced stress-strain records.

The compression responses for the Graphite-Epoxy coupons and tubes, for all the investigated laminate configurations, are shown in Figs. 6A and 6B, and those for the Boron-Epoxy specimens in Figs. 7A and 7B.

Before proceeding with a detailed discussion and describing the achieved results for each laminate configuration individually, some common comments regarding the whole test program as to the reduced test data and its presentation should be noted:

(a) The response of many of the coupons configurations is presented by two different figures, with one of them marked "damaged" and given in Appendix A. This stems from the fact that for these configurations two batches of specimens were delivered by the manufacturer, one of them assumed to be damaged and hence replaced by another one. (As can be seen from Table 1 some of these "damaged" specimens were tested by the manufacturer and the results obtained are reported in this Table). The damage occurred along the free unloaded edges of the coupons due to inappropriate cutting procedure and was repaired by glueing epoxy along the edges. This might have strengthened the specimen by improving the way load is being sheared from one noncontinuous diagonal fiber into the adjacent one through the matrix.

(b) As mentioned in the preceding chapter, edge effects far away from the loaded boundaries were observed in the compression coupons which have laminated facings possessing high Poisson's ratio values (almost all of the angle-plied laminates). This influence results in an uneven stress-strain distribution even as far as the central line of the coupon, transverse to the applied load direction. However, in the present test program only the total applied compression load was recorded and consequently

the corresponding "average stress" was obtained by dividing the total load by the appropriate laminate area. Hence, the stresses reported in this discussion are calculated as being uniformly distributed, leading to lower ultimate values than actually exist for the corresponding strain values, and are a conservative representation of both the ultimate strength and elastic modulus.

(c) The stresses calculated for representation of the tubular specimens are based on the nominal tube wall thickness, i.e. number of plies in laminate times nominal ply thickness. Preliminary calculations based on actual measured wall thickness were felt to be misleading as they led to very low ultimate values when compared with the results obtained for the coupons. As a matter of fact the measured thicknesses are thicker because of excess matrix material in the laminate which makes almost no contribution to the load carrying capacity of the laminates, except for very high angle plied laminates.

(d) Test data was reduced and curve-fitted by the following relation: $\epsilon=A\tau+B\tau^N$.

3.1. GRAPHITE-EPOXY LAMINATES

3.1.1 Unidirectional [0°] Laminates

This type of laminate configuration consisted of compression coupons only. Two batches of specimens were tested and their responses are shown in Figs. 8A and APA1 (for the so-called "damaged" specimens). It can be observed in these figures that the replacing batch of Fig. 8A yielded higher ultimate values than those experienced by the "damaged" ones of Fig. APA1, with slightly lower stiffness. In either case there exists a scatter among the ultimate values achieved for each individual specimen, but repetition of the obtained responses for all the specimens is very good up to their failure point. Figs. 8A and APA1 also present the locally obtained Poisson's ratio versus the axial strain (at the center of the specimen), and it is observed that the batch of Fig. 8A displays lower Poisson's ratio values than those experienced by the "damaged" batch for corresponding axial strain values. Also the increase in these values in Fig. 8A with increasing axial strain is less pronounced and more nonlinear in its nature. However, comparing these two figures and the results of Table 1 it is seen that the damage caused to the specimens mostly affected their strength allowables.

3.1.2 [±15°] Laminates

Again two batches of coupons were tested. The response of the coupons is shown in Fig. 9A, that of the tubes in Fig. 9B, and that of the "damaged" batch in Fig. APA2. It is seen that the "damaged" specimens, Fig. APA2, sustained higher ultimate values and a slightly higher modulus than the coupons of Fig. 9A. No scatter of results is observed in either one of the groups. In spite of their common compression response, it is observed from the two figures that variation of Poisson's ratio with increasing axial strain is different for the two groups of coupons due to the stiffer response of the "damaged" specimens in the transverse direction.

Comparison of the results obtained for the tubes, Fig. 9B, with those obtained for the coupons, Fig. 9A and APA2, reveals that the tubes experienced significantly lower ultimate values than did the coupons (about 75 percent), but on the other hand yielded a considerably higher modulus value (about 131 percent). It can be shown that if the true stresses of the tube (based on measured thickness from Table 2), rather than nominal ones (based on nominal ply thickness) are used, the modulus of the tubes will be exactly as that measured for the coupons, but on the other hand this will mean further significant reduction of the ultimate values of the tubes. Poisson's ratio versus axial strain of the tubes, Fig. 9B, does not at all resemble the curves obtained for the coupons, neither in its values nor in its shape.

3.1.3 [±30°] Laminates

In Figs. 10A and APA3 the responses for the replacing group of coupons and the "damaged" ones are presented respectively, and in Fig. 10B the response of the tubes is shown. It is seen from Fig. 10A that both the ultimate values and modulus are considerably lower for the corresponding group of specimens than those yielded for the "damaged" batch of Fig. APA3. Some scatter of results is observed among the coupons of Fig. 10A, whereas none exists for the "damaged" ones. Figs. 10A and APA3 also reveal a difference in their Poisson's values, with increasing axial strains.

Edge effects mentioned above are observed in Fig. 10A. It is seen that the axial edge gages (inner curves on the lefthand side of

the figure) experienced much lower strains than the central ones and also responded in a linear mode up to failure.

The results of Fig. 10B reveal that the cylindrical specimens yielded much lower ultimate values (about 64 percent) and a considerably higher modulus (about 118 percent) when compared to the batch of specimens corresponding to Fig. 10A. However, had the actual stress been considered for the tubes, it would have reduced the modulus to a lower value than presented in Fig. 10B, in addition to further decreasing significantly the ultimate stress. It should be noted that the modulus of Fig. 10B is only slightly higher than that obtained for the coupons of Fig. APA3.

It is observed in Fig. 10B that the nature of Poisson's ratio with increasing values of axial strain is completely different from that obtained for the coupons, both qualitatively and quantitatively.

3.1.4 [±45°] Laminates

The responses of the coupons are given in Figs. 11A and APA4, and of the tubes in Fig. 11B. Figs. 11A and APA4 reveal that the two batches of coupons responded completely differently. They experienced almost the same strength, but the ultimate strain of the "damaged" group is about 50 percent of that observed for the other group. Consequently the moduli as well as Poisson's ratio versus applied axial strain are completely different, see also Table 1. It is noted from this table that the "damaged" coupons sustained higher ultimate loads than presented in Fig. APA4, but from the strain records it appears that some kind of failure occurred at a lower load value, resulting in very irregular behavior of the strain gages - they recorded either zero strain values or very high strains which were beyond their range of response, namely, ±6% of strain. This phenomenon occurred at a load slightly lower than that corresponding to the ultimate of the "replacing" batch, Fig. 11A. It is also seen that no scatter exists among the coupons of Fig. 11A, whereas a considerable one is observed in Fig. APA4 regarding the ultimate values of the individual specimens.

Fig. 11A exhibits very pronounced edge effects; the axial edge gages responded linearly up to failure, experiencing a very low

strain compared with the very high and nonlinear strain recorded by the axial central gages (about 20 percent at ultimate). Hence the remarks made earlier about conservative presentation of the strength as well as the modulus are emphasized in the present case.

Fig. 11B shows that the tubes yielded significantly lower strengths than those sustained by the coupons (about 76 percent) and a higher modulus (about 137 percent) than that experienced by the specimens of Fig. 11A. Again, if the "true" stress is considered, the modulus of the tubes approaches from above that of Fig. 11A, but is significantly lower than that of the "damaged" specimens. Also the nature of Poisson's ratio of the tubes is different from that obtained from the coupons.

3.1.5 [±60°] Laminates

Figs. 12A and APA5 present the responses of the compression coupons, and Fig. 12B that of the tubes. It is observed from Table 1 that the "damaged" coupons sustained higher ultimate strengths than did the "replacing" group, though in Fig. APA5 the records had to be truncated at low stress values due to irregular response of the gages. It should be noted that one of the coupons in Fig. 12A (Test 497, Run 1) experienced the same behavior at about the same stress level. It is observed from Figs. 12A and APA5 that scatter of results is negligible and that the "damaged" coupons responded almost identically to those of Fig. 12A up to their failure.

Concerning edge effects, Fig. 12A displays severe differences between the strains recorded from the edge gages and the central ones (42 percent difference of ultimate). Again, the remarks made about conservative representation also apply here.

Fig. 12B shows that the tubes yielded considerably lower strength values (about 85 percent) than did the coupons, with noticeable scatter among the individual specimens. Like for previous laminates, the modulus obtained for the tubes is quite a bit higher (about 146 percent) than that of the coupons, but again if "true" rather than "nominal" stresses are considered for the tubes, their modulus approaches from above that corresponding to the coupons. The mode of variation of

Poisson's effect of the tubes with increasing axial strain is very similar to that of the coupons of Fig. 12A but yields lower Poisson's values.

3.1.6 [±75°] Laminates

The responses corresponding to the coupons are given in Figs. 13A and APA6, and that to the tubes in Fig. 13B. It is seen from Figs. 13A and APA6 that the "damaged" specimens sustained slightly lower ultimate values than did the coupons of Fig. 13A, but yielded a slightly higher modulus. It is also seen from these figures that there is more scatter among the strength values of the coupons of Fig. APA6 than there is among the specimens of Fig. 13A. Nevertheless there is no difference in the mode of response corresponding to the specimens of each batch. Comparing the two figures it is observed that the "damaged" specimens exhibit a more pronounced nonlinear response. The two figures also show a variation of Poisson's ratio values with increasing axial strain which is very much alike for the two batches. Edge effects presented in Fig. 13A seem to be insignificant for this type of laminate configuration.

In Fig. 13B the response of the tubes is presented. It is observed that these specimens experienced very low ultimate stresses relative to the coupons (about 59 percent). Also the modulus is lower than that yielded by the coupons (about 92 percent). If the "true" stresses are again considered, the modulus as well as the ultimate strength are drastically decreased relative to the coupons. It is also observed from this figure that the nature of variation of Poisson's ratio is very similar to that observed for the coupons, but quantitatively yields lower values for corresponding strain values.

3.1.7 [90°] Laminates

Figs. 14A and APA7 present the results obtained for the coupons, and figure 14B the response corresponding to the tubes. It is observed that the "damaged" coupons, Fig. APA7, yielded lower ultimate values, a more pronounced nonlinearity, and a lower modulus than the specimens of Fig. 14A. However, it is seen from Fig. 14A and Table 1 that one of the coupons corresponding to this group failed at a very low load

even when compared with the "damaged" specimens. It is noted in Table 1 that this coupon experienced end failure which precipitated early failure. Variation of Poisson's ratio is observed to be alike for the two groups, as seen from Figs. 14A and APA7.

The response of the tubes given in Fig. 14B shows that these specimens yielded considerably lower strength and modulus values (about 70 and 80 percent respectively). All the tubes responded almost identically with the exception of one failing at a very low load level. Variation of Poisson's ratio with increasing axial strain is very similar to that obtained for the coupons. Considering the "true" stresses will further decrease appreciably the strength and modulus relative to the coupons.

3.1.8 [0°/90°] Laminates

The responses of the coupons are given in Figs. 15A and APA8, and that of the tubes in Fig. 15B. The coupons of Fig. 15A reveal considerably higher strength values and a lower modulus value relative to the "damaged" ones of Fig. APA8. On the other hand these specimens exhibit noticeable scatter in shape of response and very appreciable difference in ultimate strength, due to end failure of one of the coupons (see also Table 1),whereas the coupons of Fig. APA8 responded identically with a small scatter in strength values. No significant difference in variation of Poisson's ratio is observed from Figs. 15A and APA8 for the two groups of specimens.

The response of the tubular specimens shown in Fig. 15B reveals that the tubes experienced significantly lower ultimate stresses (about 43 percent) and a slightly lower modulus (about 95 percent) relative to the coupons. Noticeable scatter of both the shape of response and ultimate strength among the individual specimens is observed. Variation of Poisson's ratio for low axial strain values is similar to that obtained for the coupons. It is seen from this figure that these ratio values decrease with increasing axial strain values whereas for the coupons they remain almost constant for all strain values. As can be seen from Table 2 the results of Fig. 15B won't change significantly when "true" rather than "nominal" stresses are being considered.

3.1.9 [0°/±45°/90°] Laminates

The response of the coupons is shown in Fig. 16A, and that of the tubes in Fig. 16B. It is observed from these figures that the coupons yielded considerably higher strength values than did the tubes (about 206 percent), whereas the tubes experienced a higher modulus (about 115 percent). If "true" stresses are considered for the tubes their ultimate stress will further decrease and their "corrected" modulus will be considerably lower relative to the planar specimens. Minor scatter is observed among the coupons, whereas Fig. 16B exhibits noticeable scatter among the tubes. Fig. 16A reveals a variation of Poisson's ratio with increasing values of axial strain tending towards a constant value, whereas the tubes exhibit no variation with a constant value equal to the assymptotic values corresponding to the coupons.

3.2 BORON-EPOXY LAMINATES

3.2.1 Unidirectional [0°] Laminates

Only compression coupons were investigated for this type of configuration, the response of which is shown in Fig. 17A. Noticeable scatter is observed from this figure among the ultimate strengths obtained for the individual specimens.

3.2.2 [±15°] Laminates

The responses of the coupons are presented in Figs. 18A and APA9, and that corresponding to the tubes in Fig. 18B. It is seen from Figs. 18A and APA9 that both batches of coupons responded almost identically. They also exhibit some type of irregularities at about the same stress level which is particularly pronounced in the transverse direction of the specimens as well as along their edges. At a stress level of about 105 ksi the gages recording the transverse and edge strains pick up strain with no increase in stress, and above this stress level the response can no longer be presented by a smooth curve. Variation of Poisson's ratio with increasing axial strain differs in its shape for each group of specimens, though quantitatively the two groups experienced similar ratio values. Edge effects mentioned earlier are observed in Fig. 18A, especially in the very high strain region.

The response of the tubes given in Fig. 18B reveals a considerably lower strength value (about 66 percent) and a higher modulus (about 159 percent) relative to those yielded by the coupons. No irregularities are observed for these specimens. Eventually, these specimens didn't reach the stress level corresponding to the appearance of irregularities in the coupons. Considering "true" stresses still yields a modulus considerably higher than that observed for the coupons while further decreasing significantly the ultimate strength relative to the coupons. No correlation is observed between variation of Poisson's ratio obtained for the tubes and that achieved for the coupons, neither qualitatively nor quantitatively.

3.2.3 [±30°] Laminates

In Figs. 19AI and 19AII the responses corresponding to the coupons are shown, and in Fig. 19B that corresponding to the tubes is given. Figs. 19AI and 19AII display a completely different response for each batch of coupons: the specimens of Fig. 19AI reveal a very pronounced transverse straining of the coupons near their ultimate strength, which might have precipitated their early failure when compared with the almost twice as high strength values experienced by the specimens of Fig. 19AII. As can be seen from this figure these specimens didn't undergo any high transverse straining and almost ceased to strain transversely at a stress level corresponding to the high rate transverse straining of the coupons in Fig. 19AI. It is also observed from Fig. 19AII that the coupons presented by this figure yielded a considerably higher modulus relative to the specimens of Fig. 19AI.

Very pronounced edge effects are observed for the two groups of coupons which exhibit a reversal in strain at about the same stress level, regardless of the batch the specimens belong to. Therefore the remarks stated earlier about conservative presentation of the results apply to this type of laminate configuration.

It should be noted that in spite of the peculiar difference in the responses obtained for the two batches, no scatter exists among the results obtained for the individual coupons of each group. Looking for a reason for this difference it was noticed in the manufacturing records that the curing process was different for the two groups.

The response obtained for the tubes in Fig. 19B reveals that they yielded significantly lower ultimate values than did the coupons, and a modulus slightly higher than the coupons of Fig. 19AI. This figure reveals that like the coupons of Fig. 19AI, the tubes experienced a very high rate of transverse straining at a stress level close to their ultimate. Hence they have experienced a transverse failure mode, too. The mode of variation of Poisson's ratio of the tubes is observed to be similar in shape to that obtained for the coupons in Fig. 18AI. However, there is an appreciable quantitative difference between the two.

3.2.4 [±45°] Laminates

In Fig. 20A the response obtained for the coupons is presented, and in Fig. 20B that corresponding to the tubes is shown. It is observed that the planar specimens sustained considerably higher strength values relative to the tubes (about 125 percent), whereas the tubes yielded an appreciably higher modulus (about 128 percent). If "true" stresses are considered for the tubes it will further decrease the ultimate strength as well as now yielding a low modulus relative to the coupons. Variation of Poisson's ratio with axial strain for the two batches has no resemblance, neither shapewise nor qualitativewise.

The coupons of Fig. 20A display very strong edge effects. The edge gages behave linearly with almost no strain, whereas the central gages reveal a very pronounced nonlinear response and high rate of straining when approaching the ultimate strength. The edge gages experienced at ultimate about 8 percent of the strain experienced by the central gages. Hence the presented results are again conservative as stated earlier in the discussion.

3.2.5 [±60°] Laminates

Fig. 21A presents the response corresponding to the coupons, and Fig. 21B that corresponding to the tubes. It is revealed that for this type of laminate configuration the tubes experienced higher strength values (about 121 percent) and a significantly higher modulus (about 245 percent) than did the coupons. Considering "true" stresses will reduce the strength yielded by the tubes to about only 86 percent of that experienced by the coupons, while still yielding a very high modulus relative to the coupons (about 174 percent). It is revealed from the two figures that both types of specimen

experience quantitatively the same variation of Poisson's ratio with increasing axial strain.

It is observed from Fig. 21A that the coupons exhibit very severe edge effects, where the gages recorded a very weak nonlinear response when approaching the ultimate strength, compared to the very high strain and very pronounced nonlinear response of the central gages when approaching the ultimate (about 31 percent). Consequently these coupons are presented in a conservative manner, as commented on above.

3.2.6 [±75°] Laminates

The response corresponding to the coupons is given in Fig. 22A. There is no figure to present the response corresponding to the tubes due to the fact that these specimens had to be rejected because of their poor manfacturing quality. Nevertheless these tubes were tested and the ultimate strengths achieved for them are given in Table 2. In spite of their "poor" quality it is observed that these tubes sustained "nominal" ultimate stresses, about 81 percent of those yielded by the tubes. However, if "true" stresses are considered instead, the ultimate values are significantly reduced.

3.2.7 [90°] Laminates

The response corresponding to the coupons is shown in Fig. 23A, and that corresponding to the tubes in Fig. 23B. Fig. 23A shows that the coupons yielded a significantly higher ultimate strength (about 146 percent) and a considerably lower modulus (about 88 percent) than did the tubes. Considering "true" stresses will further decrease the ultimate strength corresponding to the tubes, besides yielding a considerably lower modulus relative to the coupons. Variation of Poisson's ratio is very much alike, both qualitatively and quantitatively, for the two types of specimens.

3.2.8 [0°/90°] Laminates

In Fig. 24A the response of the coupons is presented, and in Fig. 24B that corresponding to the tubes is given. It is observed from these figures that both types of specimens yielded similar ultimate

stresses but the tubes, see Fig. 24B, experienced a considerably higher modulus (about 148 percent). Considering "true" stresses it is seen that the "actual" ultimate stresses corresponding to the tubes are appreciably reduced relative to the coupons, whereas the modulus of the tubes becomes almost equal to that achieved for the coupons. Fig. 24A reveals significant scatter among the ultimate value obtained for the individual coupons, whereas Fig. 24B shows a small scatter among the strength values obtained for each tube, but exhibits more scatter among the individual modes of response. Fig. 24B also reveals some irregularities in the responses of the tubes, especially pronounced in the specimen of Test 609, Run 15. However, this irregular behavior didn't affect the strength of this tube as can be seen from Table 2 and Fig. 24B. It is worthwhile noting in Table 2 that the laminate of the tube of Test 609, Run 11, consisted of 20 plies whereas all the other tubes were fabricated from 16-ply laminate. As can be observed from Table 2 and Fig. 24 neither the strength nor the response of this tube were influenced by this fact. Variation of Poisson's ratio obtained for the coupons does not resemble that obtained for the tubes, as can be observed from the two figures.

3.2.9 [0°/±45°/90°] Laminates

The responses corresponding to the coupons are presented in Fig. 25A and APA10, and those corresponding to the tubes in Fig. 25B. The results of Fig. 25A and APA10 show that the "damaged" specimens experienced similar ultimate strength values to those observed for the coupons of Fig. 25A, but a slightly higher modulus than that yielded by the "replacing" coupons. Variation of Poisson's effect seems to be very similar for the two groups of specimens. Edge effects were studied for the group of Fig. 25A, but seem to be insignificant.

It is observed from Fig. 25B that the tubes sustained ultimate values similar to those corresponding to the coupons. However they yielded a higher modulus (about 145 percent) relative to the coupons. When "true" stresses are evaluated for the tubes, it is seen from Table 2 that the stresses are reduced to about only 60 percent of their "nominal" values, and the modulus is reduced considerably below that

yielded for the coupons. It is observed in Fig. 25B that one of the tubes, Test 537, Run 6, exhibits some irregularities in its response, mainly in the transverse direction, but this has no influence on the ultimate strength sustained by this tube. The variation of Poisson's ratio with axial strain in Fig. 25B seems to yield similar values to those obtained for the coupons, Fig. 25A and APA10, but the mode of variation differs from that corresponding to the coupons.

4. CONCLUSIONS

(a) The considerably better and higher performance displayed by the compression coupons relative to the tubes favors and prefers them for defining the nonlinear/inelastic response and allowables of heavy high performance composite laminated materials.

(b) The "sensitivity" to edge effects observed for the coupons of present dimensions (aspect ratio) calls for a study on adequate coupon dimension for appropriate application in similar experimental studies.

(c) The conclusion (b) will result in a long specimen which is susceptible and sensitive to buckling. Hence, different types of specimens should be designed, tested and evaluated to achieve the objectives of the present test program.

REFERENCES

1. J. T. Muha - "Users Manual for The Laminate Point Stress Analysis Computer Program SQ5 as Revised by AFDL/FBC" - AFFDL-TM-74-107 FBC, July (1974).

2. G. C. Grimes, L. F. G. Reimann, T. Wah, G. E. Commerford, W. D. Blackstone and J. E. Wolfe - "The Development of Nonlinear Analysis Methods for Bonded Joints in Advanced Filamentary Composite Structures" - AFDL-TR-72-97, Sept. (1972).

3. C. H. Wu - "Buckling of Anisotropic Cylindrical Shells" - Dept. of Solid Mechanics, Structures and Mechanical Design, Case Western Reserve University, June (1971).

4. W. D. Whetstone - Structural Network Analysis Program" - Users Manual, Static Analysis Version V70E, LMSC-HREC D162812, Dec. (1970).

APPENDIX A

It was mentioned in Section 3 (Experimental Results and Discussion) that some groups of the coupons were observed to be damaged by the manufacturer and replaced by other ones. However, these specimens were delivered and tested. The results obtained for these coupons, presented in Table 1, and their responses, shown in Figs. APA1 through APA10, have already been discussed in the abovementioned section. In general it appears that due to being glued along the "hurt" edges all of the angle plied specimens experienced a slightly higher strength than did the "replacing" coupons. This might have resulted from the improved way in which load is sheared from one noncontinuous diagonal fiber into the adjacent one through the matrix.

APPENDIX B

The advantageous application of advanced composites is strongly dependent, among other requirements, upon better knowledge and physical insight into their loading and unloading characteristics, and the effect of cyclic loading on their response and performance. Though the present test program was not aimed at studying these phenomena, an attempt was made to obtain information concerned with the loading and unloading of the specimens during the course of the test program for many of the tubes. They were gradually loaded and unloaded and the recorded results corresponding to this loading procedure are presented in Figs. APB1 through APB11.

Fig. APB1 presents the cycling test of a [±30°] GR/E tube. It is observed from this figure that the modulus of the tube decreases the more the tube experienced strain during a preceding cycle, to which the modulus corresponds. It is also seen that the decrease becomes noticeable once the preceding cycle has exhibited a nonlinear mode.

In Fig. APB2 the effect of loading and unloading is presented for a [±45°] GR/E tube. this figure exhibits similar results to those discussed above for the [±30°] GR/E tube.

Figs. APB3I and APB3II show the effect of load cycling on two [±75°] GR/E tubes. It is seen from these figures that the two tubes were influenced in a similar manner, and that the modulus increased after the first loading was removed and the cylinder reloaded.

In Figs. APB4I and APB4II the effect of load cycling on two [90°] GR/E tubes is shown. It is observed that noticeable influence is experienced after the tubes have been considerably strained at a preceding cycle, resulting in a significant reduction of the modulus.

Fig. APB5 presents the cycling test of a [0°/90°] GR/E tube. This figure reveals that the more the tube was loaded and strained in the preceding cycle the more the modulus increased.

Loading and unloading effects are shown in Figs. APB6I and APB6II for two [0°/±45°/90°] GR/E tubes. No meaningful effects are

observed in either one of these figures.

In Figs. APB7I and APB7II the cycling effects of two [±15°] B/E tubes are presented. It is observed that after the tube had been unloaded and then reloaded the modulus of the tube in Fig. APB7I slightly increased, whereas the tube of Fig. APB7II insignificantly decreased.

Fig. APB8 shows the influence of loading and unloading on a [±45°] B/E tube. A slight decrease in the modulus is observed for each cycle in the sequence.

In Figs. APB9I, APB9II and APB9III cycling tests are shown for three [±60°] B/E tubes. These figures reveal a tendency to a further increase in modulus the more the tube is stressed in the preceding cycle.

Loading and unloading effects are presented in Figs. APB10I and APB10II for two [0°/90°] tubes. The tube of Fig. APB10I reveals an insignificant increase in modulus due to the cycling procedure, whereas no influence is observed at all for the tube of Fig. APB10II.

In Figs. APB11I and APB11III the results of cycling tests for two [0°/±45°/90°] GR/E tubes are shown. No effect of loading and unloading is observed in these figures.

TABLE 1A **Compression Coupons - Dimensions and Test Results**

GRAPHITE-EPOXY LAMINATES (3M SP-286T3)												
						"Damaged Batch"					Tested By SWRI "Damaged"	
Laminate Construction	t" Measured Thickness	$P_{ult.}$ (kips)	$(\sigma_c)_{ult.}$ ksi	$(Ex)_c$ $x10^6$ psi (best fit)	$(\epsilon_x)_{max}$ $x10^{-3}$	t"	$P_{ult.}$	$(\sigma_c)_{ult}$	$(Ex)_c$	$(\epsilon_x)_{max}$ $x10^{-3}$	$P_{ult.}$	$(\sigma_c)_{ult.}$
[0°]	.043	30.27 32.88 28.16	176 191 164	16.07	13.7	.043	— 22.4 26.3	— 130 153	16.41	9.8	25.7	149
[±15°]	.043	20.16 19.74 20.03	117 115 116	13.94	9.0	.044	— 23.56 22.96	— 134 130	14.14	10.3	21.45	122
[±30°]	.044	10.4 9.65 9.77	59.1 54.8 55.5	6.87	9.8	.046	— 11.73 11.93	— 63.7 64.8	7.84	10.2	9.94	54.1
[±45°]	.044	6.59 6.72 6.60	37.4 38.2 37.5	2.27	45.2	.044	— 7.55 7.39	— 42.9 42.0	3.01	26.	7.05	39.7
[±60°]	.044	6.62 6.29 6.23	37.6 35.7 35.4	1.72	52	.045	7.05 — 7.03	41.0 — 40.9	1.71	*	6.35	35.5
[±75°]	.043	5.75 6.20 **5.37	33.4 36.0 31.2	1.91	31.6	.046	6.29 — 4.58	34.2 — 24.9	2.06	30.2	5.19	28.1
[90°]	.043	5.91 5.67 **2.98	34.4 33.0 17.3	1.91	26.0	.043	3.55 4.29 —	20.6 24.9 —	1.79	15.7	2.72	16.0
[0°/90°]	.044	20.22 **7.08 19.61	115. 40.2 111.	8.79	14.0	.045	16.4 14.44	91.1 80.2	9.20	10.8	14.85	82.5
[0°/±45°/90°]	.042	16.43 15.08 15.5	97.8 89.8 92.3	6.74	18.0	—	—	—	—	—	—	—

(Laminate nominal thickness: GR/E - 8x(.0052) = .0416")

* Strain gages ceased to respond regularly with increasing load.

** End doubler debonded - End failure.

1" (inch) = $2.540x10^{-2}$ metre (m)

1 pound force = 4.448222 Newton(N)

1 kip = 10^3 pound force

1 psi = $6.894757x10^3$ Pascal (Pa)

1 ksi = 10^3 psi

TABLE 1B **Compression Coupons - Dimensions and Test Results**

BORON-EPOXY LAMINATES (AVCO 5505/5.6 MIL. DIA.)												
						"Damaged Batch"					Tested By SWRI Damaged	
Laminate Construction	t" Measured Thickness	$P_{ult.}$ (kips)	$(\sigma_c)_{ult.}$ ksi	$(Ex)_c$ $x10^6$ psi (best fit)	$(\epsilon x)_{max.}$ $x10^{-3}$	t"	$P_{ult.}$	$(\sigma_c)_{ult.}$	$(Ex)_c$	$(\epsilon x)_{max.}$ $x10^{-3}$	$P_{ult.}$	$(\sigma_c)_{ult.}$
[0°]	.052	54.71 71.05 64.53	263 342 310	31.27	10.5	.055	**45.99	209	—	—		
[±15°]	.055	29.19 30.65 30.27	133 139 138	23.65	6.6	.056	30.25 31.75 —	135 142 —	24.00	6.4	24.65	111
[±30°]I	.056	20.45 20.75 20.46	94.7 96.1 94.7	13.57	9.5							
[±30°]II		13.19 13.01 12.44	58.9 58.1 55.5	10.98	8.0							
[±45°]	.053	7.17 7.44 7.14	33.8 35.1 33.7	2.53	44.0	.054	5.85	27.1	—	—	5.70 5.52 5.71	26.1 25.3 26.1
[±60°]	.053	6.74 6.64 6.54	31.8 31.3 30.8	1.62	48.0						6.84 6.78	30.5 30.3
[±75°]	.056	7.47 7.64 7.79	33.3 34.1 34.8	2.79	21.0							
[90°]	.055	6.98 6.55 6.73	31.7 29.8 30.6	2.98	15.4						6.24 6.54 6.12	28.5 30.0 27.9
[0°/90°]	.053	43.69 48.74 37.96	206 230 179	17.17	13.5							
[0°/±45°/90°]	.053	32.74 30.98 33.47	154 146 158	11.47	14.0	.053	32.27 — 31.96	152 — 151	12.08	12.8		

(Laminate nominal thickness: B/E - 8x(.0067) = .0536")

* Strain gages ceased to respond regularly with increasing load.

** End doubler debonded - End failure.

1 (inch) = $2.540x10^{-2}$ metre (m)
1 pound force = 4.448222 Newton(N)
1 kip = 10^3 pound force
1 psi = $6.894757x10^3$ Pascal (Pa)
1 ksi = 10^3 psi

TABLE 2A Compression Tubes - Dimensions and Test Results

GRAPHITE-EPOXY LAMINATES (3M SP-286T3)																	
Laminate Construction	Geometry				Ultimate Load & Strength					Loading & Unloading Procedure							
	t" nom. (No. of plies x ply thick.)	t" meas. thick.	L" (Fig. 1B)	O.D." (Fig. 1B)	$P_{ult.}$ (kips)	(σ_{ult}) nom. (ksi)	(σ_{ult}) meas. (ksi)	$(Ex)_c$ (best fit) $x10^6$psi	$(\epsilon_x)_{max.}$ $x10^{-3}$	P_I (kips)	Ex_I $x10^6$psi	P_{II} (kips)	Ex_{II} $x10^6$psi	P_{III} (kips)	Ex_{III} $x10^6$psi	P_{IV} (kips)	Ex_{IV} $x10^6$psi
$[\pm 15°]_{4S}$	.083	.108	6.98	3.027	63.75	80.77	62.07			-	-	-	-	-	-	-	-
		.108	6.99	3.023	52.31	66.36	51.00	18.42	–	-	-	-	-	-	-	-	-
		.106	6.99	2.998	79.55	105.49	82.60	[14.25]		15.15	-	30.23	-	59.91	-	79.55	-
$[\pm 30°]_{2S}$	.042	.050	6.00	3.018	11.45	29.24	24.56	-		-	-	-	-	-	-	-	-
		.054	5.99	3.022	13.99	35.72	27.78	8.11	5.2	5.14	7.48	7.65	7.50	10.21	7.26	12.24	6.75
		.052	6.01	3.037	13.96	35.44	28.63	[6.55]		5.10	-	13.96	-	-	-	-	-
$[\pm 45°]_{2S}$	.042	.051	6.00	3.029	11.18	28.45	23.43			-	-	-	-	-	-	-	-
		.053	6.00	3.035	11.38	28.92	22.92	3.12	18.0	-	-	-	-	-	-	-	-
		.053	6.00	3.038	11.14	28.28	22.41	[2.51]		5.16	3.54	7.65	3.23	11.14	2.15	-	-
$[\pm 60°]_{2S}$	.042	.061	6.00	3.022	12.53	32.07	22.08			-	-	-	-	-	-	-	-
		.059	5.85	3.014	10.98	28.17	20.05	2.51	-	-	-	-	-	-	-	-	-
		.057	6.00	3.038	8.72	22.17	16.34	[1.79]		-	-	-	-	-	-	-	-
$[\pm 75°]_{2S}$	.042	.063	6.01	3.027	8.15	20.84	13.89			-	-	-	-	-	-	-	-
		.061	6.01	3.020	7.58	19.41	13.36	1.75	14.0	3.03	1.74	4.06	1.88	6.09	1.86	7.58	1.87
		.060	6.01	3.036	8.39	21.37	14.96	[1.20]		3.07	1.64	8.39	1.83	-	-	-	-
$[90°]_{16T}$	.083	.126	6.00	2.968	11.47	15.48	10.20			-	-	-	-	-	-	-	-
		.139	6.00	2.996	17.81	23.91	14.28	1.52	18.7	4.02	1.46	8.07	1.47	17.81	1.30	-	-
		.111	6.00	3.012	18.20	24.06	17.99	[1.01]		4.02	-	8.04	-	18.20	-	-	-
$[0°/90°]_{2S}$	.042	.049	9.00	1.106	6.87	49.26	42.22			-	-	-	-	-	-	-	-
		.043	9.00	1.097	4.39	31.57	30.83	8.35	5.7	2.06	7.27	4.05	7.56	4.39	8.49	-	-
		.043	9.00	1.088	4.05	29.37	28.69	[7.79]		-	-	-	-	-	-	-	-
$[0°/\pm 45°/90°]_{2S}$	.083	.115	7.00	2.886	33.60	46.50	33.56			-	-	-	-	-	-	-	-
		.109	7.00	3.037	29.14	38.17	29.06	7.77	7.0	10.31	8.39	20.24	8.56	29.14	8.31	-	-
		.110	7.00	3.017	36.05	47.56	35.89	[5.71]		11.17	7.64	20.22	7.53	36.05	7.48	-	-

[ ] Moduli values corresponding to "true" measured thickness

1"(inch) = 2.540×10^{-2} metre (m)

1 pound force = 4.448222 Newton (N)

1 kip = 10^3 pound force

1 psi = 6.894757×10^3 Pascal (Pa)

1 ksi = 10^3 psi

TABLE 2B **Compression Tubes - Dimensions and Test Results**

BORON-EPOXY LAMINATES (AVCO 5505/5.6 MIL.DIA)																	
Laminate Construction	Geometry				Ultimate Load & Strength					Loading & Unloading Procedure							
	t" nom. (No. of plies x ply thick.)	t" meas. thick.	L" (Fig. 1B)	O.D." (Fig. 1B)	$P_{ult.}$ (kips)	$(\sigma_{ult.})_{nom.}$ (ksi)	$(\sigma_{ult.})_{meas.}$ (ksi)	$(Ex)_c$ (best fit) $x10^6$psi	$(\epsilon_x)_{max.}$ $x10^{-3}$	P_I (kips)	Ex_I $x10^6$psi	P_{II} (kips)	Ex_{II} $x10^6$psi	P_{III} (kips)	Ex_{III} $x10^6$psi	P_{IV} (kips)	Ex_{IV} $x10^6$psi
$[\pm 15°]_{3S}$	.080	.111	8.98	3.045	66.12	89.67	64.62			50.49	36.00	66.12	37.30	-	-	-	-
		.116	9.00	3.047	61.47	83.45	57.55	37.49	2.2	25.34	38.30	61.47	36.60	-	-	-	-
		.108	9.00	3.043	67.69	91.76	67.97	[26.85]		-	-	-	-	-	-	-	-
$[\pm 30°]_{2S}$	.054	.076	7.01	3.042	14.59	29.00	20.60			10.21	-	10.13	-	14.59	-	-	-
		.074	6.99	3.025	15.33	30.62	22.35	11.11	2.7	-	-	-	-	-	-	-	-
		.075	7.01	3.023	15.07	30.13	21.70	[8.00]		10.18	-	10.16	-	15.07	-	-	-
$[\pm 45°]_{2S}$	.054	.074	5.98	3.044	14.11	28.00	20.44			-	-	-	-	-	-	-	-
		.071	5.98	3.059	12.91	25.47	19.37	3.23	3.5	2.54	3.05	4.10	3.03	5.16	2.97	12.91	2.86
		.074	6.00	3.047	13.50	26.77	19.53	[2.39]		-	-	-	-	-	-	-	-
$[\pm 60°]_{2S}$	.054	.076	6.00	3.062	16.75	33.07	23.49			5.12	2.70	16.75	2.64	-	-	-	-
		.081	6.00	3.045	17.62	35.09	23.39	3.97	19.3	7.62	2.91	17.62	3.60	-	-	-	-
		.079	6.00	3.058	19.55	38.68	26.44	[2.72]		5.16	3.12	19.55	3.28	-	-	-	-
$[\pm 75°]^*_{2S}$	.054	.074	6.00	3.056	13.85	27.38	19.93			-	-	-	-	-	-	-	-
		.079	6.00	3.045	15.65	31.10	21.39	-	-	-	-	-	-	-	-	-	-
		.079	6.00	3.050	15.35	30.46	20.82			-	-	-	-	-	-	-	-
$[90°]_{8T}$	.054	.076	5.98	3.030	8.91	17.78	12.63			-	-	-	-	-	-	-	-
		.082	5.98	3.035	10.87	21.70	14.29	3.39	7.8	-	-	-	-	-	-	-	-
		.079	5.98	3.045	10.57	20.87	14.26	[2.32]		-	-	-	-	-	-	-	-
**	.134	.204	9.00	2.868	236.32	210.76	138.44			-	-	-	-	-	-	-	-
		.160	9.00	3.035	227.82	233.19	157.40			61.63	24.60	227.82	25.80	-	-	-	-
$[0°/90°]_{4S}$	.108	.152	9.01	3.018	205.92	211.51	150.28	25.34	9.0	40.34	24.60	61.81	25.00	122.34	24.50	205.92	24.50
		.151	9.00	3.025	200.67	205.78	147.18	[17.73]		-	-	-	-	-	-	-	-
		.180	7.01	3.040	142.50	146.90	88.11			-	-	-	-	-	-	-	-
$[0°/\pm 45°/90°]_{2S}$	.108	.180	7.00	3.033	134.80	139.20	83.55	16.65	9.4	60.90	16.90	101.10	17.00	134.80	16.80	-	-
		.169	6.98	3.031	132.80	136.80	87.40	[10.20]		20.30	16.10	82.10	16.40	132.80	16.60	-	-

* Damaged tubes (see Results and Discussion)

** Note difference in nominal thickness

[ ] Moduli values corresponding to "true" measured thickness

1"(inch) = 2.540×10^{-2} metre (m)

1 pound force = 4.448222 Newton (N)

1 kip = 10^3 pound force

1 psi = 6.894757×10^3 Pascal (Pa)

1 ksi = 10^3 psi

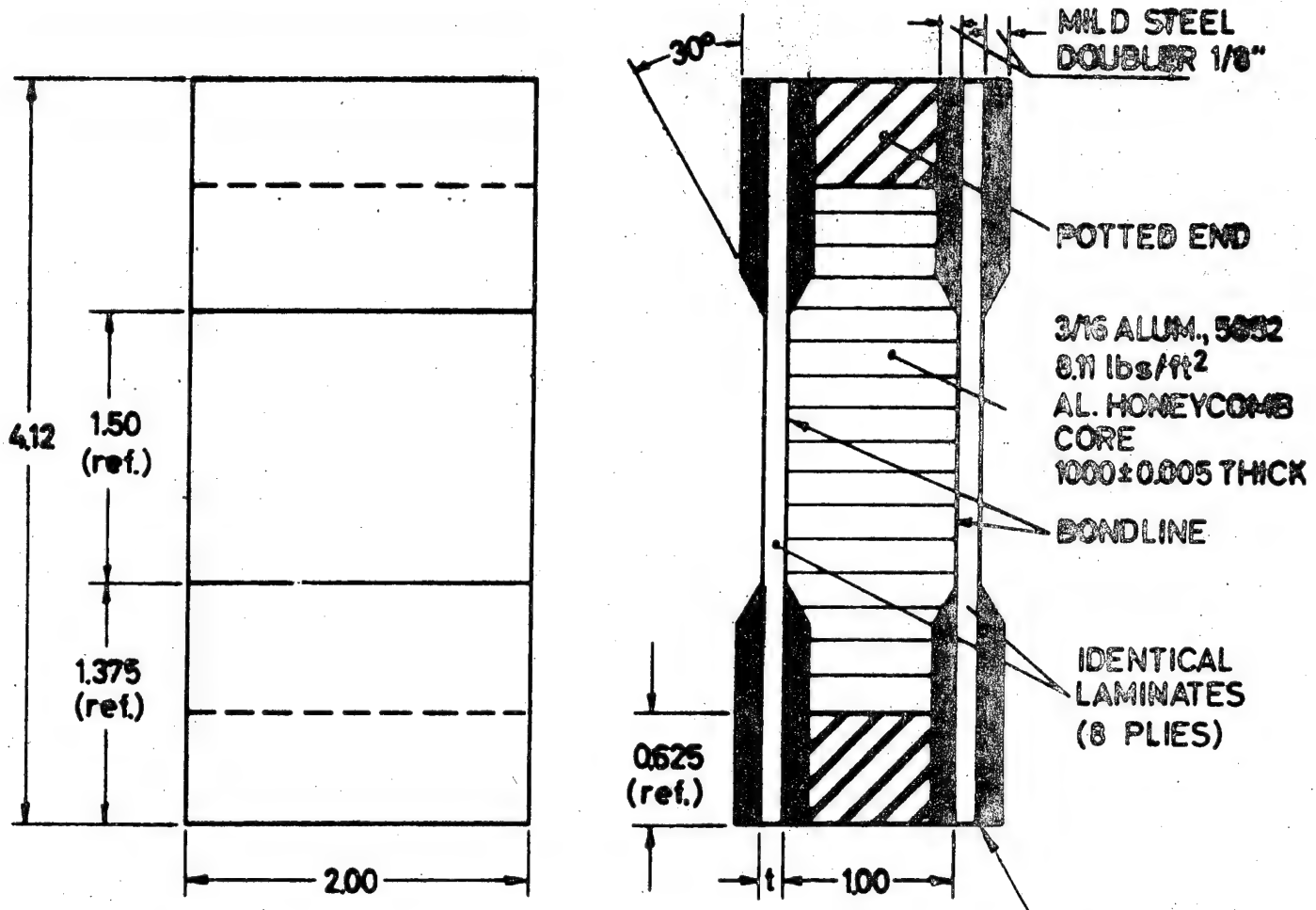

t for: GRAPHITE/EPOXY 8x(0.0052)
BORON/EPOXY 8x(0.0067)

ADHESIVE: NITRILE/EPOXY PER MMM-A-132 TYPE I
POTTING COMPOUND; MAGNABOUND 79-3
NARMCO 3150
EPON 934

FIG. 1A COMPRESSION COUPONS - DIMENSIONS AND DETAILS.

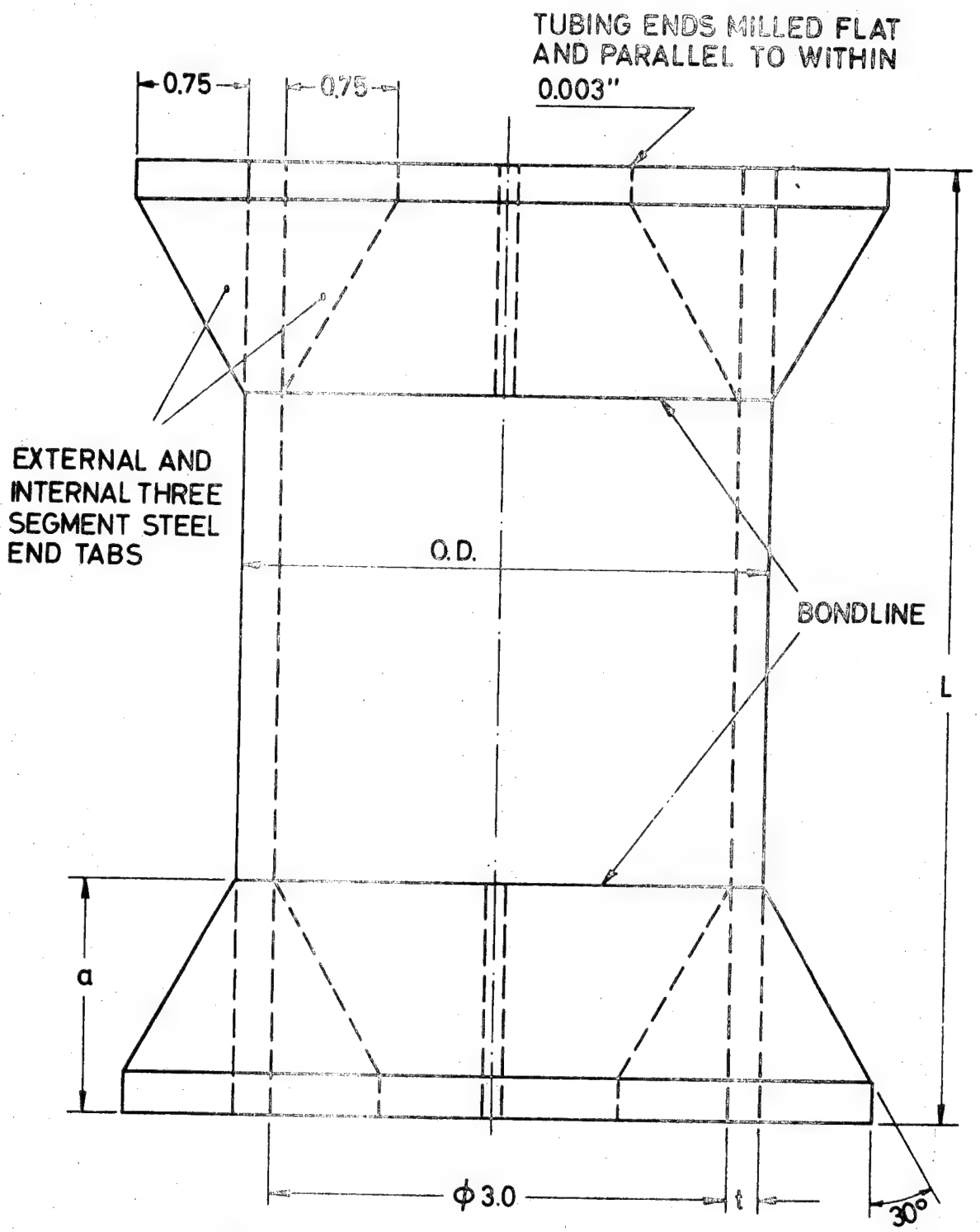

a - CALCULATED TO WITHSTAND ULTIMATE LOAD

t - NUMBER OF PLIES x (0.0052) FOR GRAPHITE/EPOXY
x (0.0067) FOR BORON/EPOXY
CALCULATED WITH [12] TO AVOID BUCKLING

ADHESIVE: NITRILE/EPOXY PER MMM-A-132 TYPE I
END TABS; 1010-1080 MILD STEEL THICK WALL TUBING

27

FIG. 1B COMPRESSION TUBES - DIMENSIONS AND DETAILS

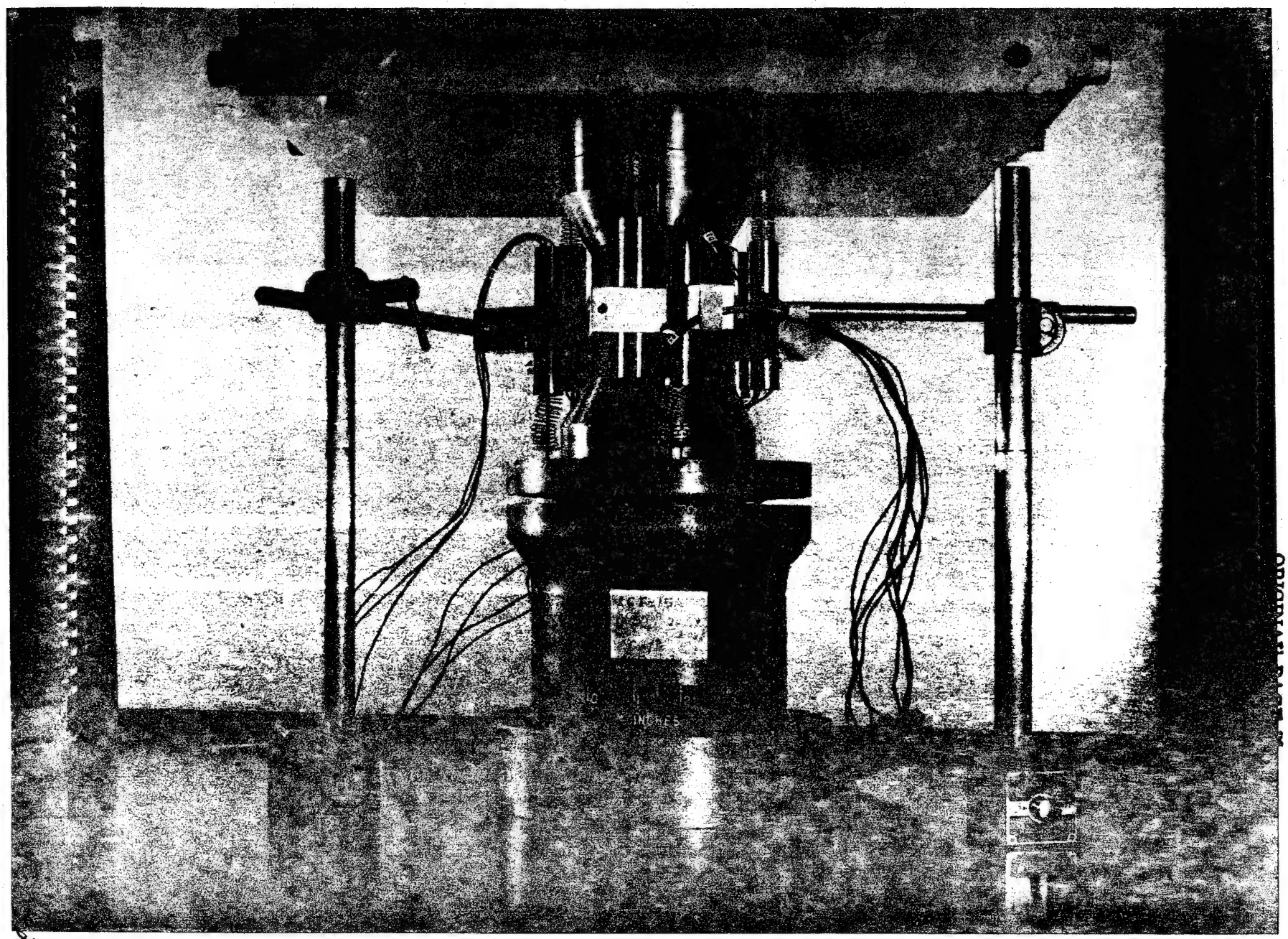

FIG. 2 COMPRESSION TEST SET UP

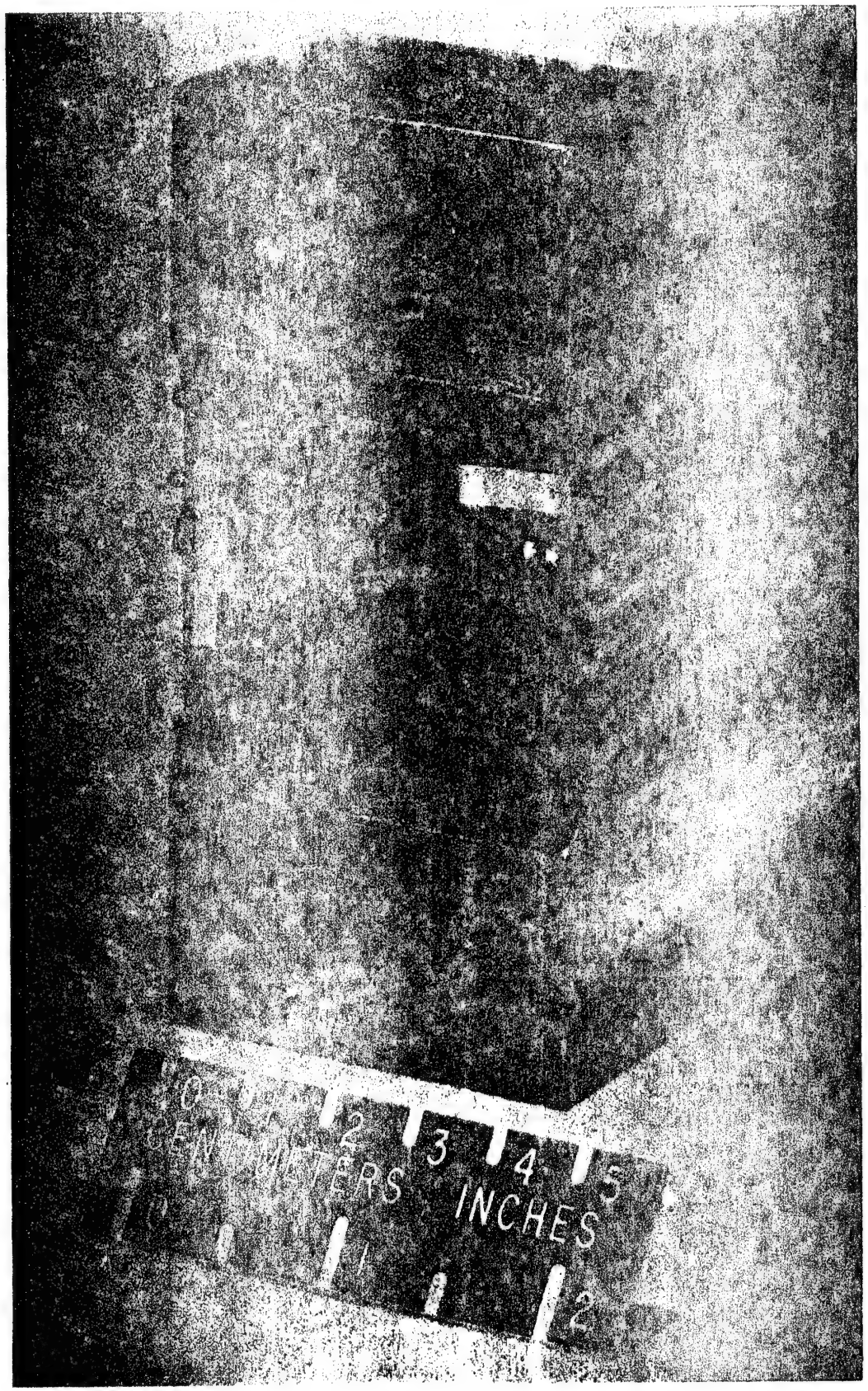

FIG. 3 COMPRESSION COUPONS - GAGE LOCATION

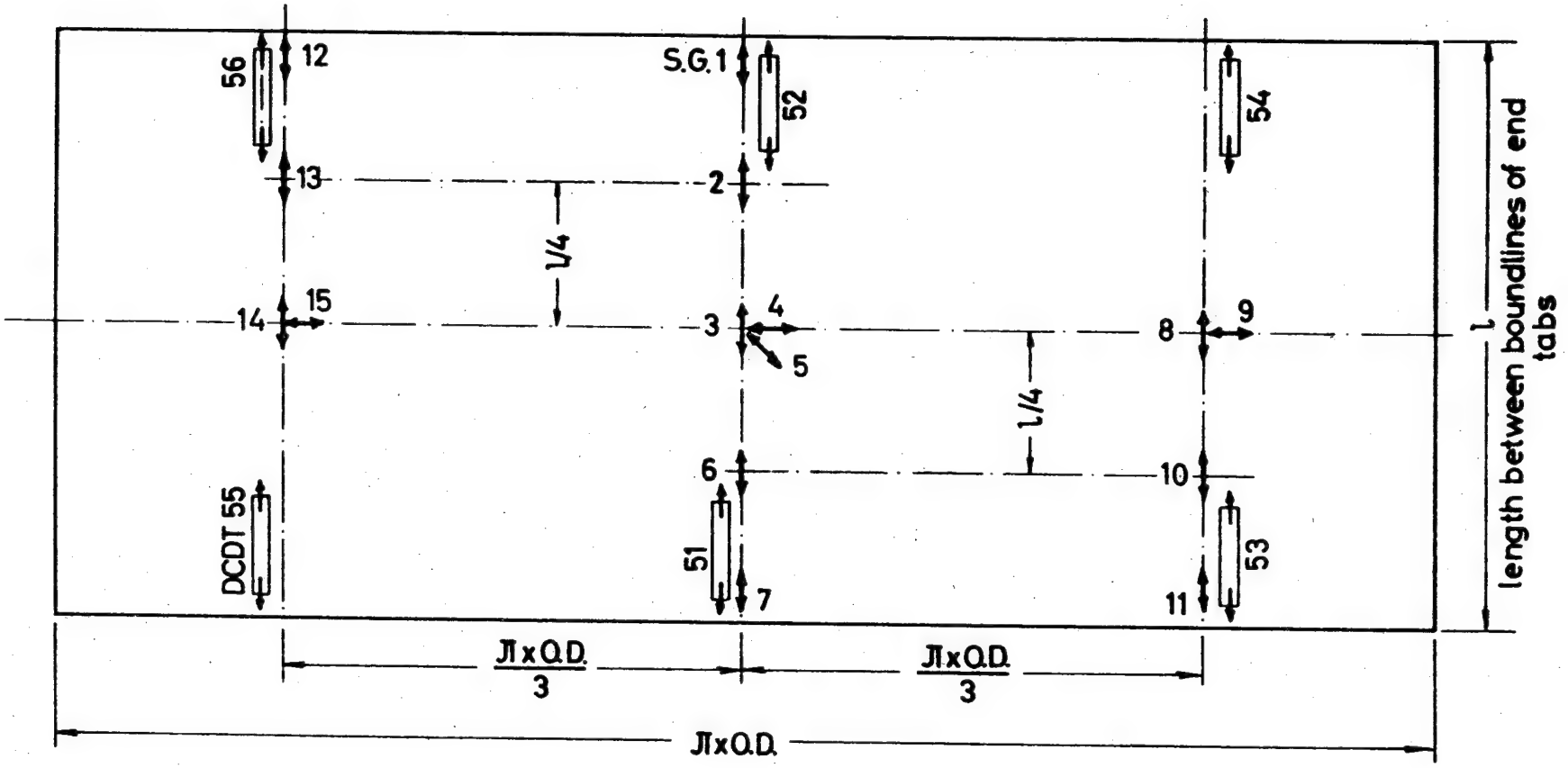

FIG. 4 DEVELOPED SURFACE OF TUBULAR SPECIMEN-STRAIN GAGE AND DCDT LOCATION

FIG. 5 COMPRESSION TUBES

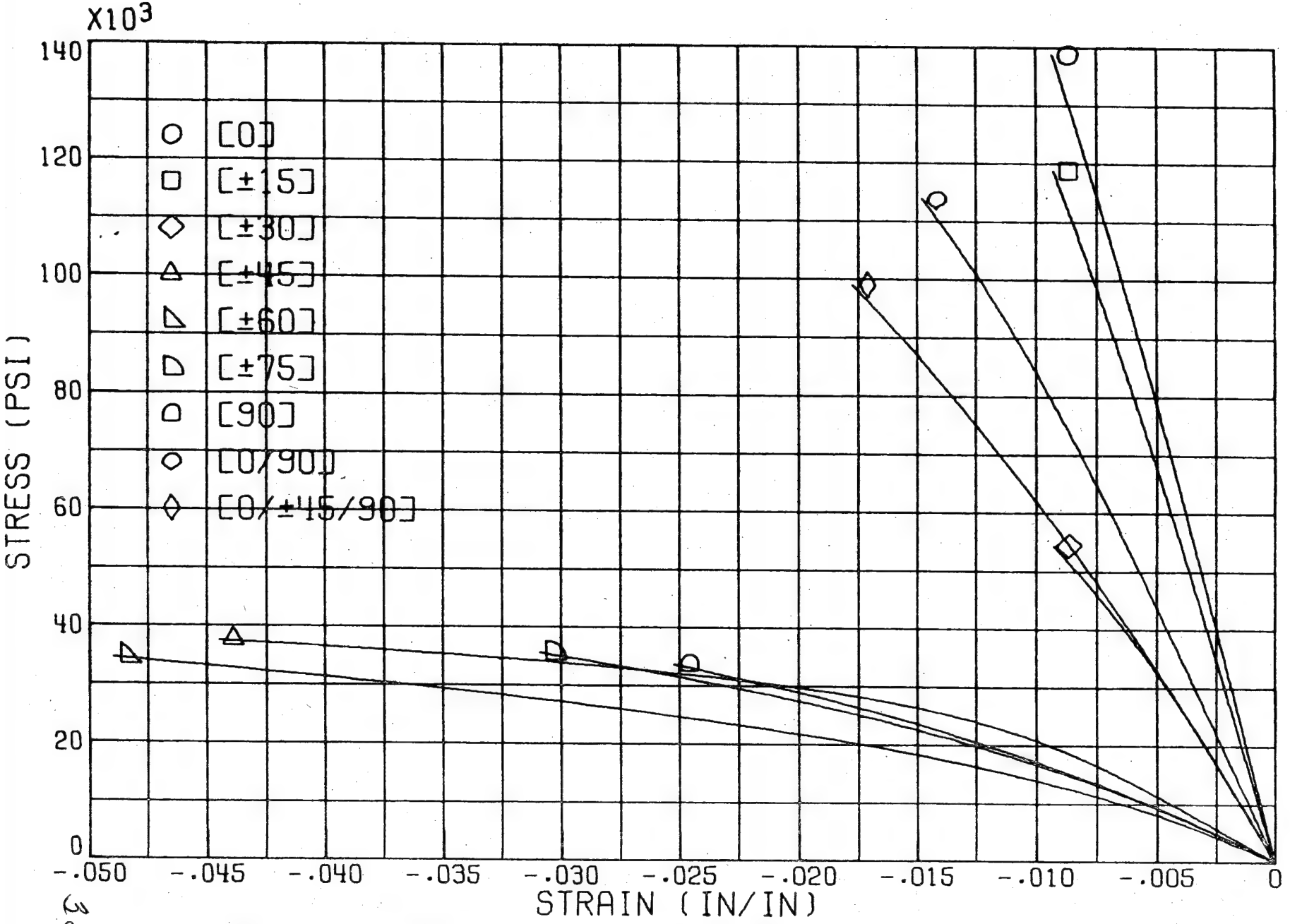

32

FIG. 6A COMPRESSION PLANAR GR/EP

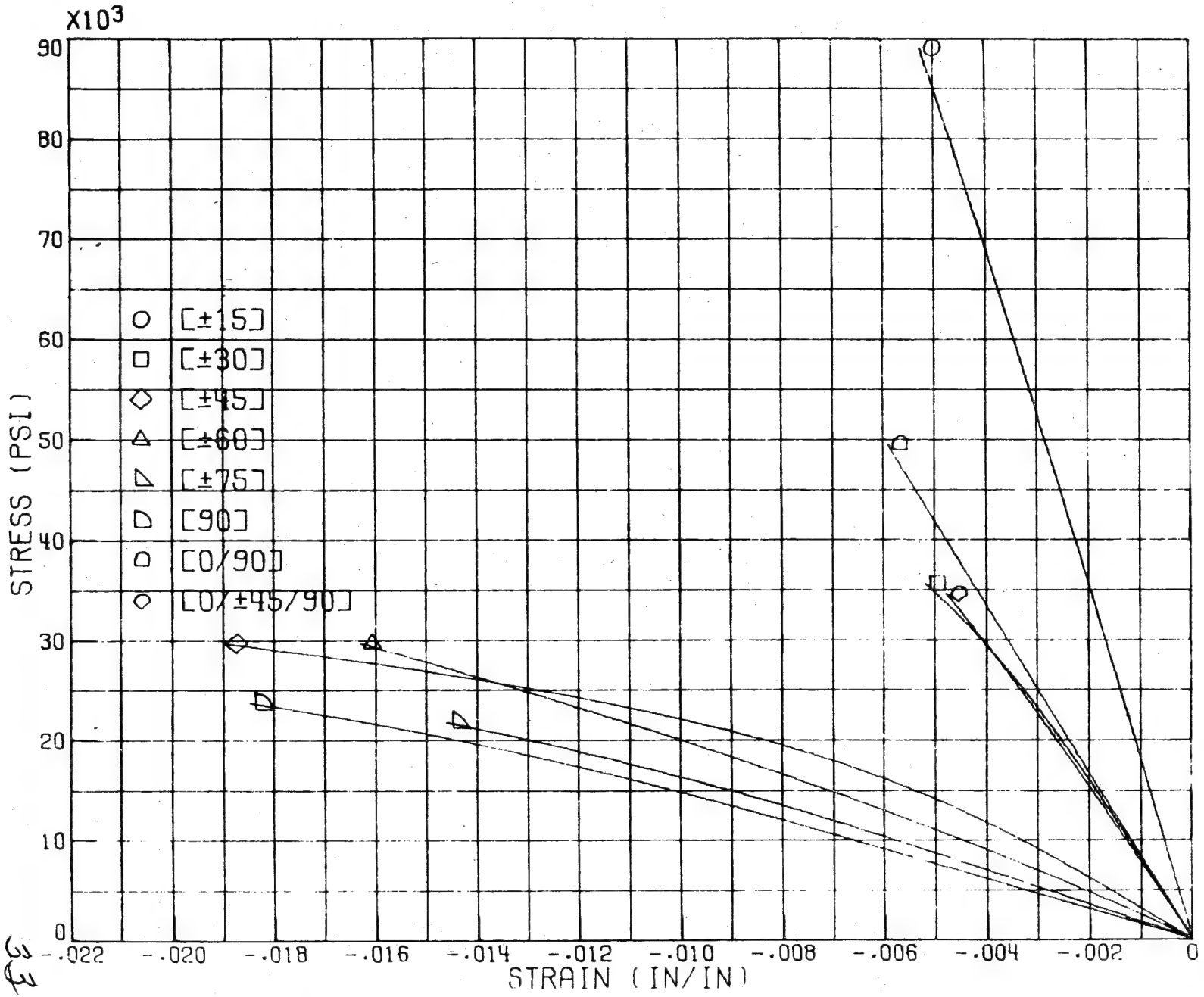

FIG. 6B COMPRESSION TUBULAR GR/E

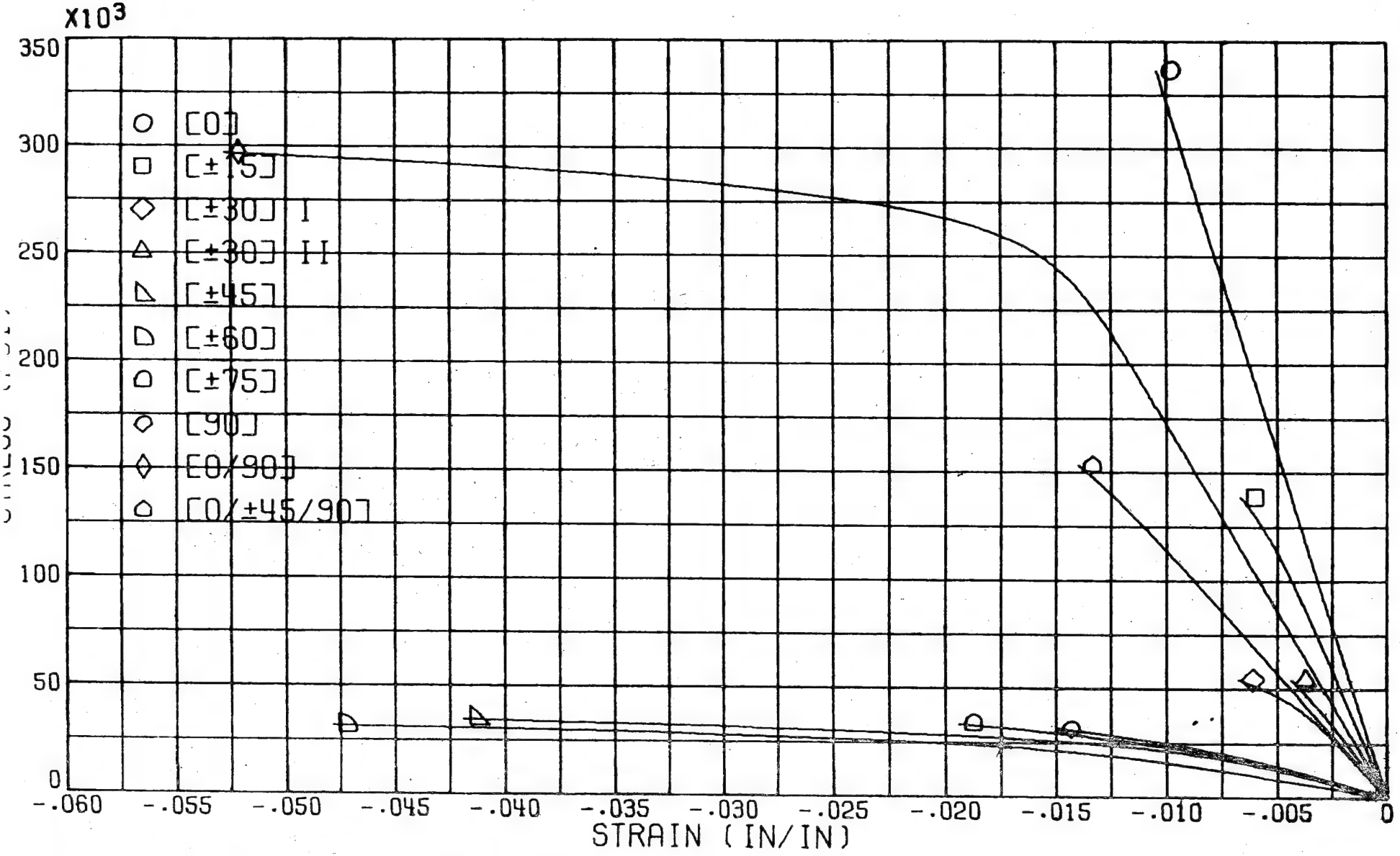

FIG. 7A COMPRESSION PLANAR B/E

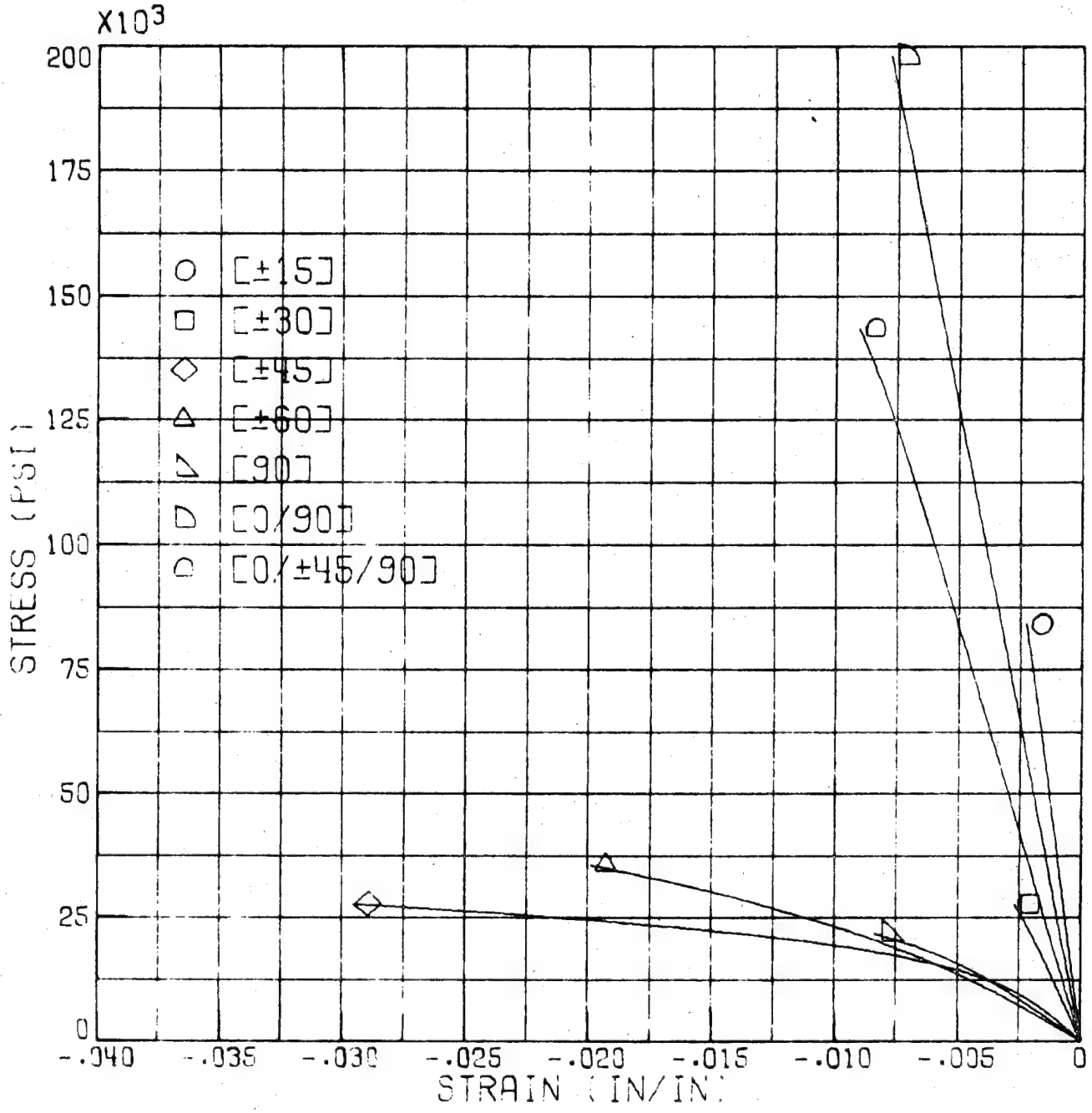

FIG. 7B COMPRESSION TUBULAR B/E

o TEST 502 RUN 7
□ TEST 502 RUN 8
◇ TEST 502 RUN 9

△ BEST FIT
A= $-.6219 \times 10^{-7}$
B= $-.2665 \times 10^{-18}$
N= 3

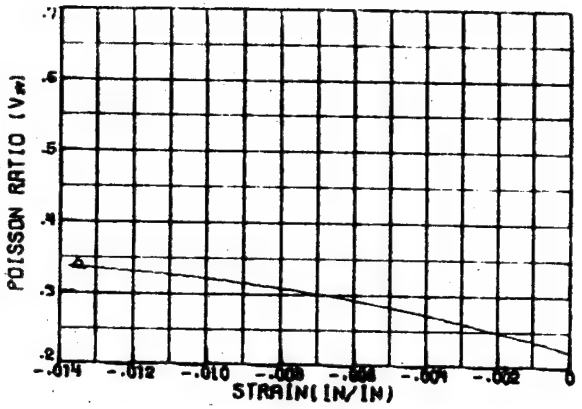

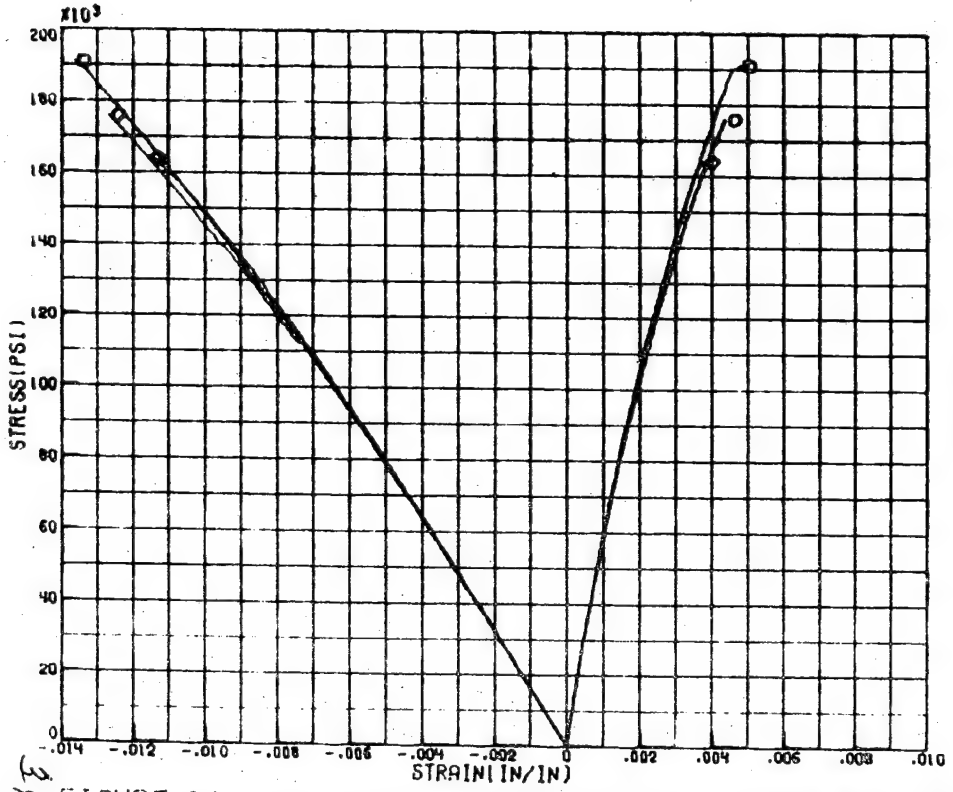

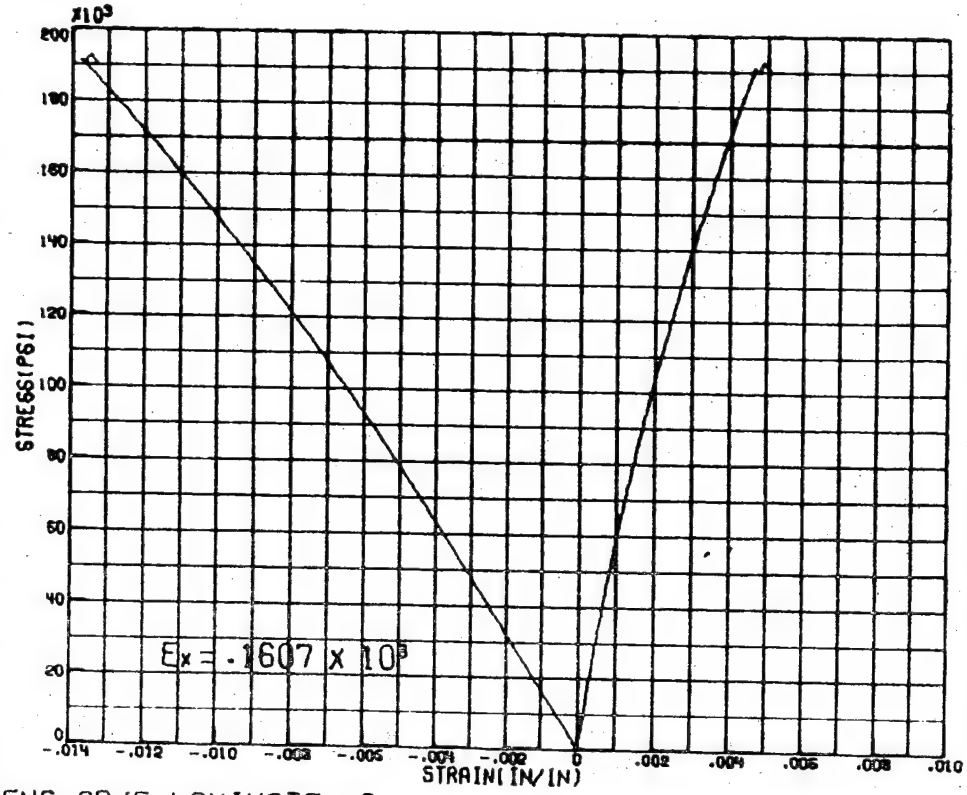

FIGURE 8A.-COMPRESSION RESPONSE OF PLANAR SPECIMENS-GR/E LAMINATE- 0

○ TEST 502 RUN 10 △ BEST FIT
□ TEST 502 RUN 11 A= $-.7171 \times 10^{-7}$
◇ TEST 502 RUN 12 B= $-.4688 \times 10^{-10}$
N= 3

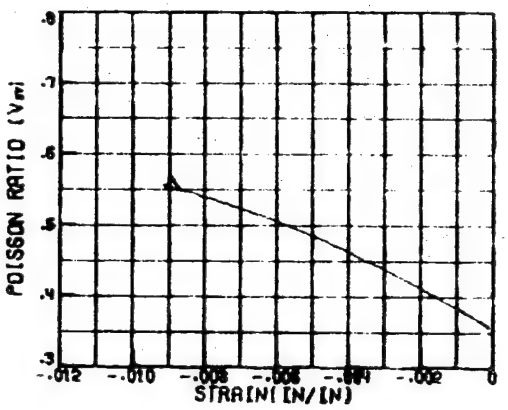

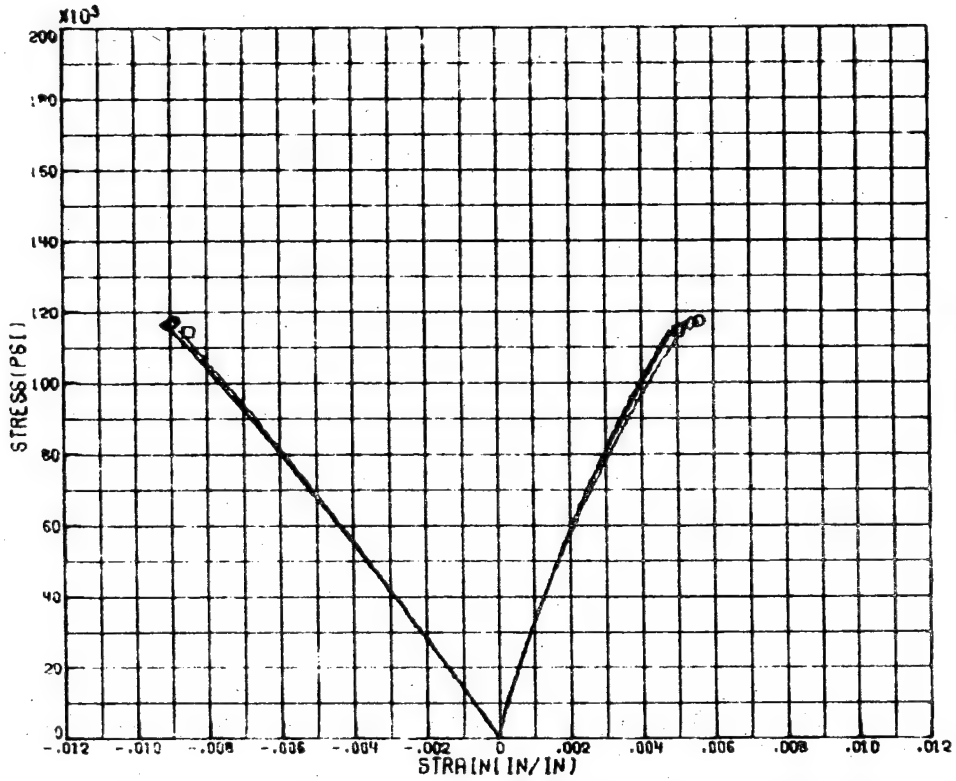

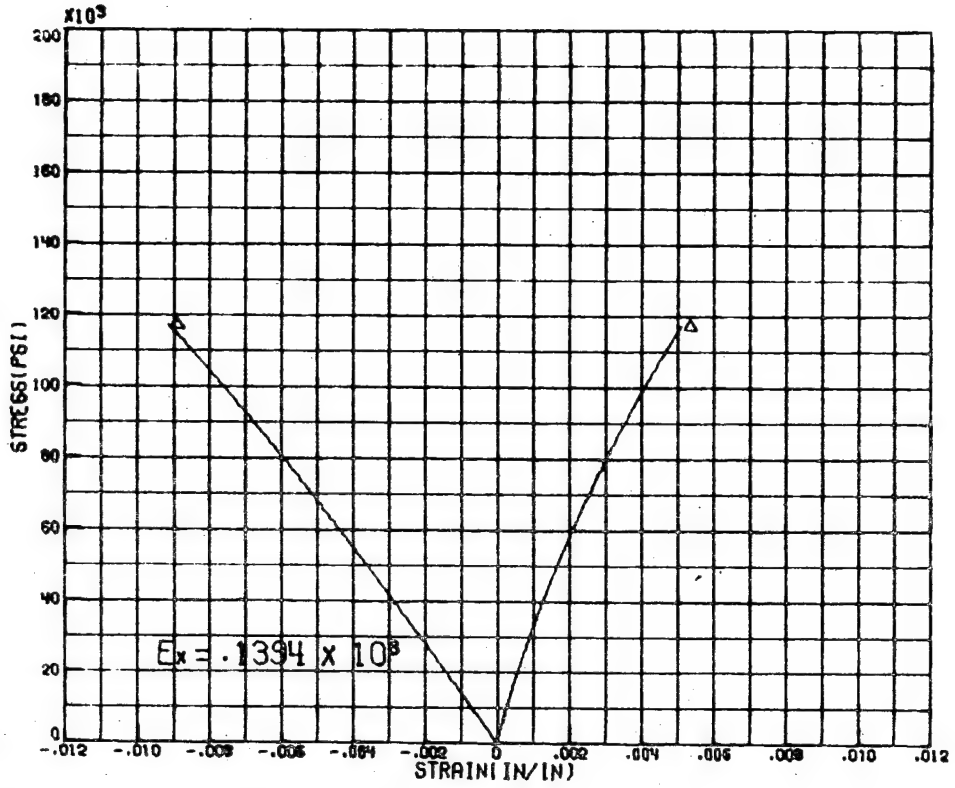

FIGURE 9A: COMPRESSION RESPONSE OF PLANAR SPECIMENS-GR/E LAMINATE-[±15]

○ TEST 537 RUN 9
□ TEST 537 RUN 10
◇ TEST 609 RUN 6

△ BEST FIT
A= -.5428 x 10^{-7}
B= -.5515 x 10^{-13}
N= 2

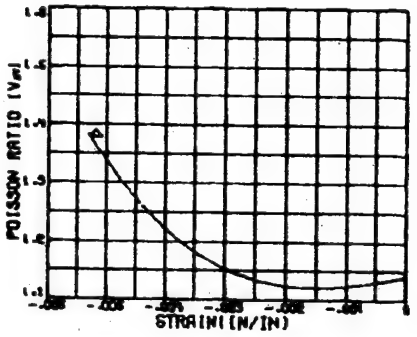

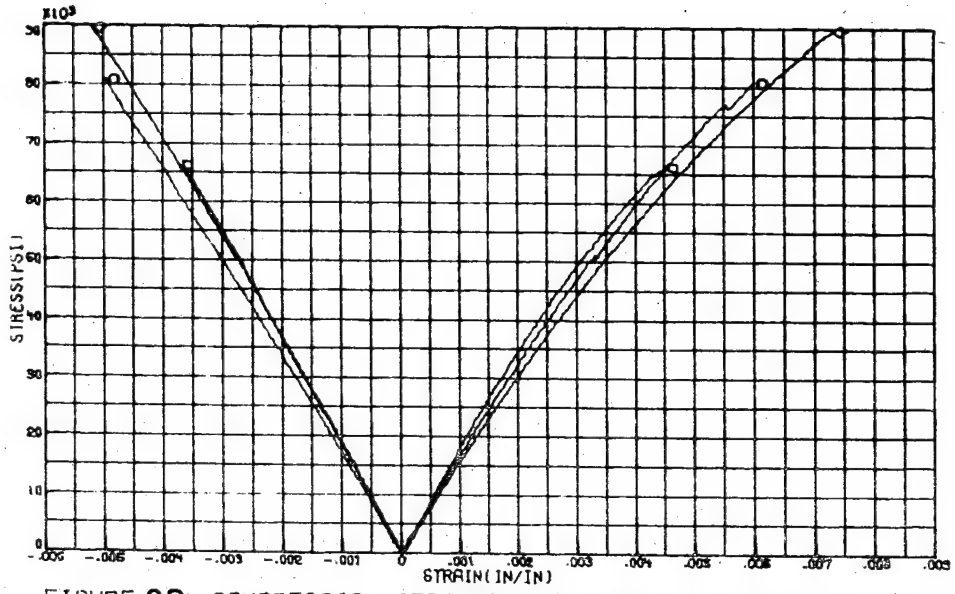

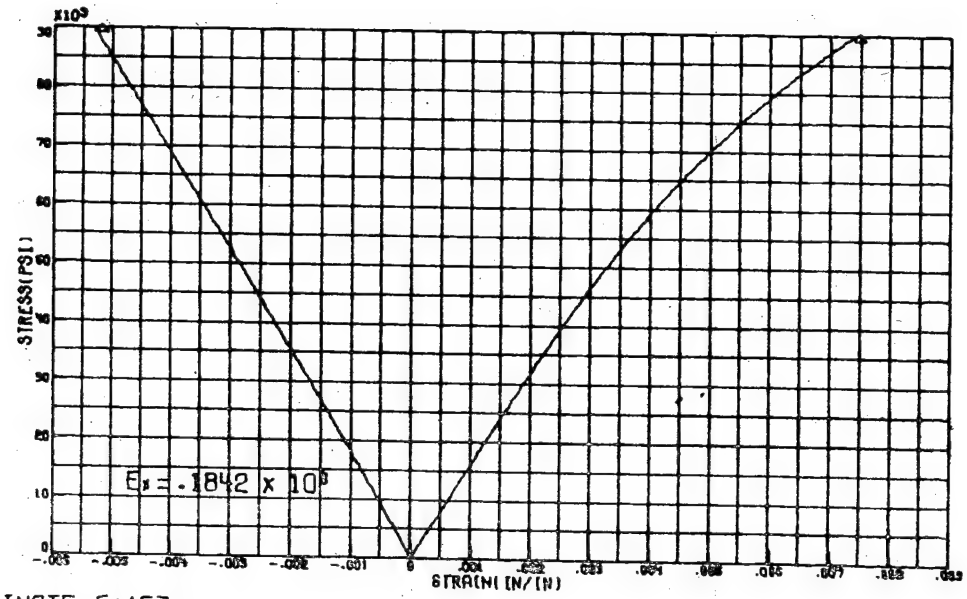

FIGURE 9B:-COMPRESSION RESPONSE OF TUBULAR SPECIMENS-GR/E LAMINATE-[±15]

○	TEST 502	RUN 34	△	BEST FIT
□	TEST 502	RUN 35		A= $-.1454 \times 10^{-6}$
◇	TEST 502	RUN 36		B= $-.8552 \times 10^{-17}$
				N= 3

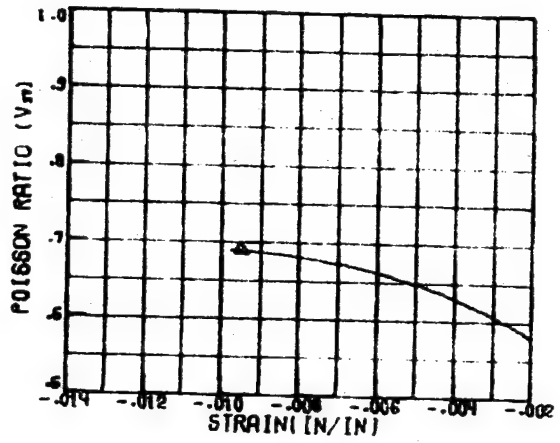

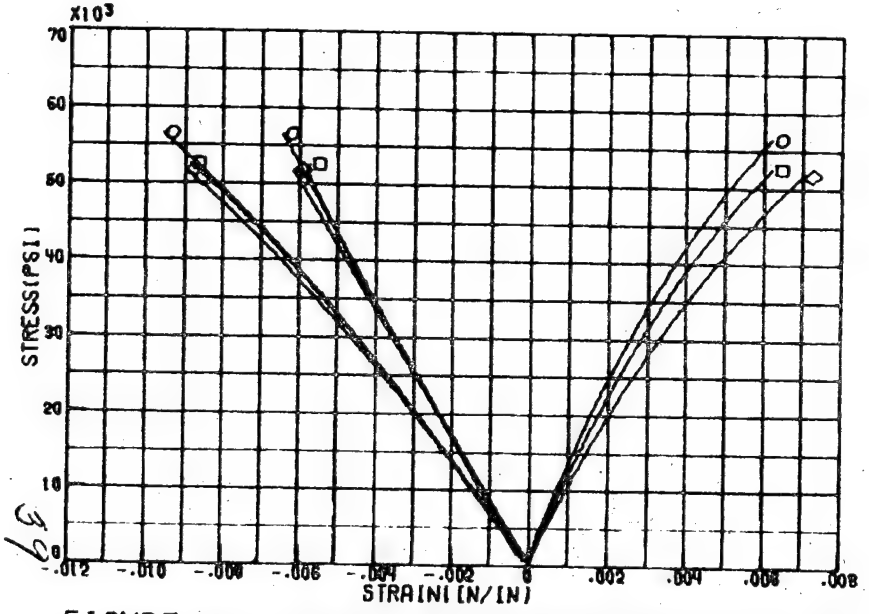

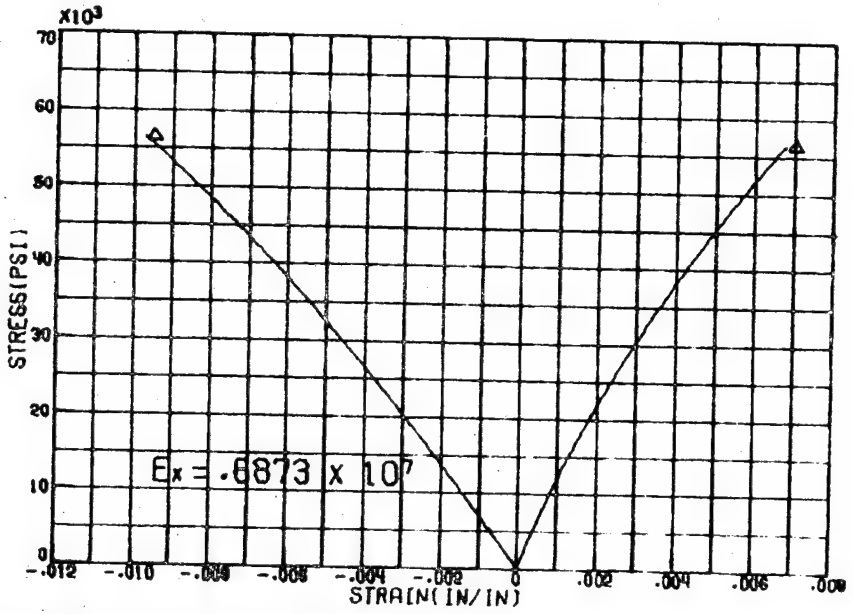

FIGURE 10A:-COMPRESSION RESPONSE OF PLANAR SPECIMENS-GR/E LAMINATE-[±30]

○ TEST 527 RUN 4 ^ BEST FIT
□ TEST 527 RUN 5 A= $-.1233 \times 10^{-6}$
◇ TEST 527 RUN 6 B= $-.4967 \times 10^{-21}$
N= 4

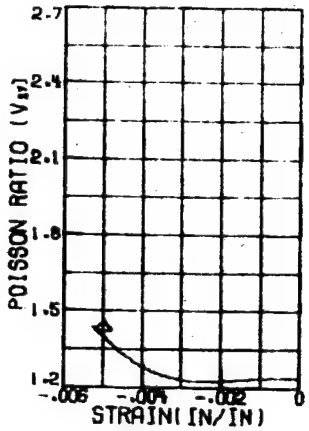

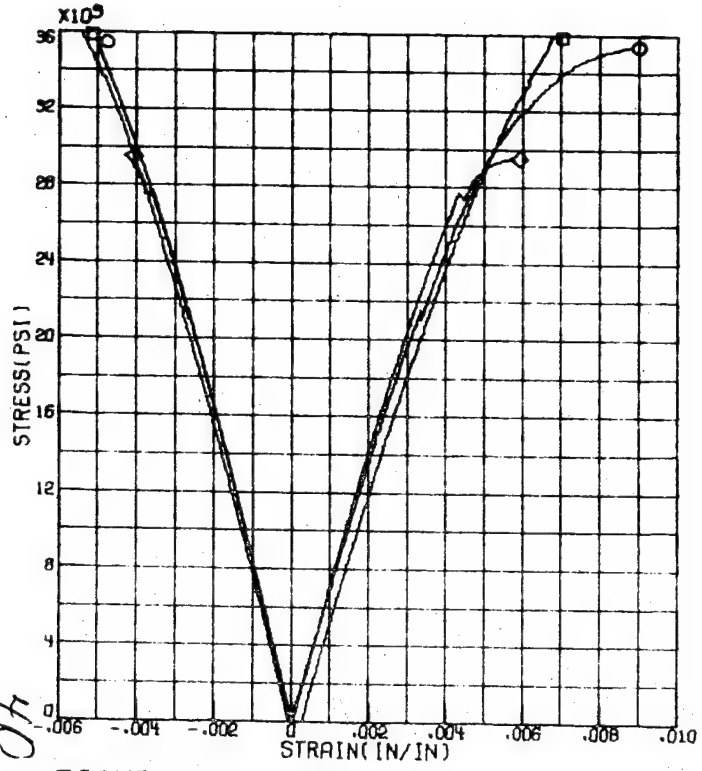

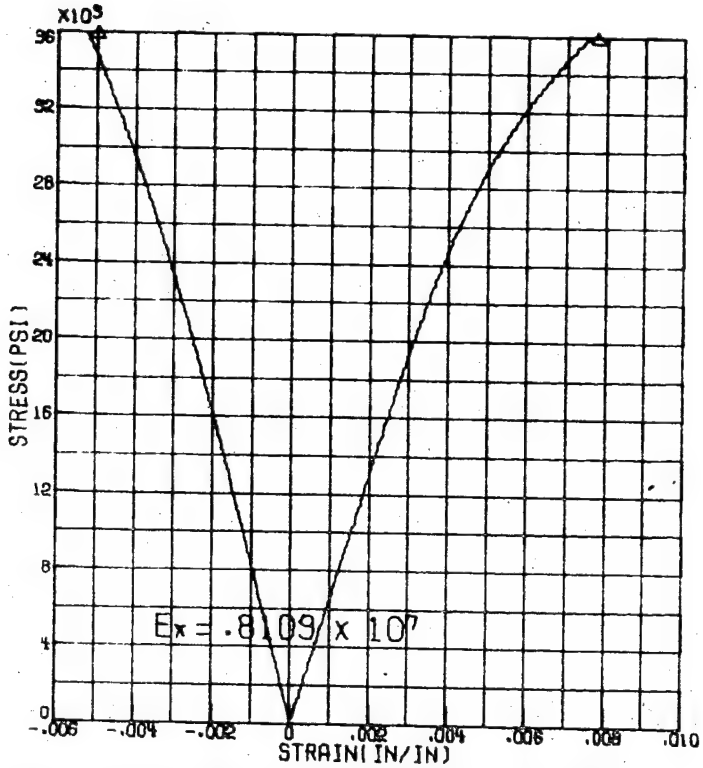

FIGURE 10B:-COMPRESSION RESPONSE OF TUBULAR SPECIMENS-GR/E LAMINATE- [±30]

- ○ TEST 501 RUN 1
- □ TEST 501 RUN 2
- ◇ TEST 501 RUN 3

△ BEST FIT

A= $-.4397 \times 10^{-6}$

B= $-.9873 \times 10^{-23}$

N= 6

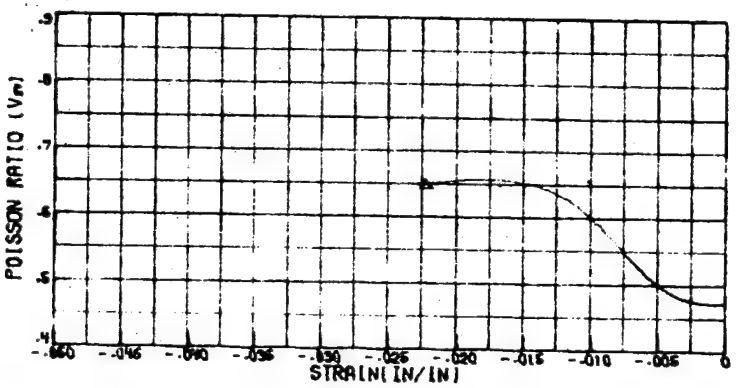

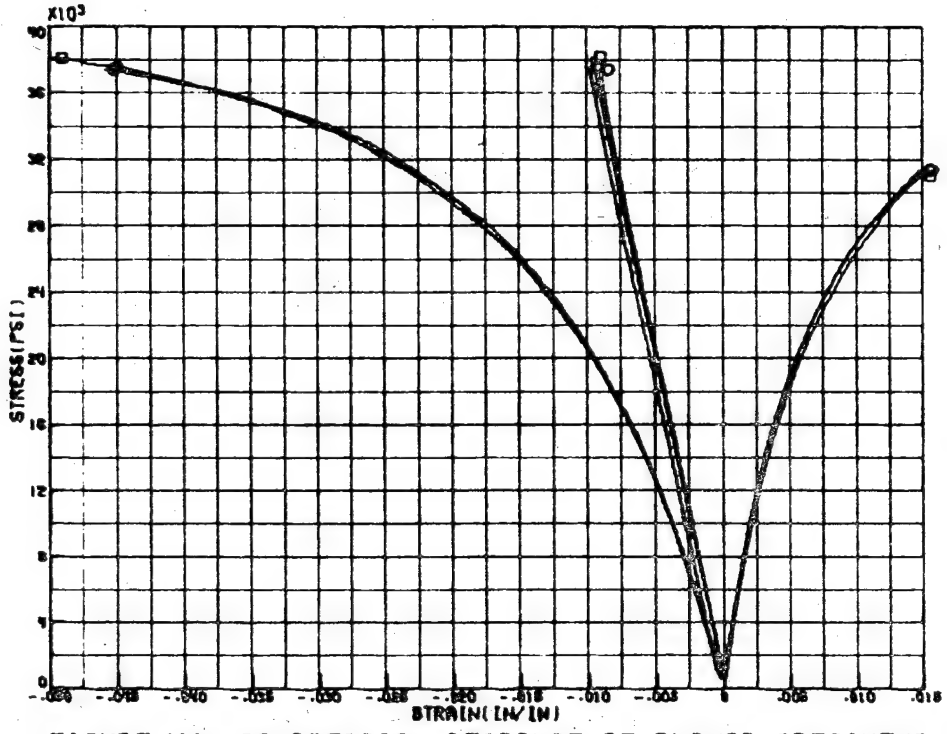

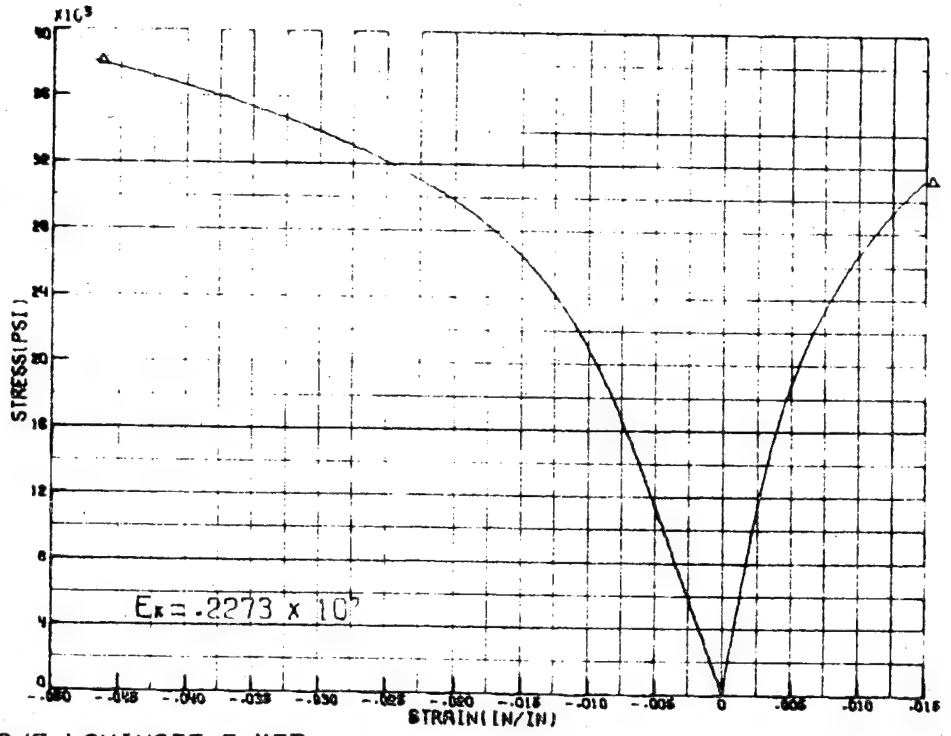

FIGURE 11A:-COMPRESSION RESPONSE OF PLANAR SPECIMENS-GR/E LAMINATE-[±45]

14

TEST 525 RUN 2 △ BEST FIT
TEST 525 RUN 3 A= -.3205 x 10^{-6}
TEST 526 RUN 5 B= -.1217 x 10^{-19}
N= 4

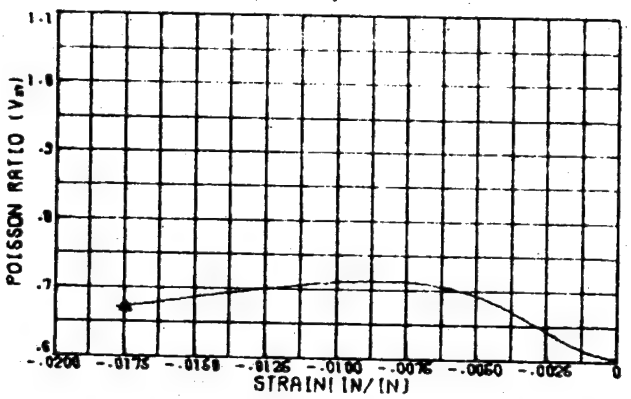

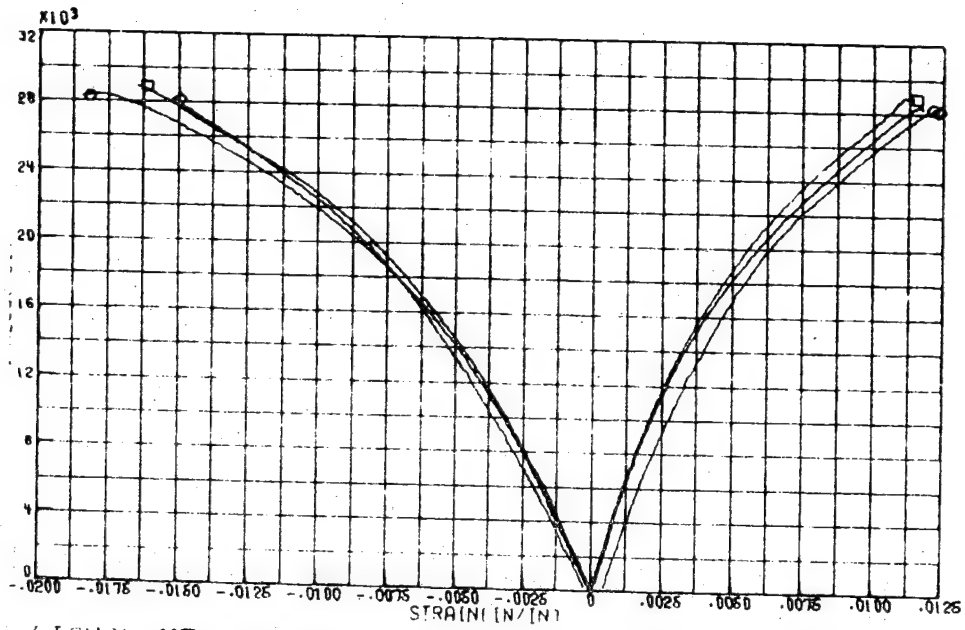

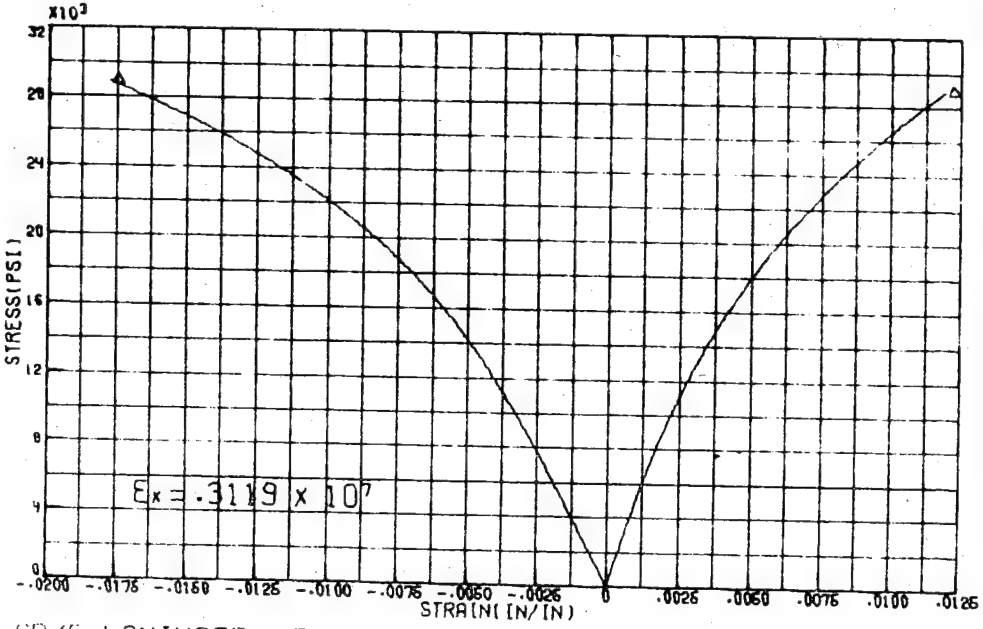

FIGURE 11B: COMPRESSION RESPONSE OF TUBULAR SPECIMENS-GR/E LAMINATE- [±45]

4/2

○ TEST 497 RUN 1 △ BEST FIT
□ TEST 497 RUN 2 A= $-.5814 \times 10^{-6}$
◇ TEST 499 RUN 1 B= $-.7006 \times 10^{-16}$
N= 3

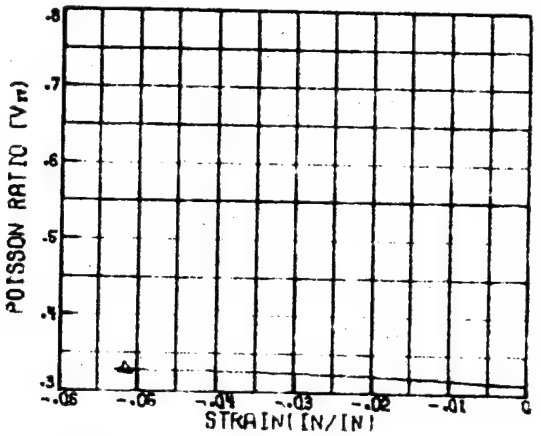

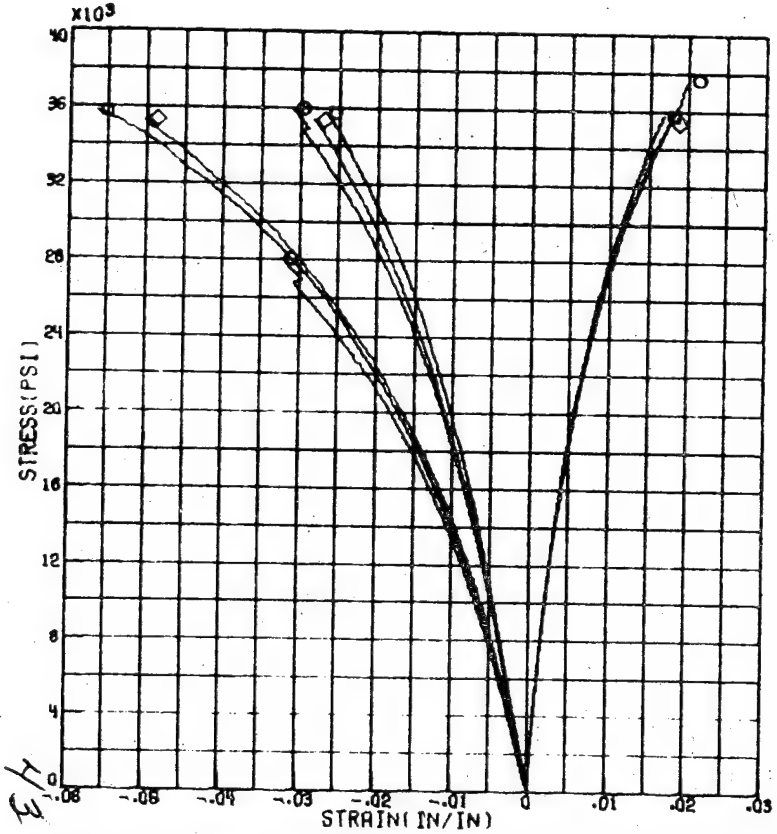

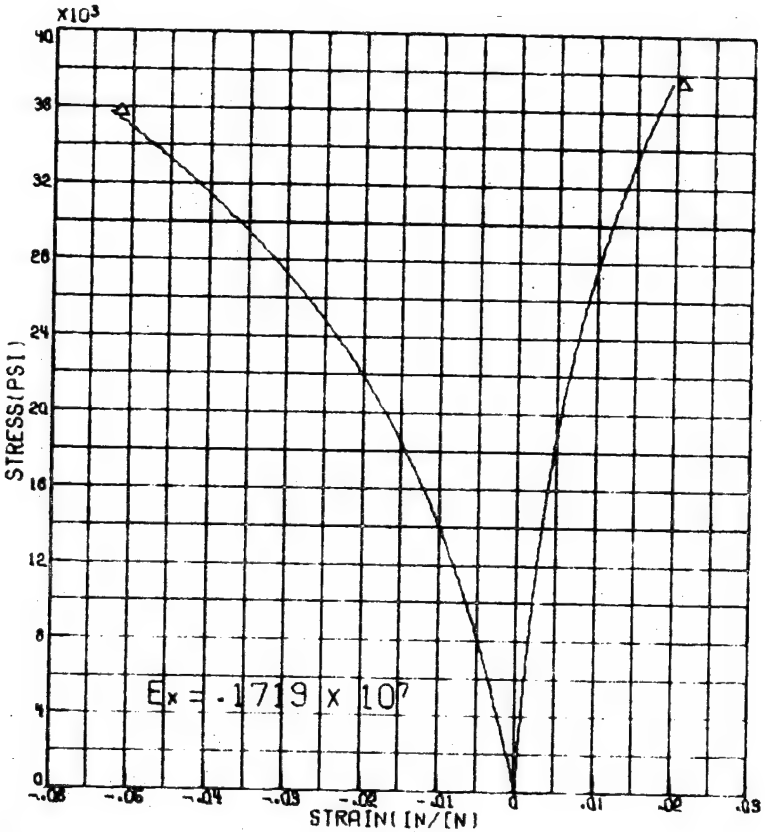

FIGURE **12A**:-COMPRESSION RESPONSE OF PLANAR SPECIMENS-GR/E LAMINATE-[±60]

○ TEST 514 RUN 1 △ BEST FIT
□ TEST 525 RUN 4 A= -.3989 x 10^{-6}
◇ TEST 525 RUN 5 B= -.5064 x 10^{-11}
N= 2

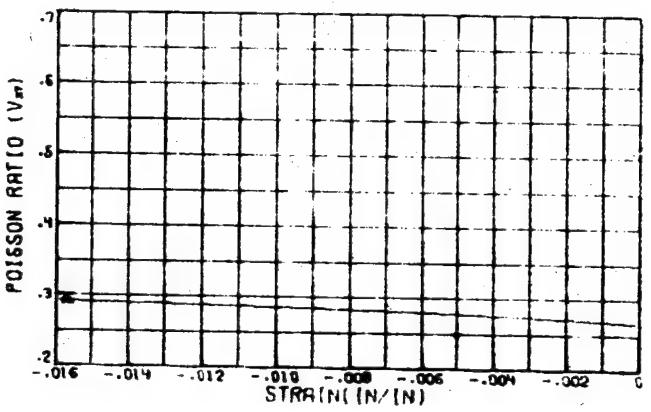

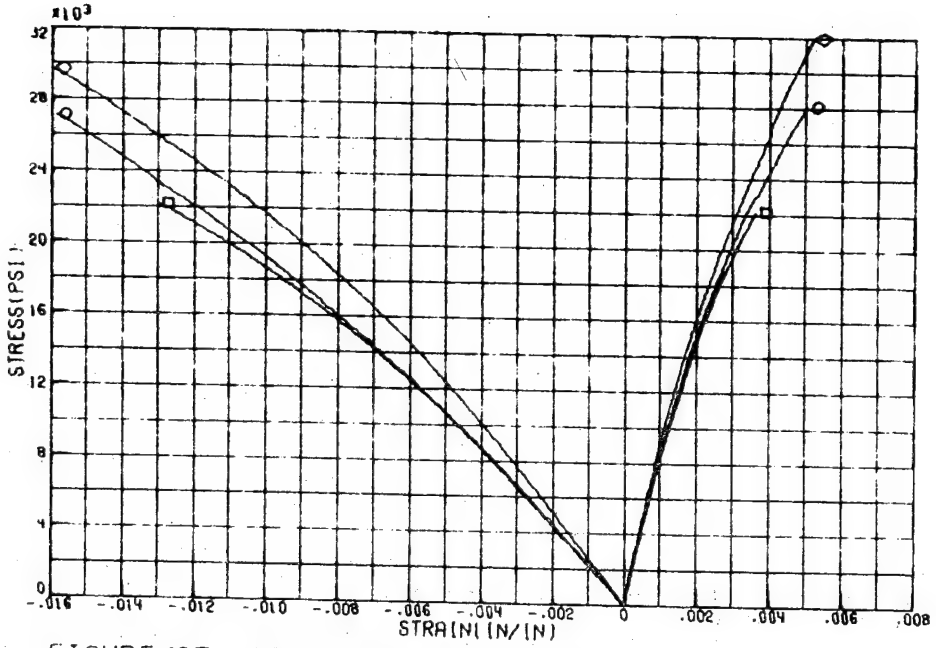

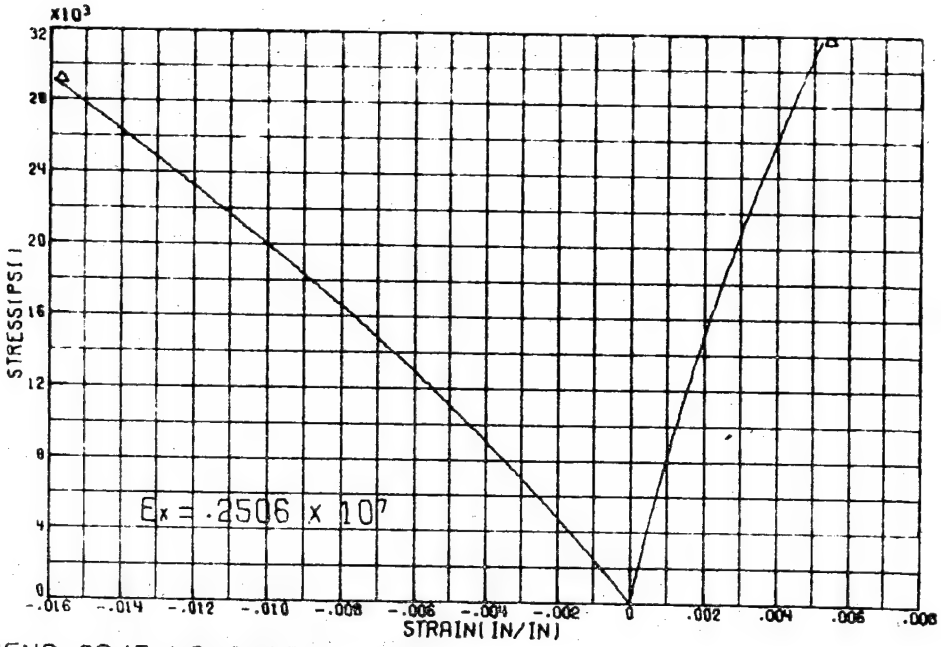

FIGURE 12B:-COMPRESSION RESPONSE OF TUBULAR SPECIMENS-GR/E LAMINATE- [±60]

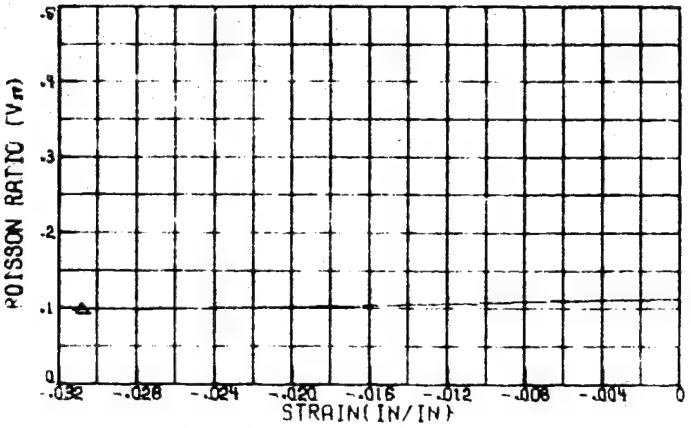

○ TEST 499 RUN 2 △ BEST FIT
□ TEST 499 RUN 3 q_x = -.5232 x 10^{-6}
◇ TEST 499 RUN 4 B= -.2721 x 10^{-16}
N= 3

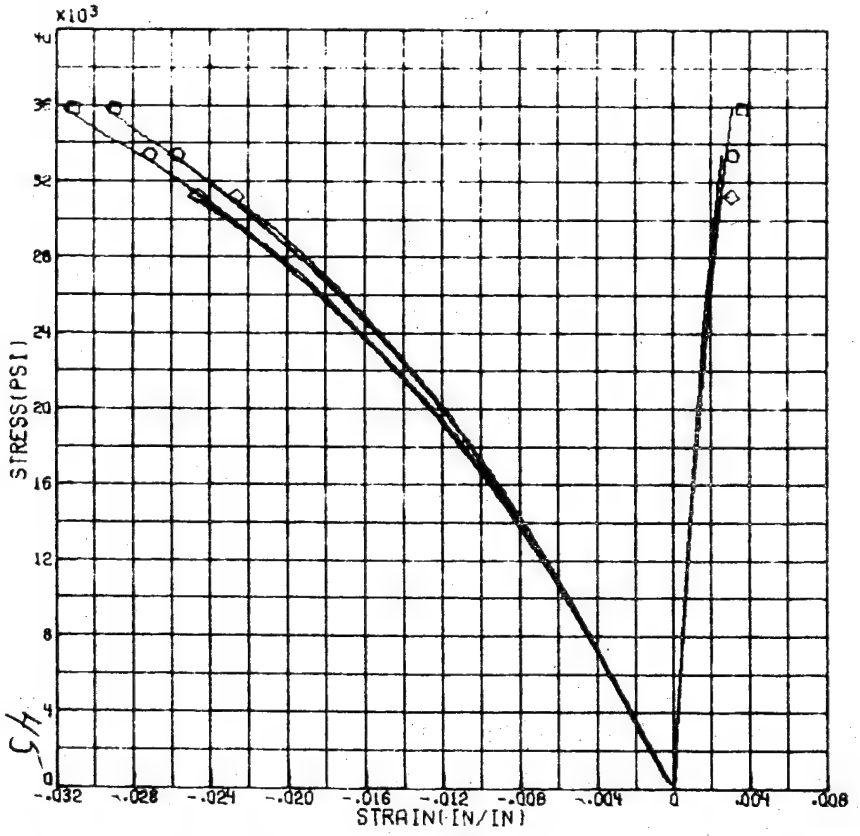

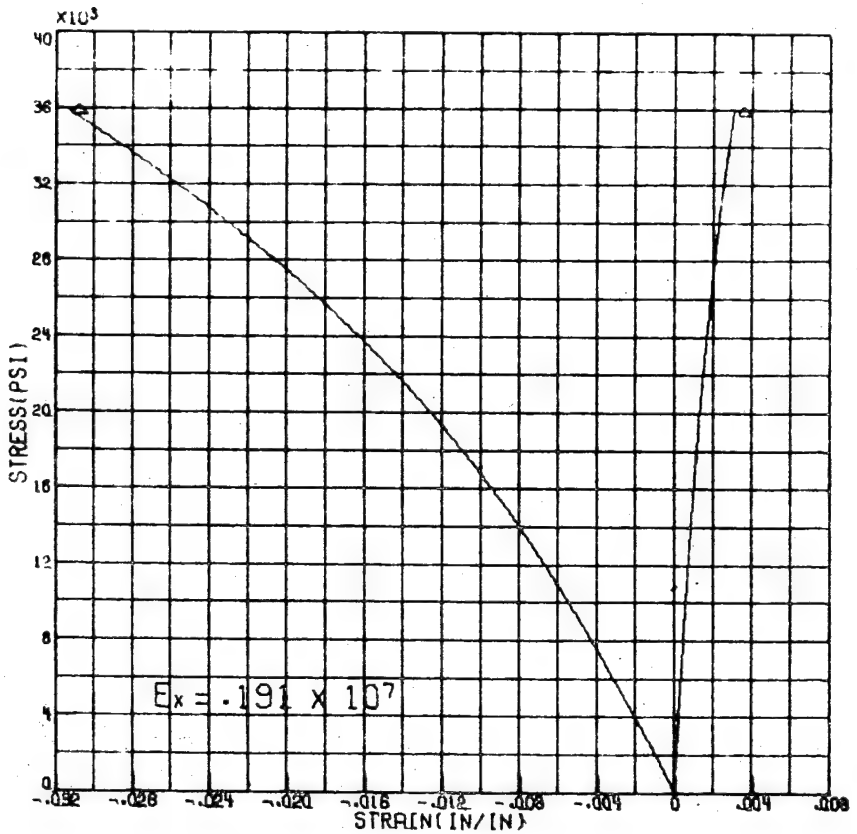

FIGURE 13A:-COMPRESSION RESPONSE OF PLANAR SPECIMENS-GR/E LAMINATE-[±75]

○ TEST 526 RUN 4 △ BEST FIT
□ TEST 526 RUN 6 A= $-.5703 \times 10^{-6}$
◇ TEST 526 RUN 7 B= $-.9751 \times 10^{-20}$
N= 4

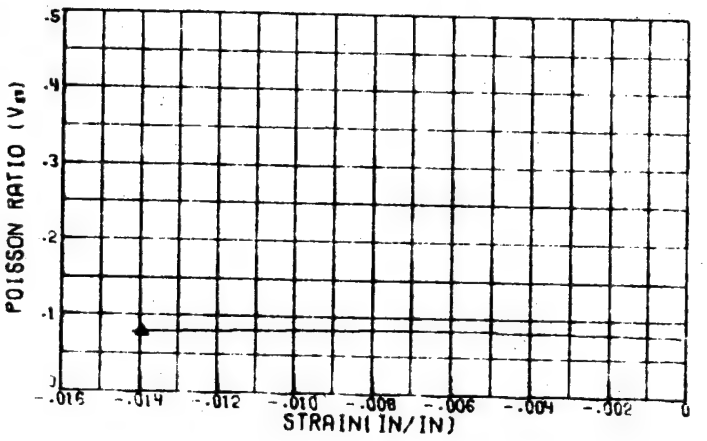

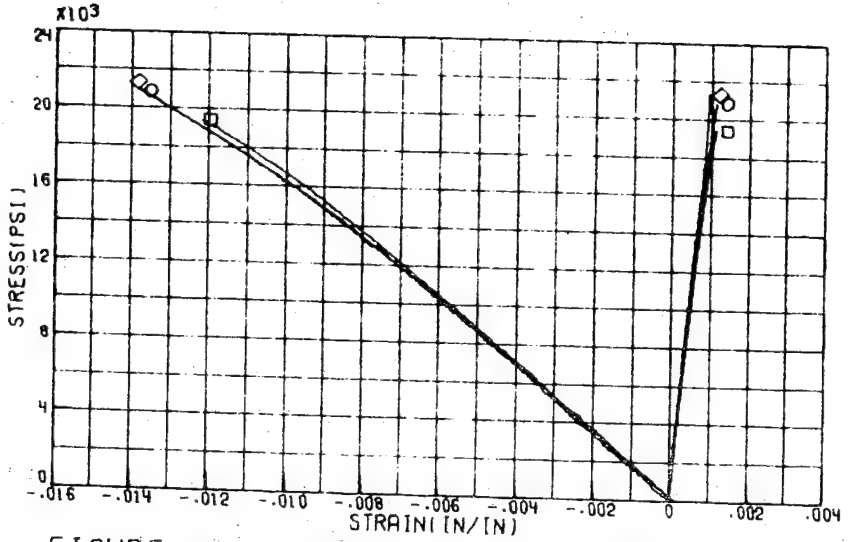

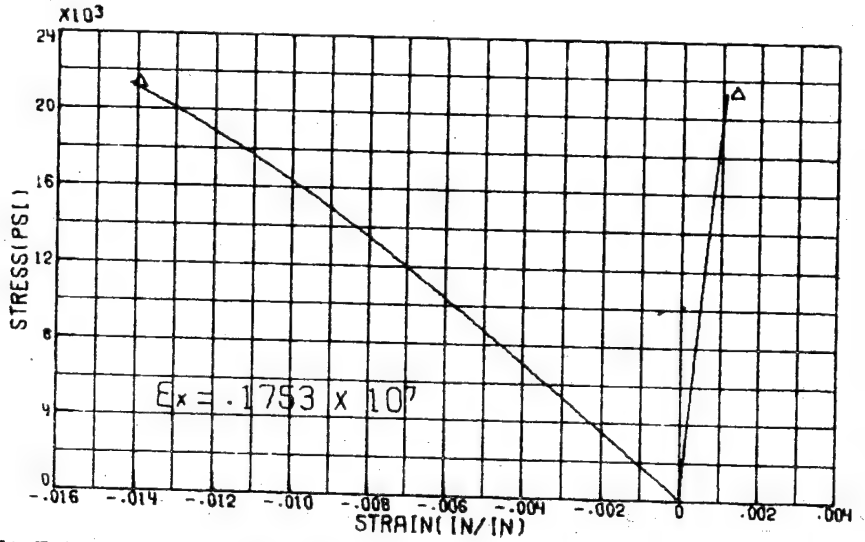

FIGURE 13B:-COMPRESSION RESPONSE OF TUBULAR SPECIMENS-GR/E LAMINATE- [±75]

○ TEST 490 RUN 29 △ BEST FIT
□ TEST 499 RUN 5 A= $-.5235 \times 10^{-6}$
◇ TEST 499 RUN 6 B= $-.1993 \times 10^{-15}$
N= 3

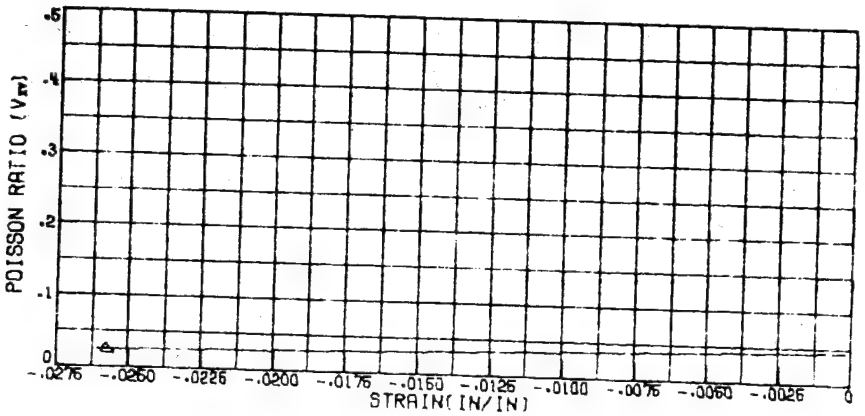

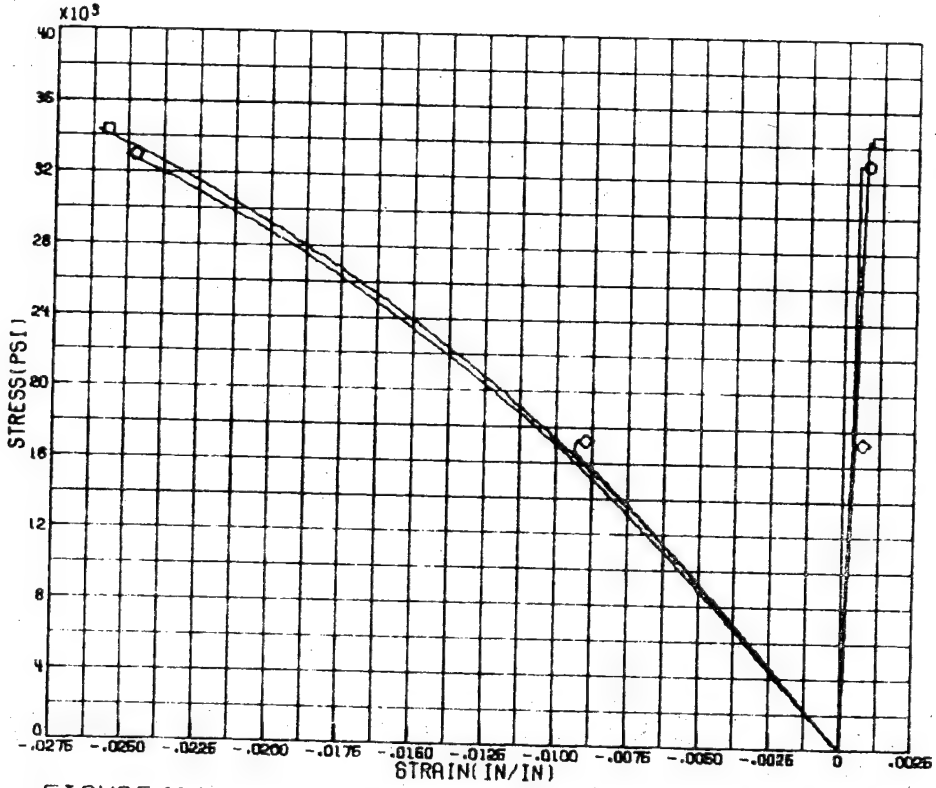

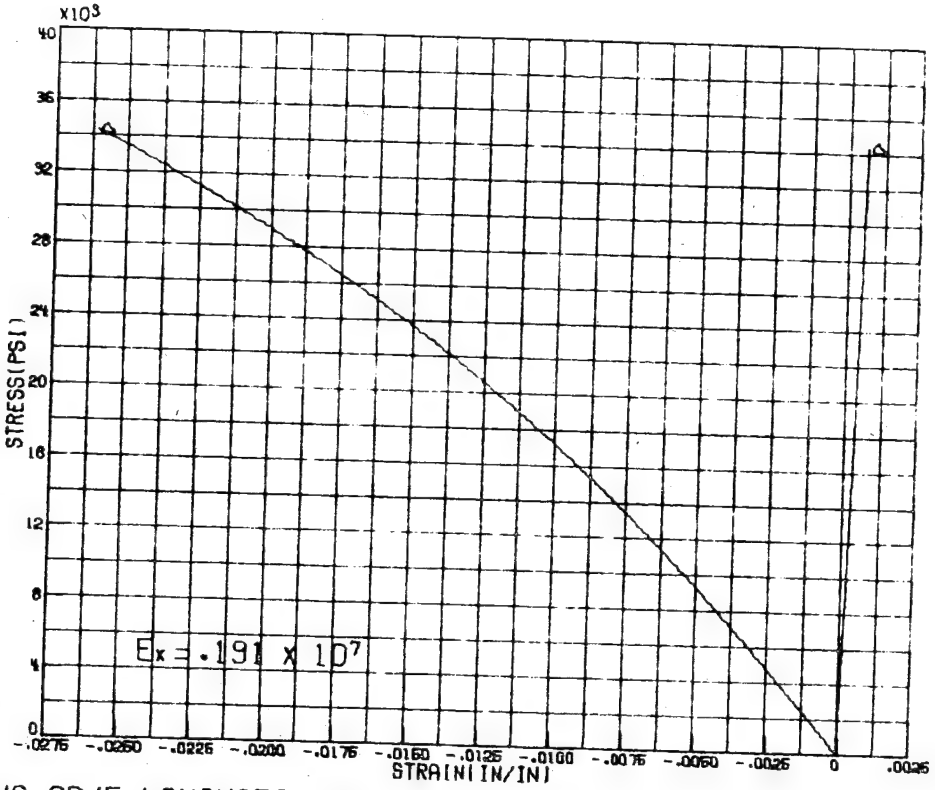

FIGURE 14A:-COMPRESSION RESPONSE OF PLANAR SPECIMENS-GR/E LAMINATE-[90]

△ BEST FIT
A= -.6579 x 10^{-6}
B= -.3776 x 10^{-24}
N= 5

○ TEST 609 RUN 2
□ TEST 609 RUN 3
◇ TEST 609 RUN 4

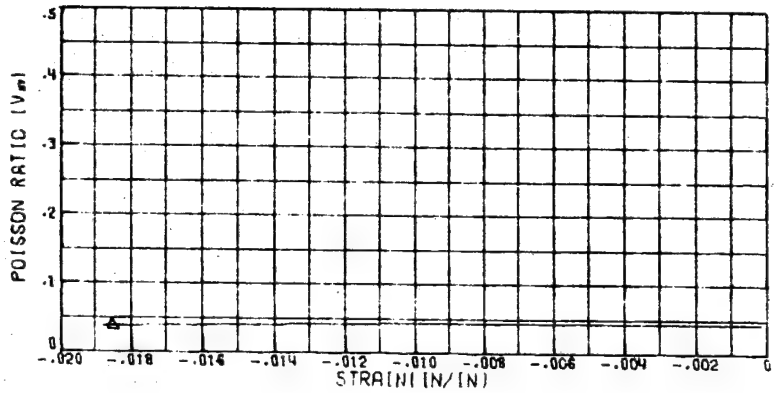

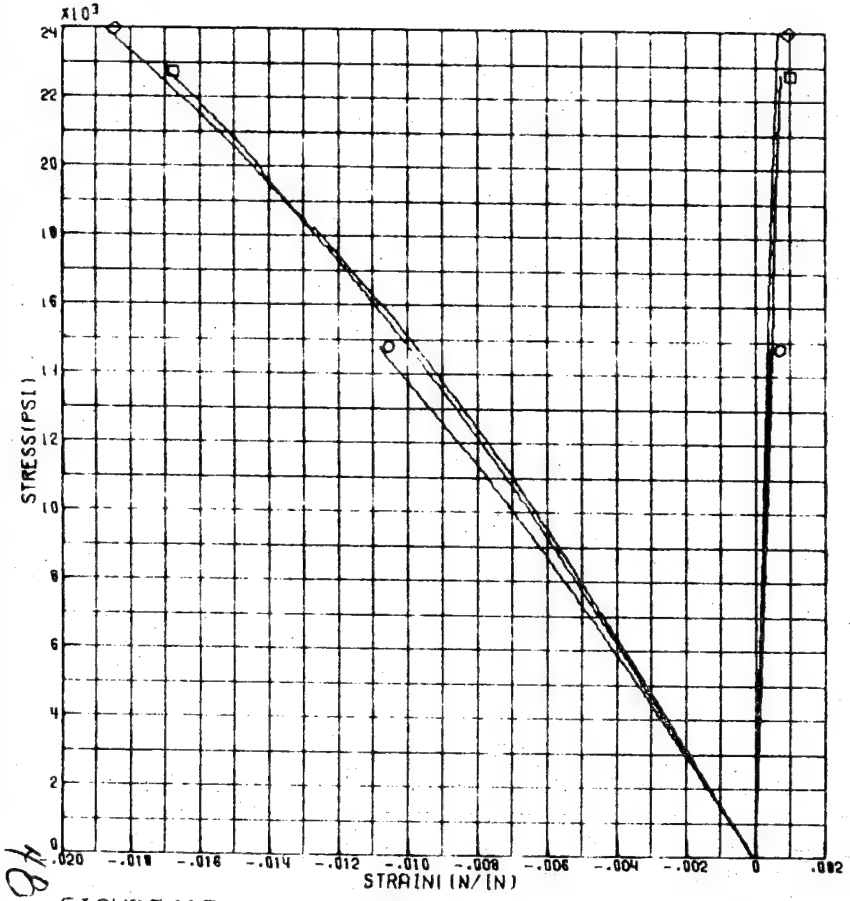

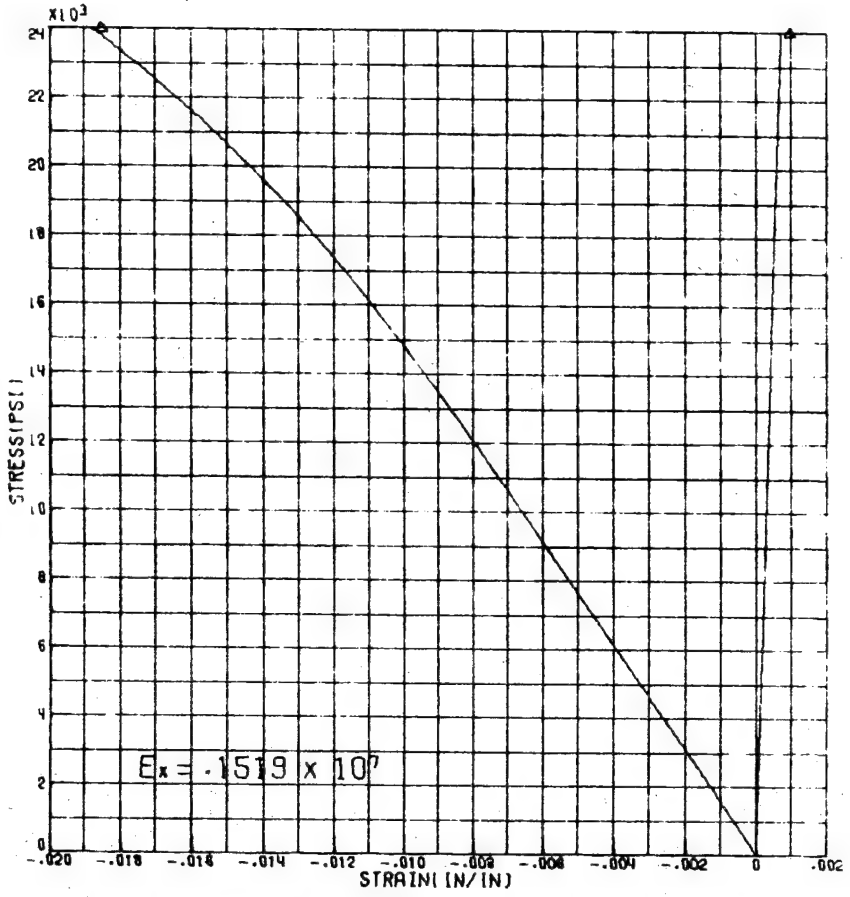

FIGURE 14B:-COMPRESSION RESPONSE OF TUBULAR SPECIMENS-GR/E LAMINATE-[90]

○ TEST 502 RUN 4 △ BEST FIT
□ TEST 502 RUN 5 A= $-.1137 \times 10^{-6}$
◇ TEST 502 RUN 6 B= $-.9631 \times 10^{-28}$
N= 5

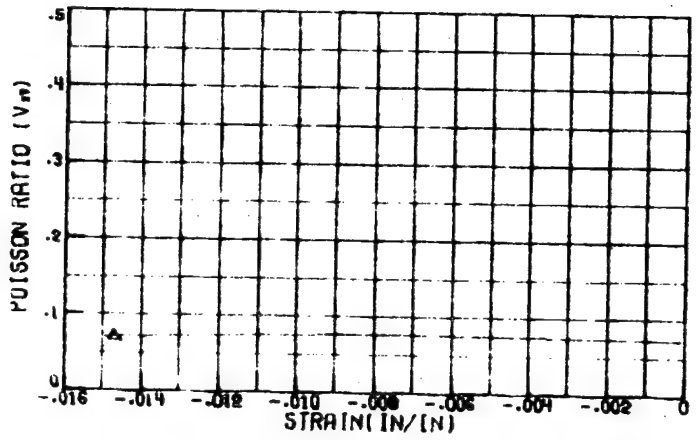

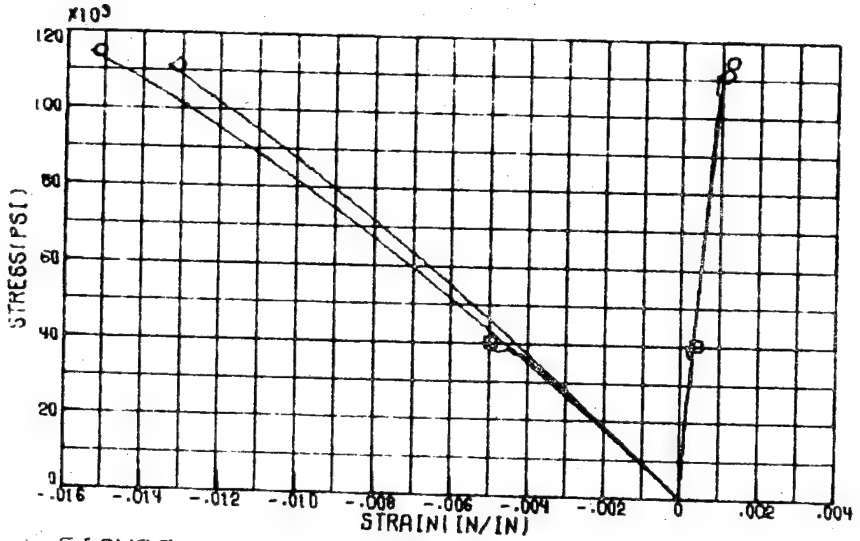

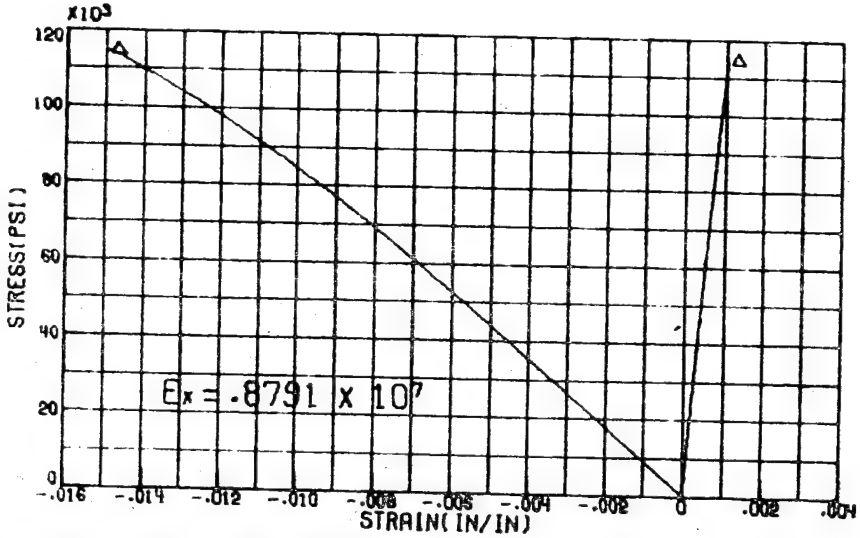

FIGURE 15A:-COMPRESSION RESPONSE OF PLANAR SPECIMENS-GR/E LAMINATE-[0/90]

64

○ TEST 620 RUN 1 △ BEST FIT
□ TEST 620 RUN 2 $A = -.1197 \times 10^{-6}$
◇ TEST 620 RUN 3 $B = .8588 \times 10^{-27}$
$N = 5$

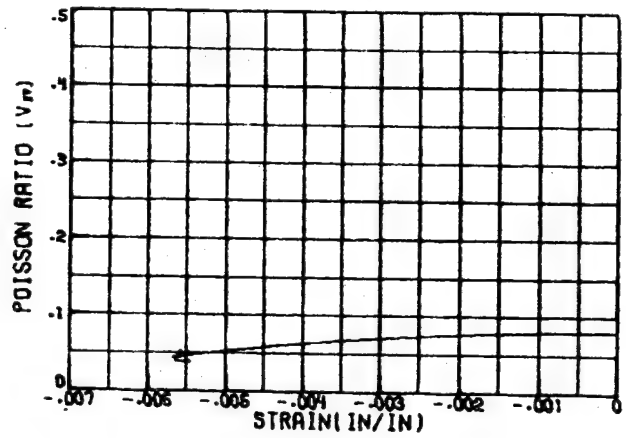

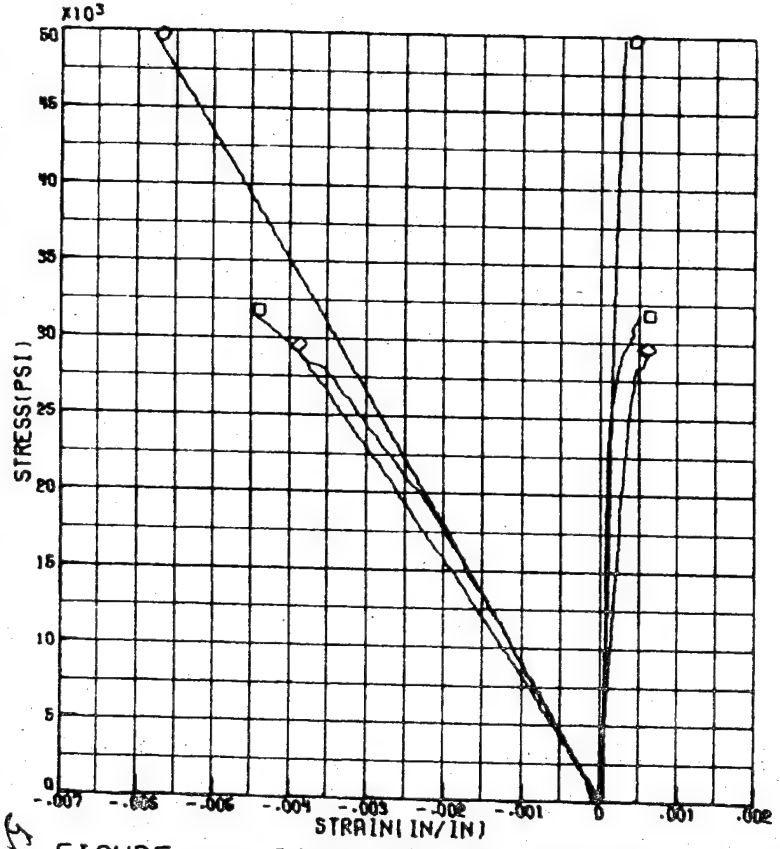

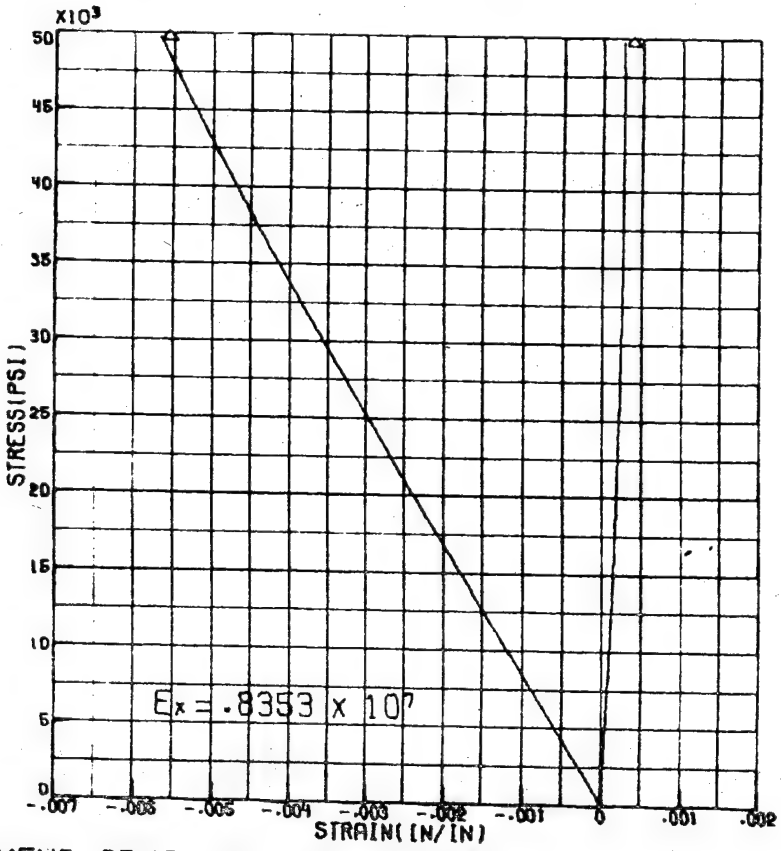

FIGURE 15B:-COMPRESSION RESPONSE OF TUBULAR SPECIMENS-GR/E LAMINATE-[0/90]

○ TEST 502 RUN 1
□ TEST 502 RUN 2
◇ TEST 502 RUN 3

△ BEST FIT
A= $-.1484 \times 10^{-6}$
B= $-.3139 \times 10^{-17}$
N= 3

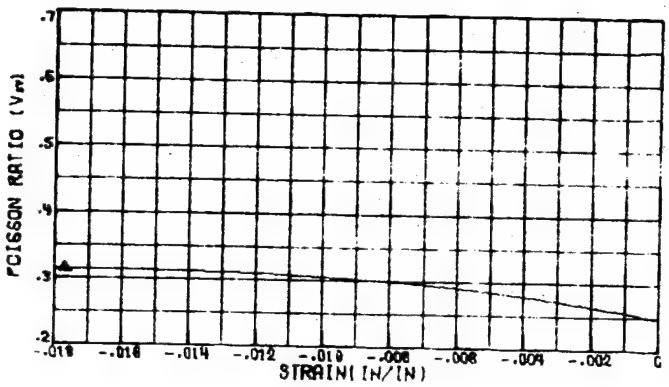

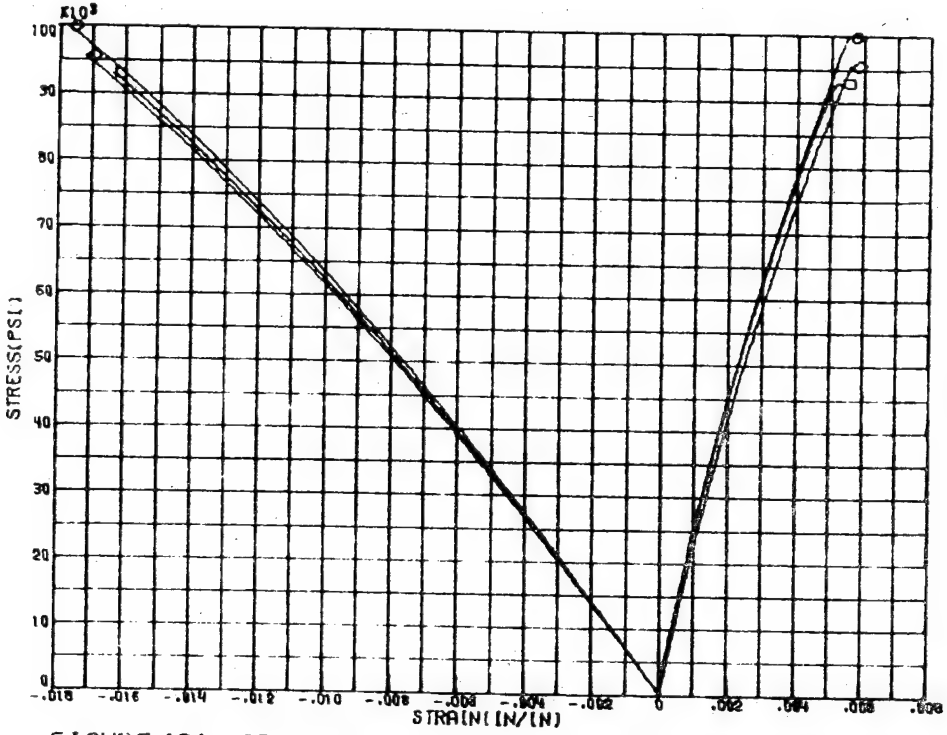

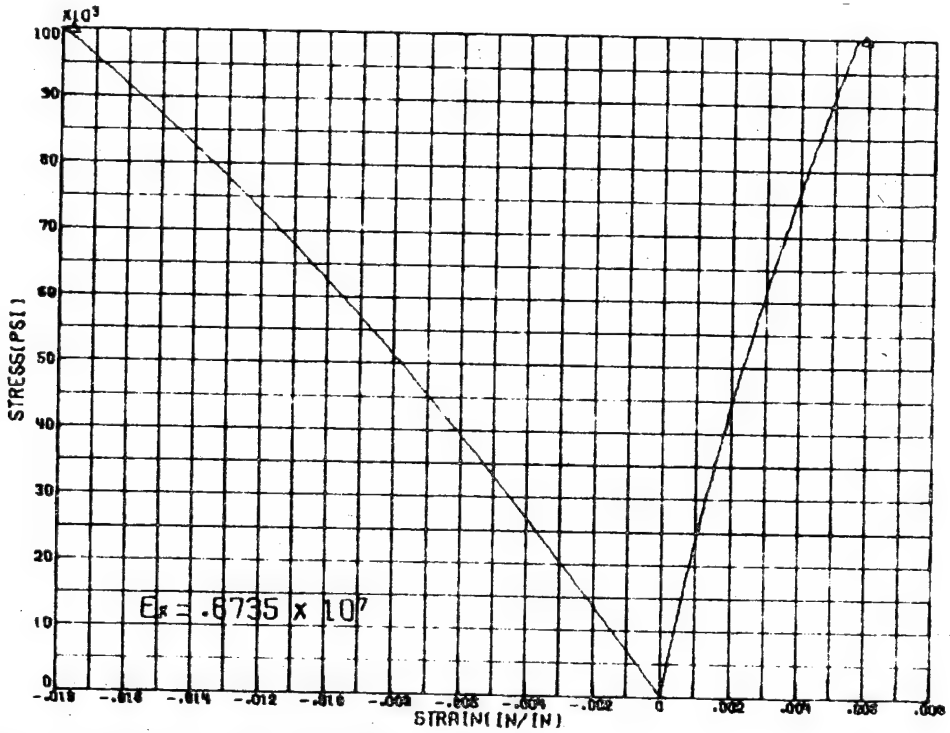

FIGURE 16A:--COMPRESSION RESPONSE OF PLANAR SPECIMENS-GR/E LAMINATE-[0/±45/90]

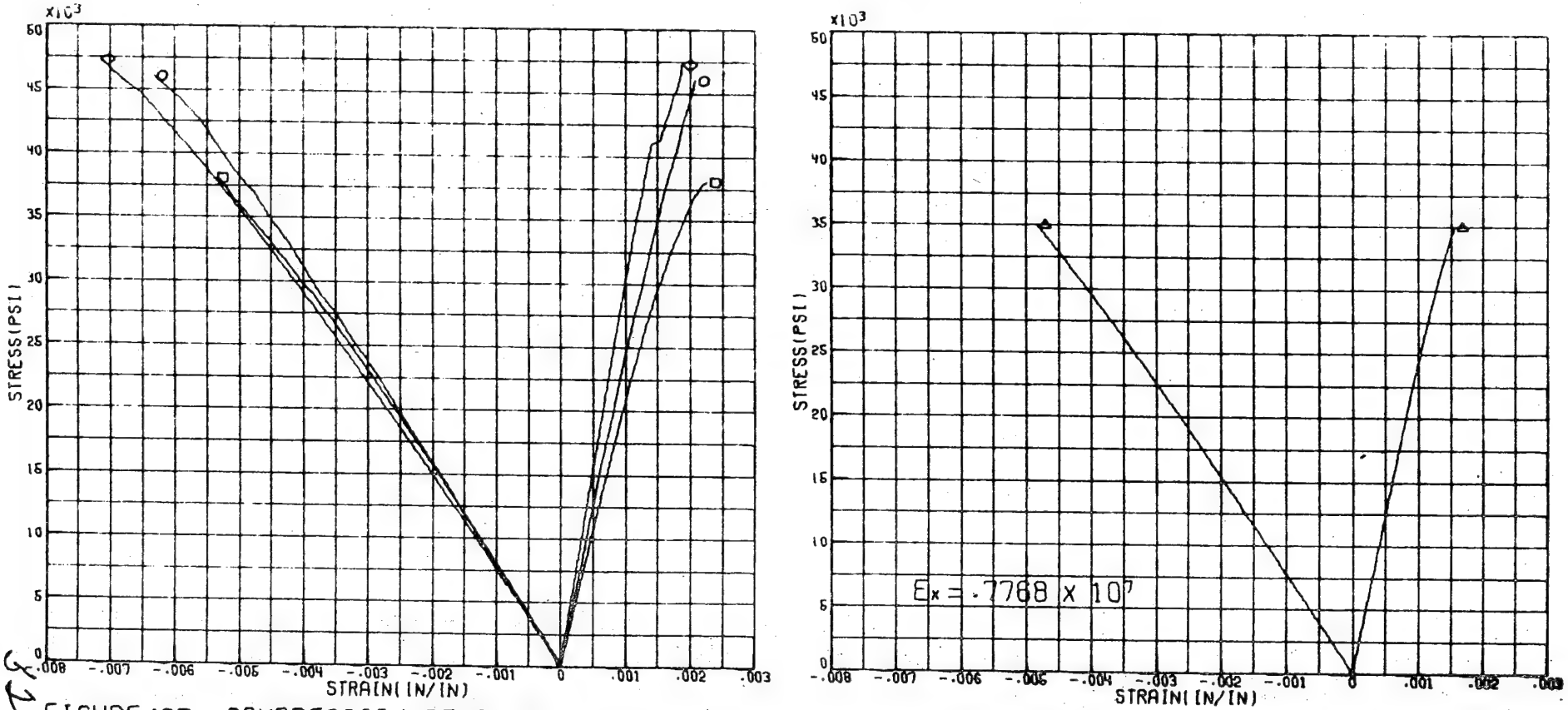

FIGURE 16B:-COMPRESSION RESPONSE OF TUBULAR SPECIMENS-GR/E LAMINATE-[0/±45/90]

◇ TEST 502 RUN 13 △ BEST FIT
□ TEST 502 RUN 14 A= $-.3197 \times 10^{-7}$
◇ TEST 502 RUN 15 B= $.2798 \times 10^{-14}$
N= 2

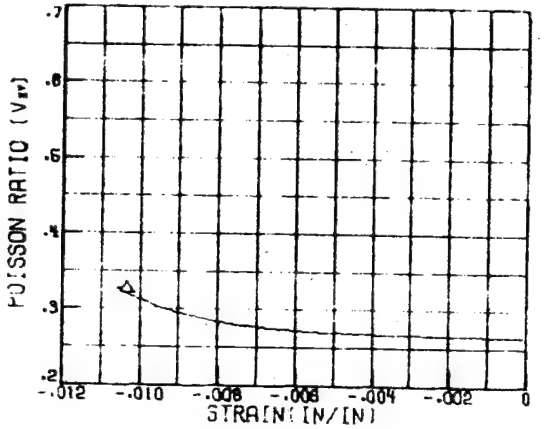

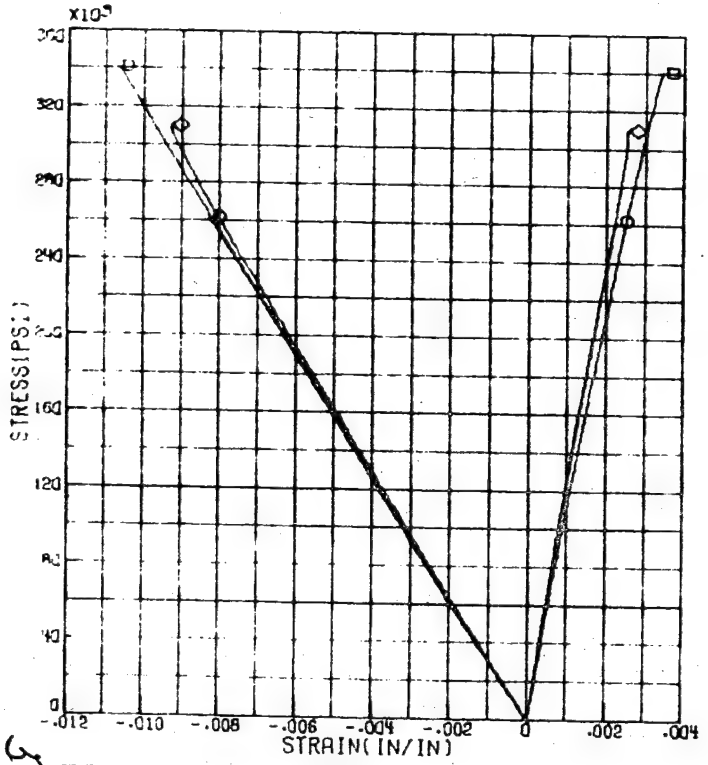

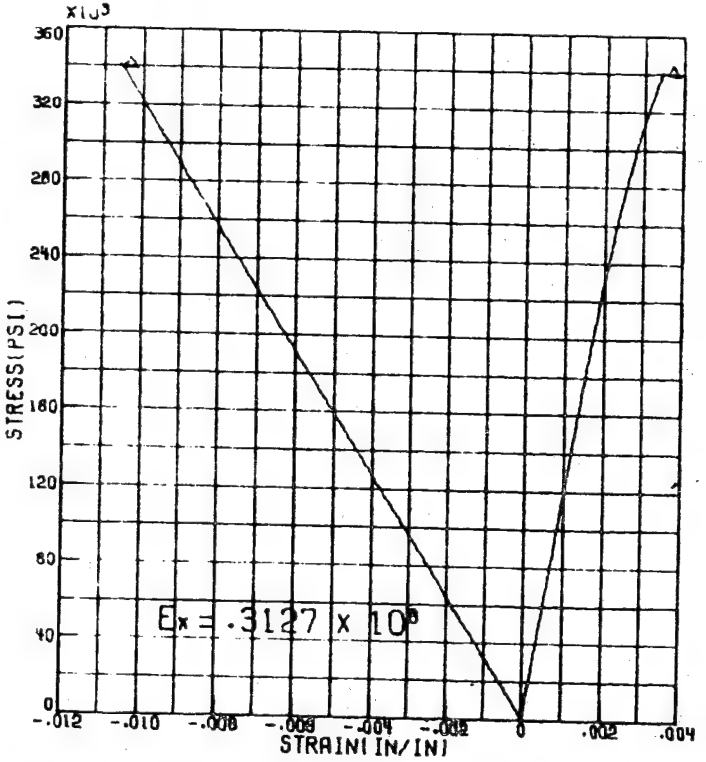

FIGURE 17A :-COMPRESSION RESPONSE OF PLANAR SPECIMENS- B/E LAMINATE- [0]

○ TEST 502 RUN 19 △ BEST FIT
□ TEST 502 RUN 20 A= $-.4264 \times 10^{-7}$
◇ TEST 502 RUN 21 B= $-.7728 \times 10^{-33}$
N= 7

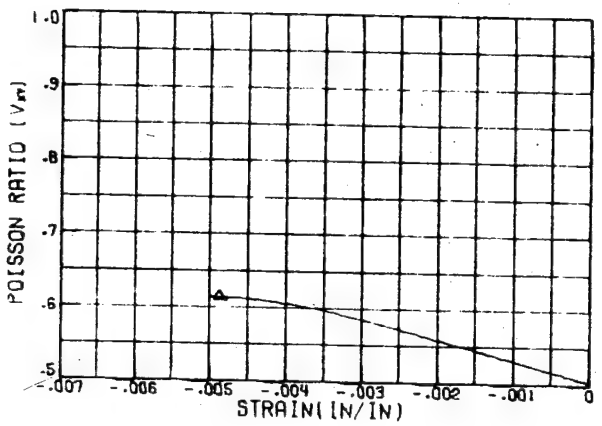

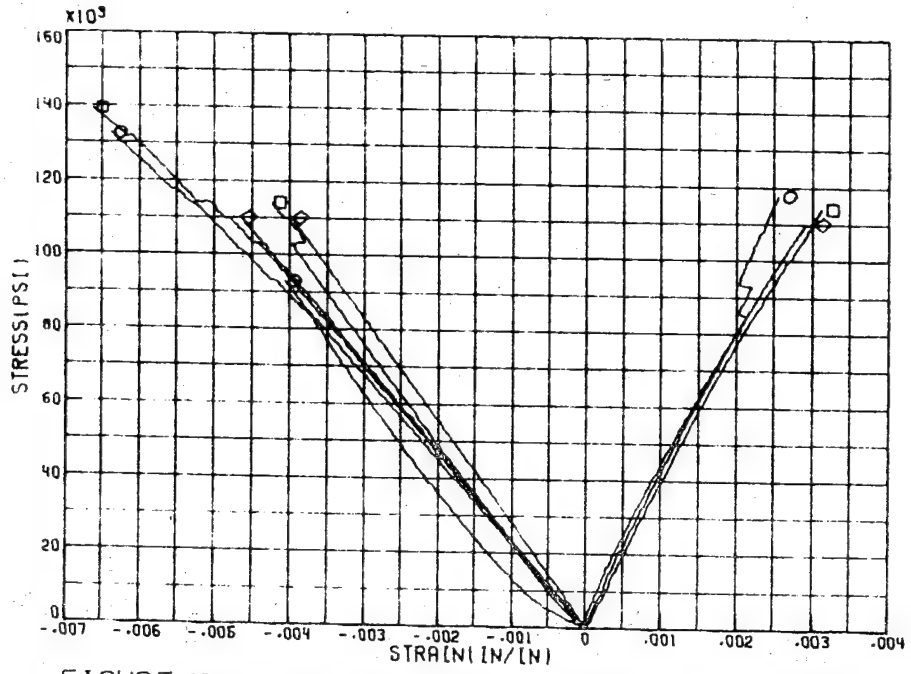

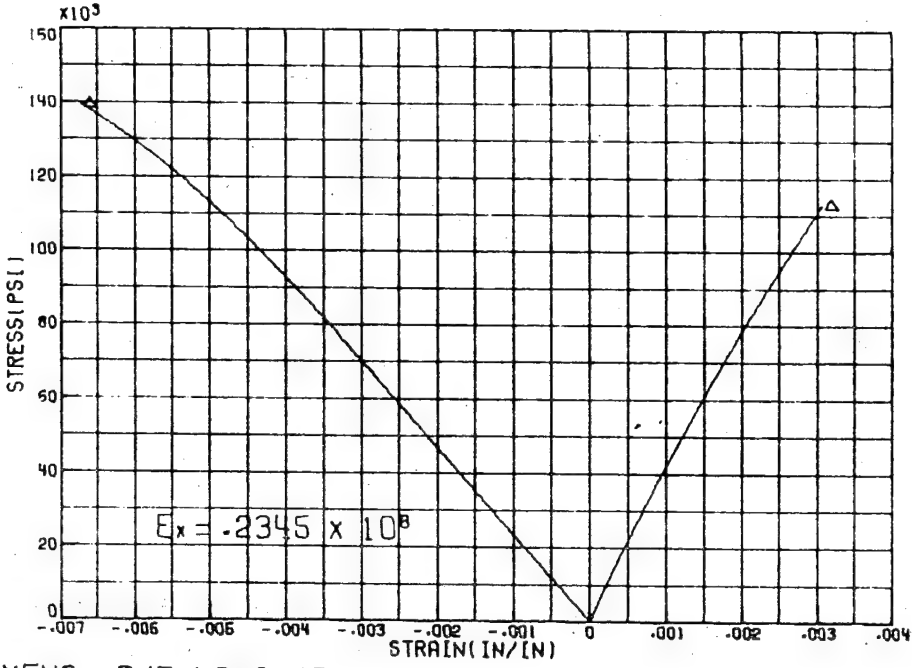

FIGURE **18A**:-COMPRESSION RESPONSE OF PLANAR SPECIMENS- B/E LAMINATE- [±15]

○ TEST 527 RUN 8 △ BEST FIT
□ TEST 527 RUN 9 A= $-.2667 \times 10^{-7}$
◇ TEST 527 RUN 10 B= $-.1165 \times 10^{-28}$
N= 5

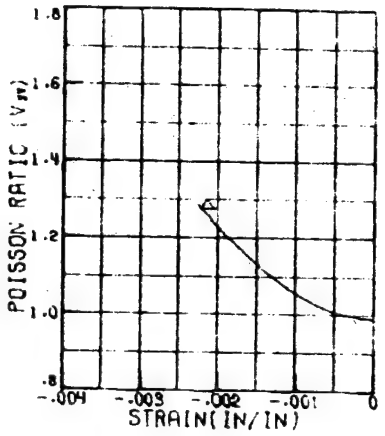

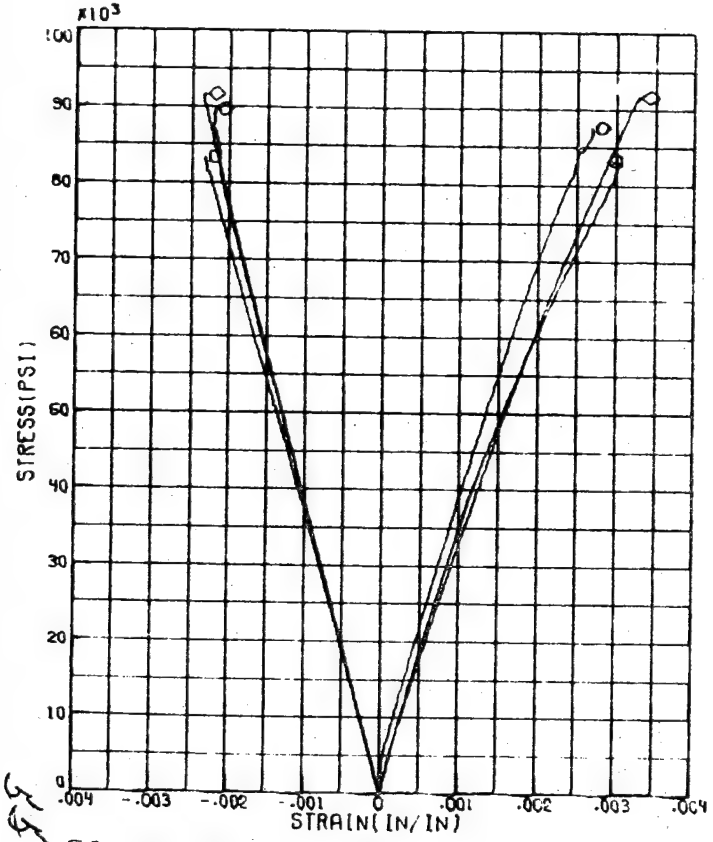

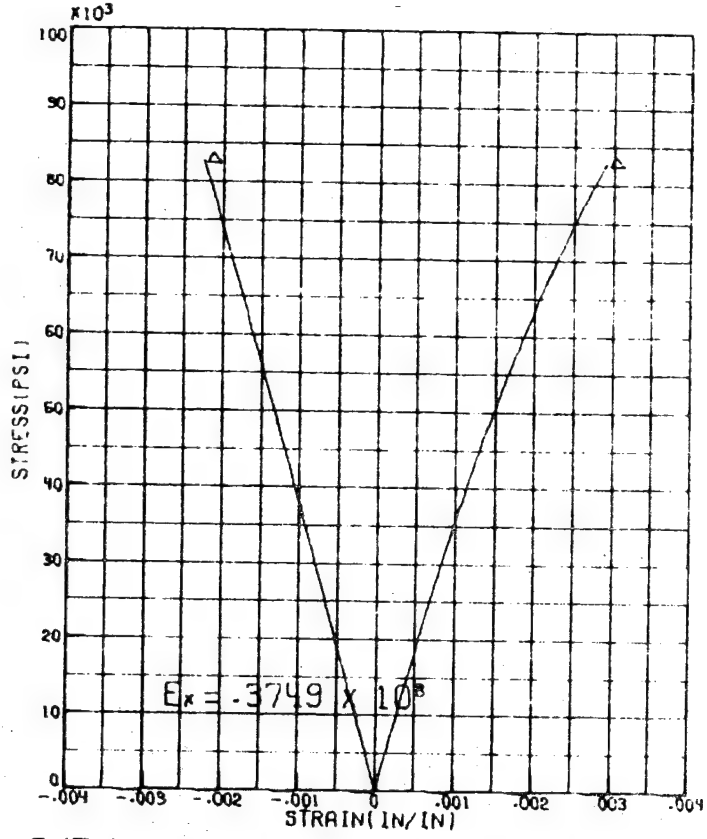

FIGURE 18B :-COMPRESSION RESPONSE OF TUBULAR SPECIMENS-B/E LAMINATE- [±15]

○ TEST 495 RUN 4 △ BEST FIT
□ TEST 495 RUN 5 A= $-.9099 \times 10^{-7}$
◇ TEST 495 RUN 6 B= $-.6914 \times 10^{-31}$
N= 6

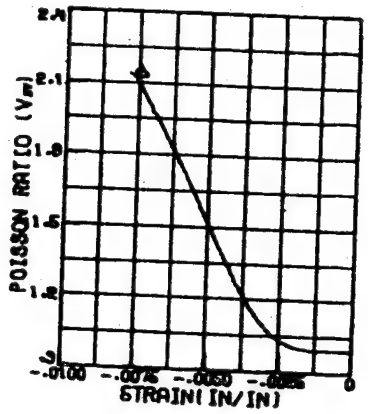

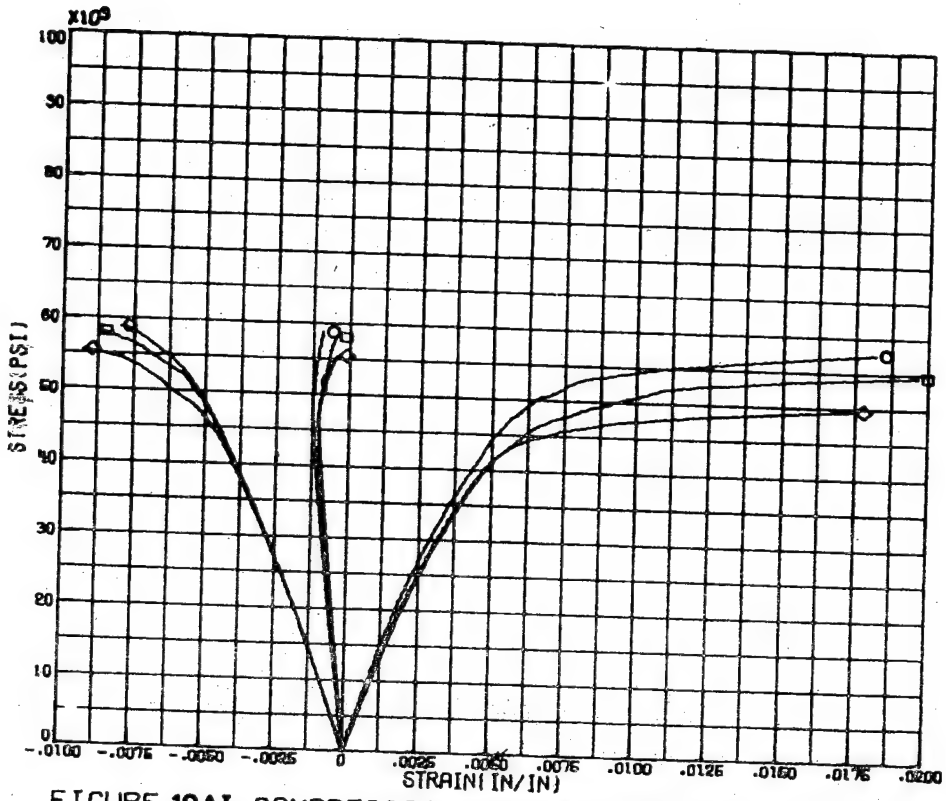

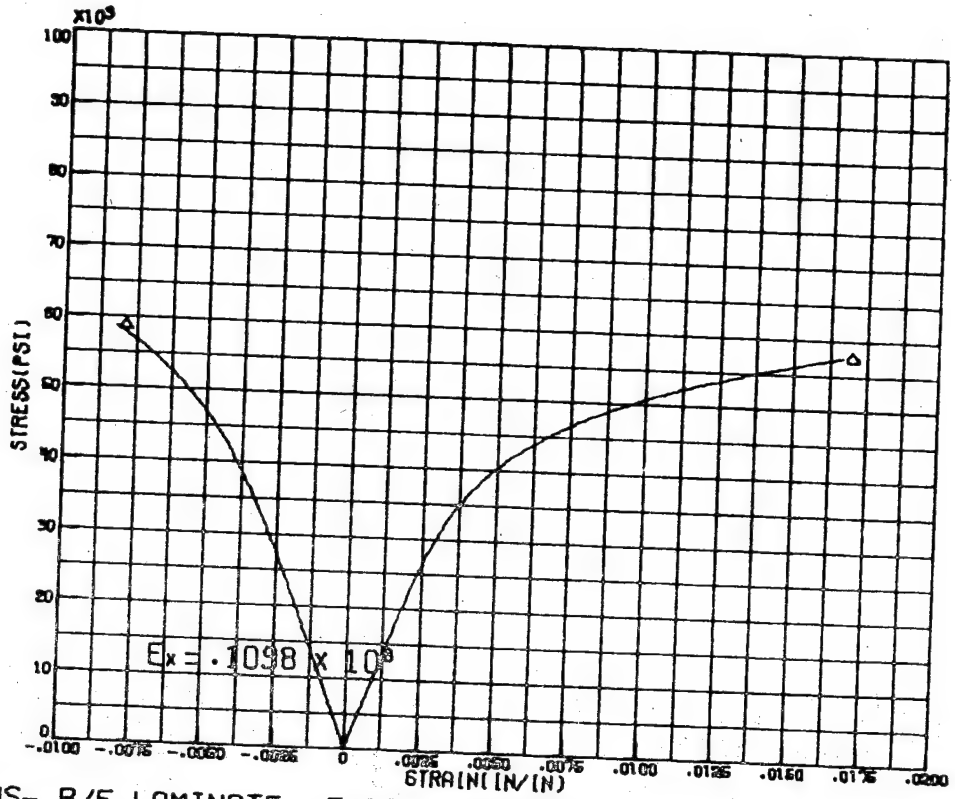

FIGURE 19AI-COMPRESSION RESPONSE OF PLANAR SPECIMENS- B/E LAMINATE- [±30] - BATCH

o TEST 502 RUN 25 △ BEST FIT

□ TEST 502 RUN 26 A= $-.7368 \times 10^{-7}$

◇ TEST 502 RUN 27 B= $-.3837 \times 10^{-22}$

N= 4

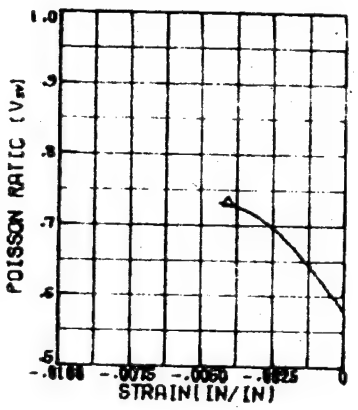

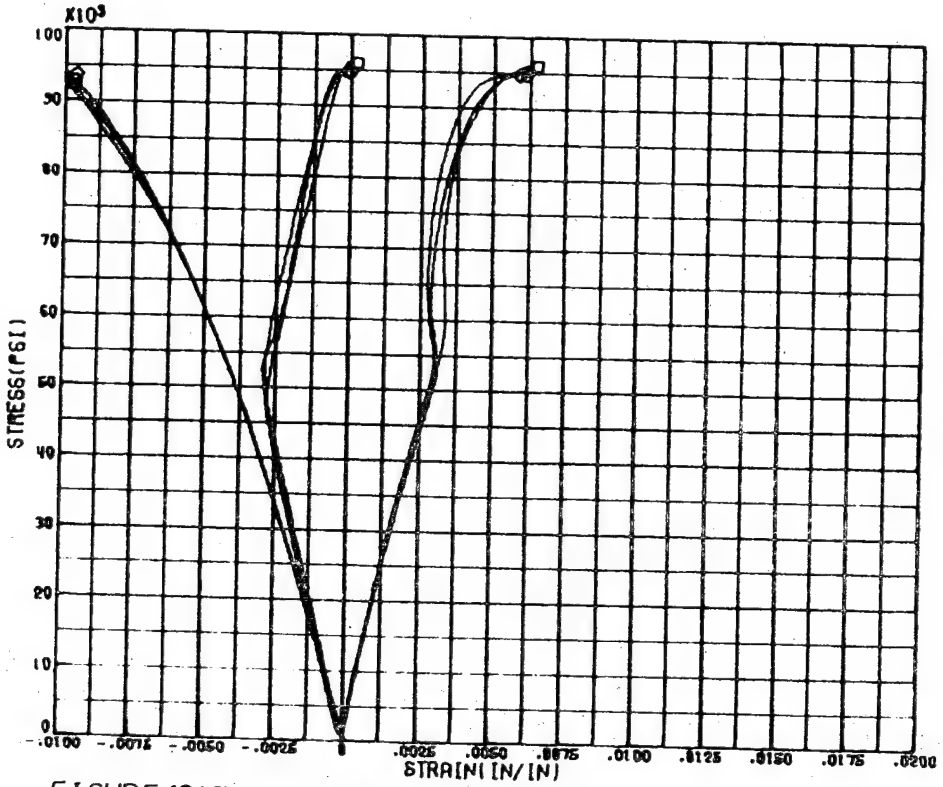

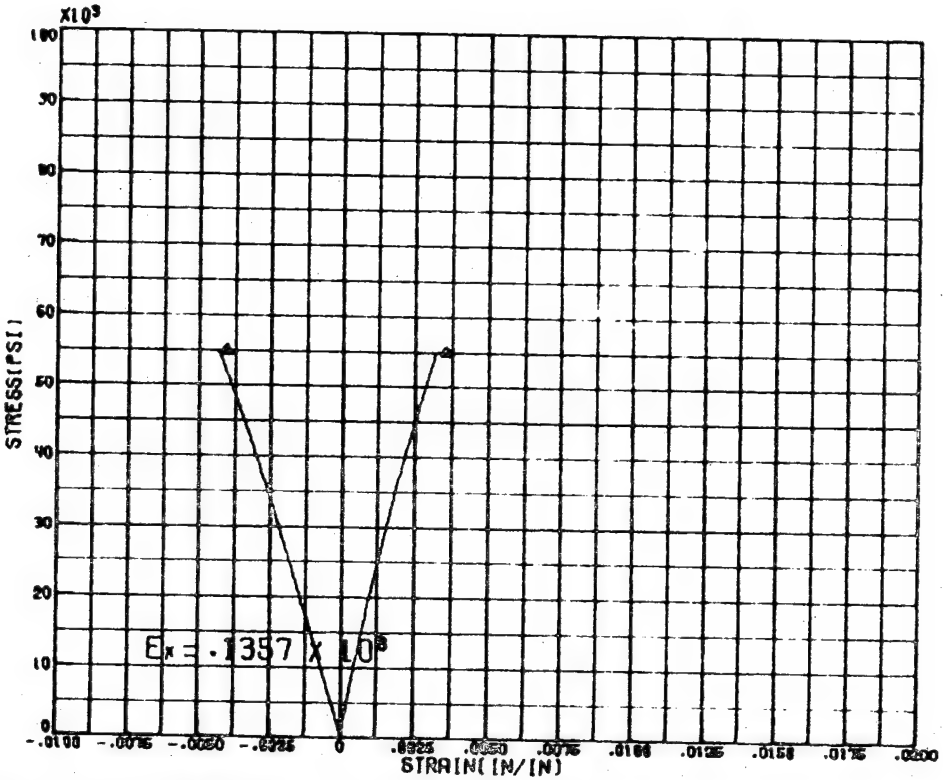

FIGURE 19AII--COMPRESSION RESPONSE OF PLANAR SPECIMENS- B/F LAMINATE- [±30] - BATCH II

○ EST 527 RUN 1 △ BEST FIT
□ TEST 527 RUN 2 A= $-.8998 \times 10^{-7}$
◇ TEST 527 RUN 3 B= $-.3911 \times 10^{-21}$
N= 4

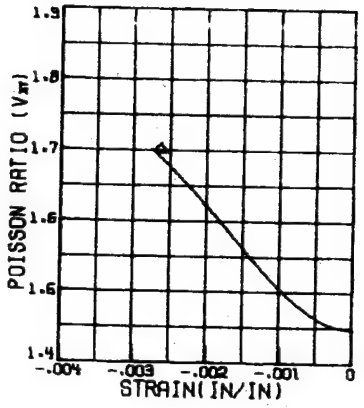

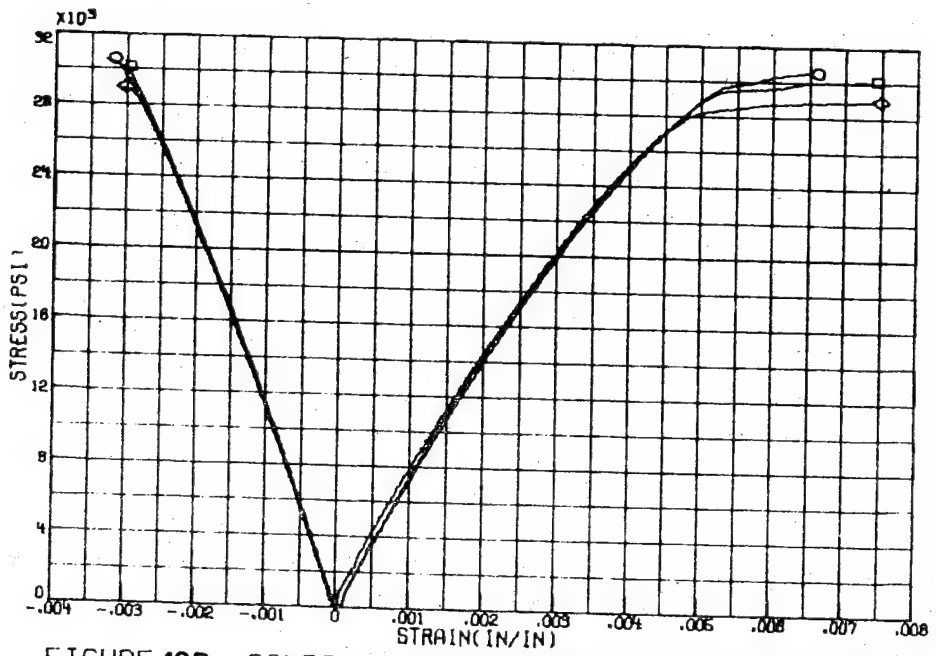

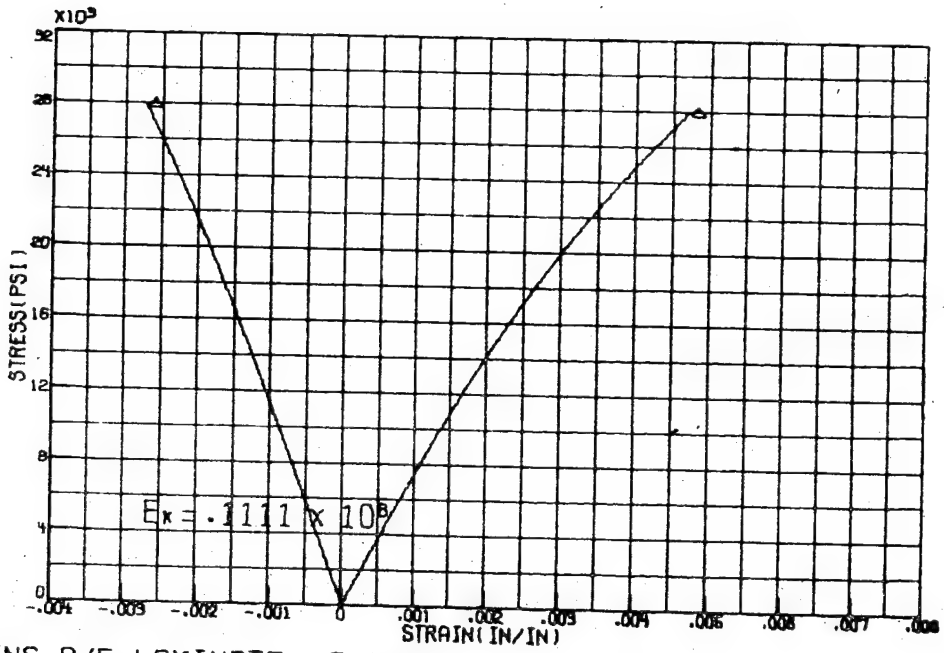

FIGURE 19B:-COMPRESSION RESPONSE OF TUBULAR SPECIMENS-B/E LAMINATE- [±30]

○ TEST 502 RUN 28 △ BEST FIT
□ TEST 502 RUN 29 A= $-.3947 \times 10^{-6}$
◇ TEST 502 RUN 30 B= $-.1632 \times 10^{-28}$
N= 6

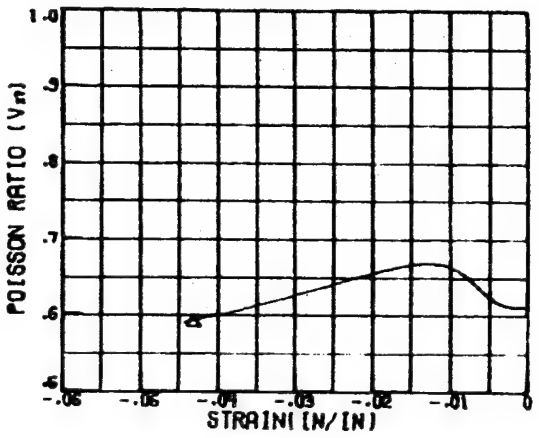

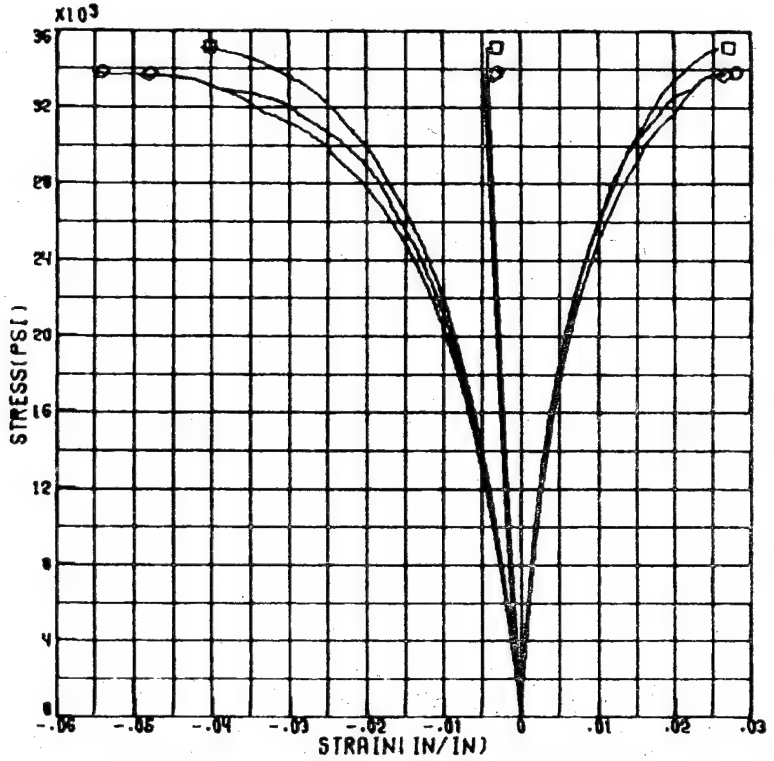

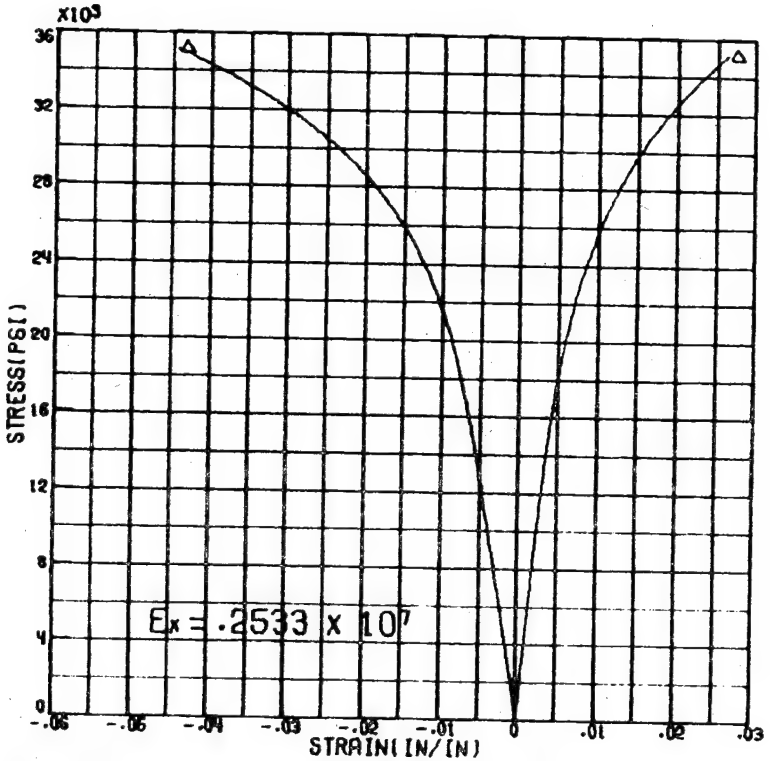

FIGURE 20A:-COMPRESSION RESPONSE OF PLANAR SPECIMENS- B/E LAMINATE- [±45]

o TEST 525 RUN 1 △ BEST FIT
□ TEST 526 RUN 1 A= $-.3093 \times 10^{-6}$
◇ TEST 526 RUN 2 B= $-.4252 \times 10^{-19}$
N= 4

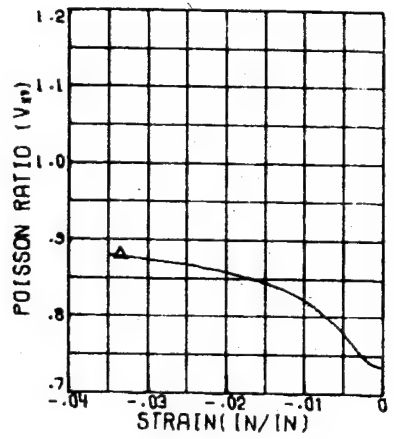

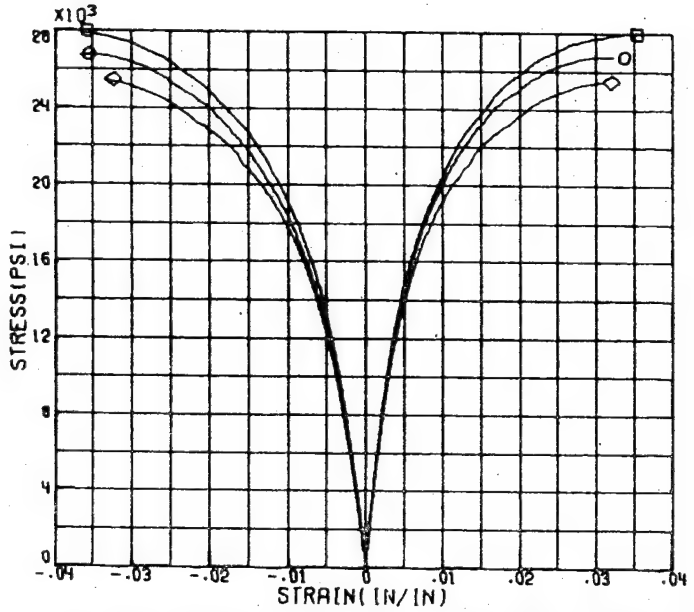

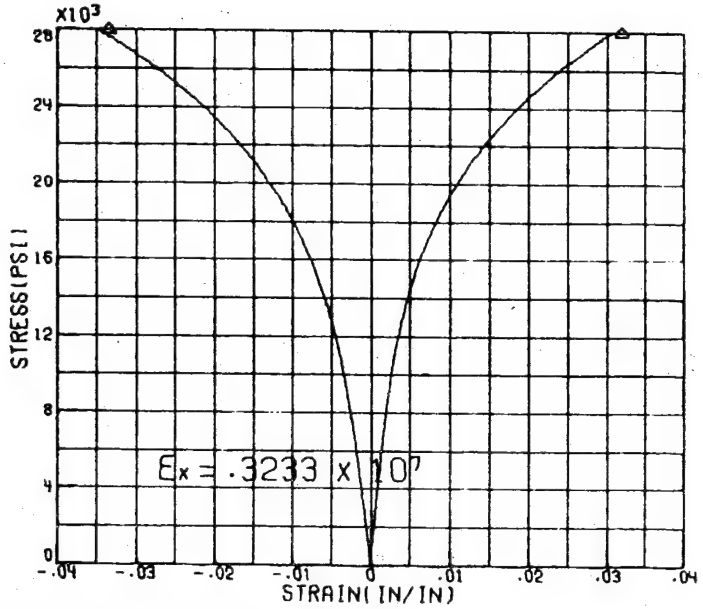

FIGURE 20B:-COMPRESSION RESPONSE OF TUBULAR SPECIMENS-B/E LAMINATE- [±45]

09

○ TEST 502 RUN 31 △ BEST FIT
□ TEST 502 RUN 32 A= $-.6173 \times 10^{-6}$
◇ TEST 502 RUN 33 B= $-.8846 \times 10^{-33}$
N= 7

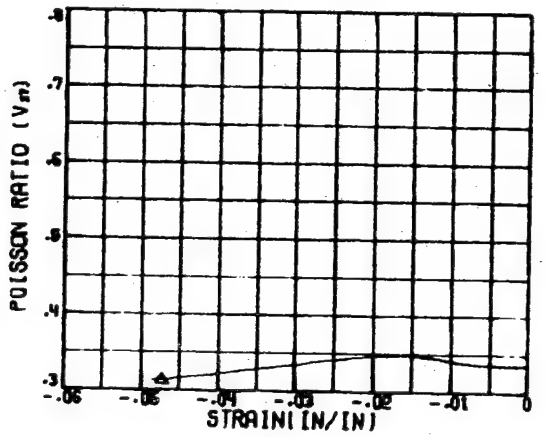

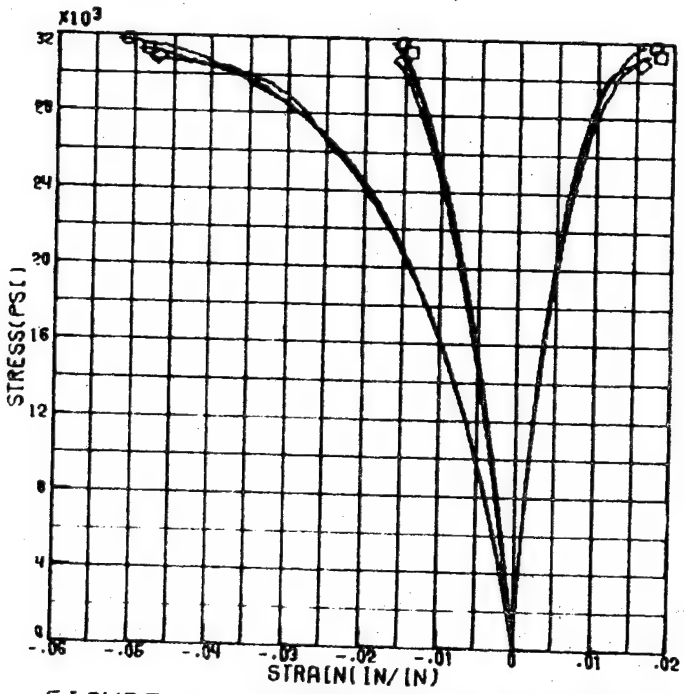

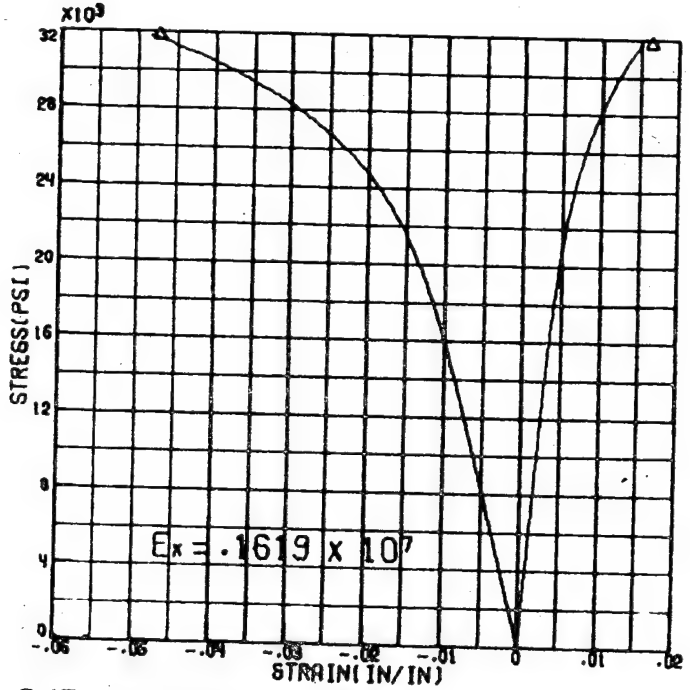

FIGURE 21A:-COMPRESSION RESPONSE OF PLANAR SPECIMENS- B/E LAMINATE- [±60]

19

○ TEST 526 RUN 3 △ BEST FIT
□ TEST 526 RUN 8 A= $-.252 \times 10^{-6}$
◇ TEST 526 RUN 9 B= $-.8126 \times 10^{-11}$
N= 2

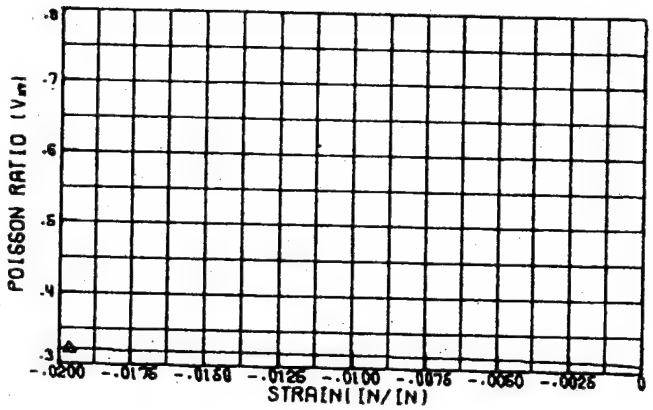

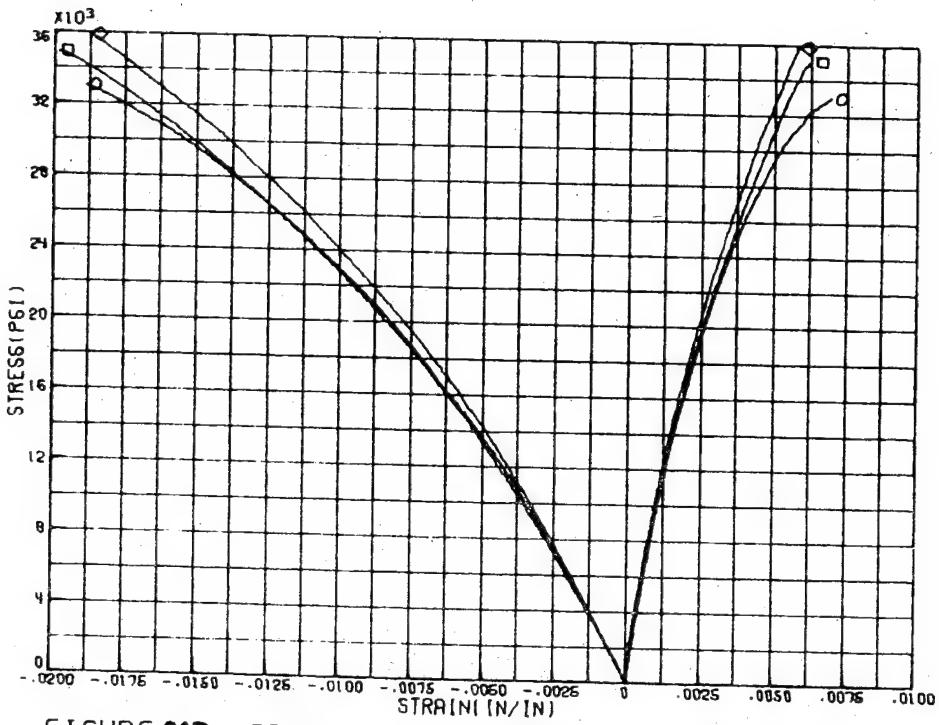

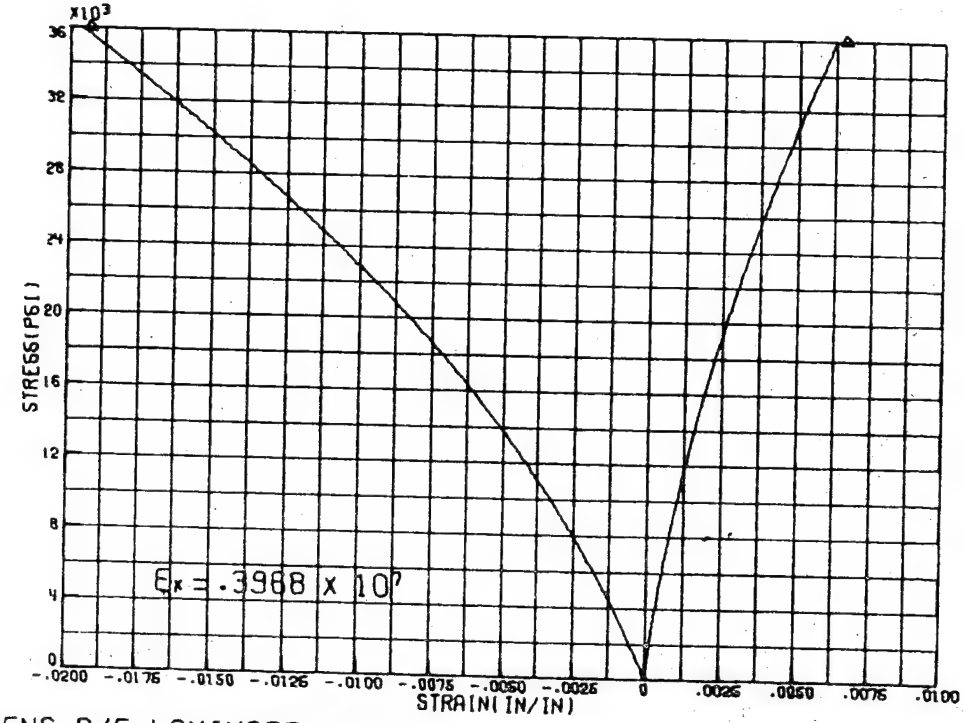

FIGURE **21B**:-COMPRESSION RESPONSE OF TUBULAR SPECIMENS-B/E LAMINATE- [±60]

○ TEST 490 RUN 21 △ BEST FIT
□ TEST 490 RUN 22 A= -.3588 x 10^{-6}
◇ TEST 490 RUN 23 B= -.5705 x 10^{-20}
N= 4

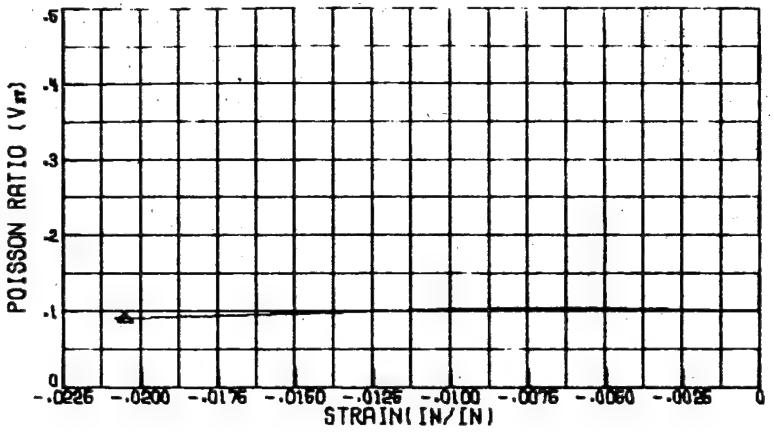

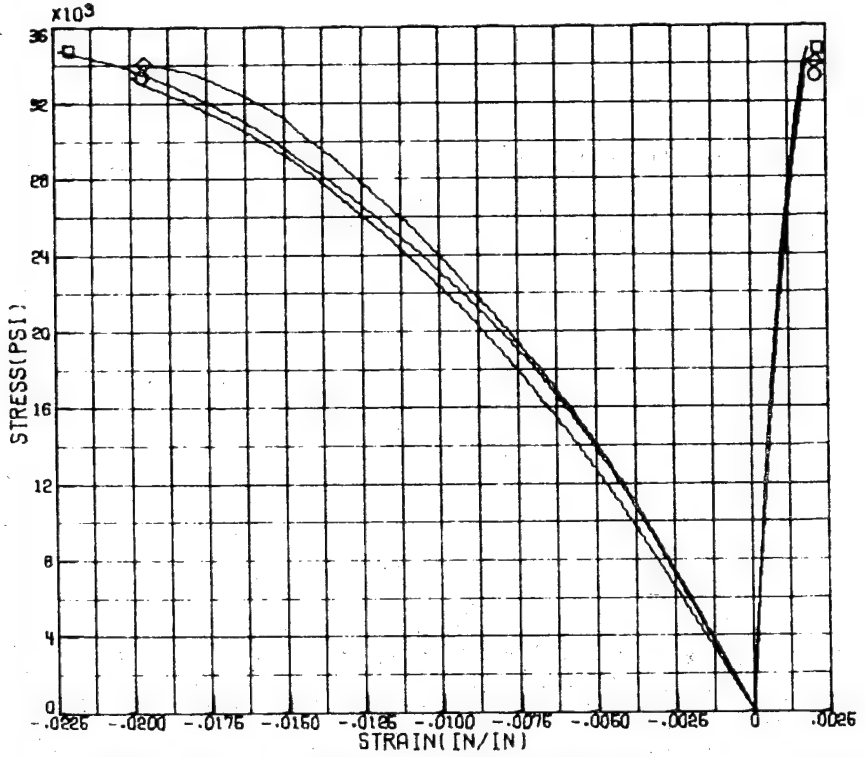

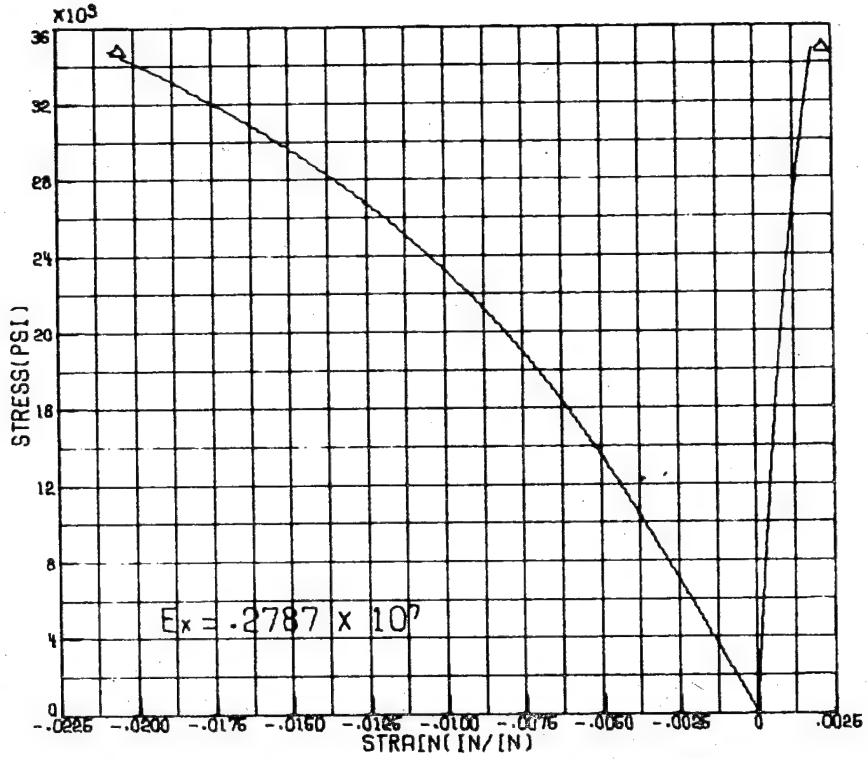

FIGURE **22A**:-COMPRESSION RESPONSE OF PLANAR SPECIMENS- B/E LAMINATE- [±75]

○ TEST 490 RUN 19 △ BEST FIT
□ TEST 490 RUN 20 A= $-.3351 \times 10^{-6}$
◇ TEST 490 RUN 24 B= $-.4316 \times 10^{-20}$
N= 4

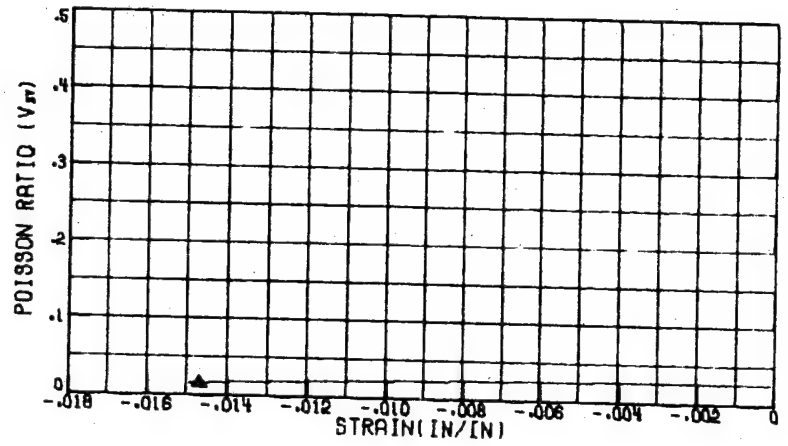

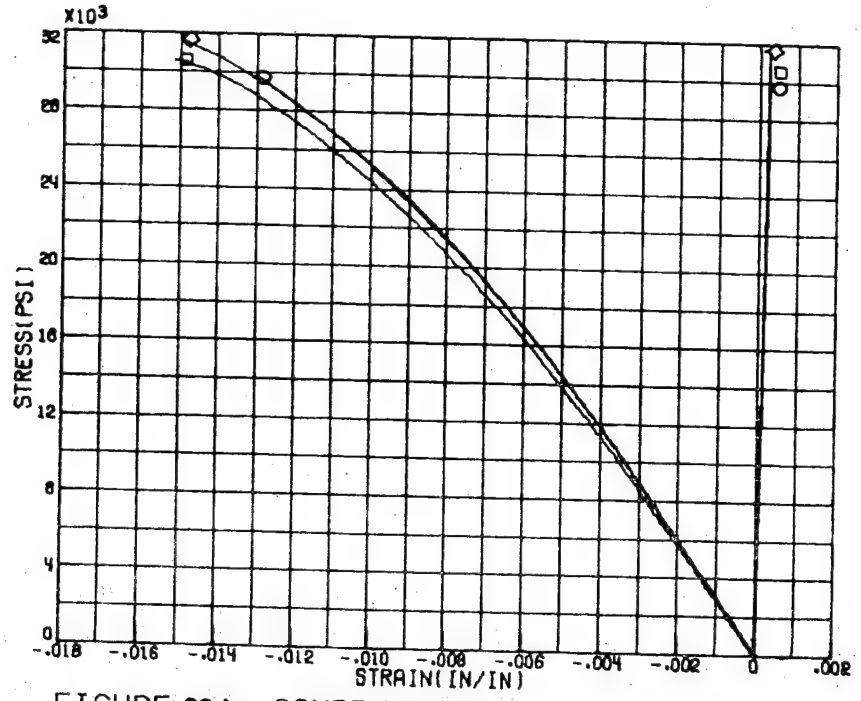

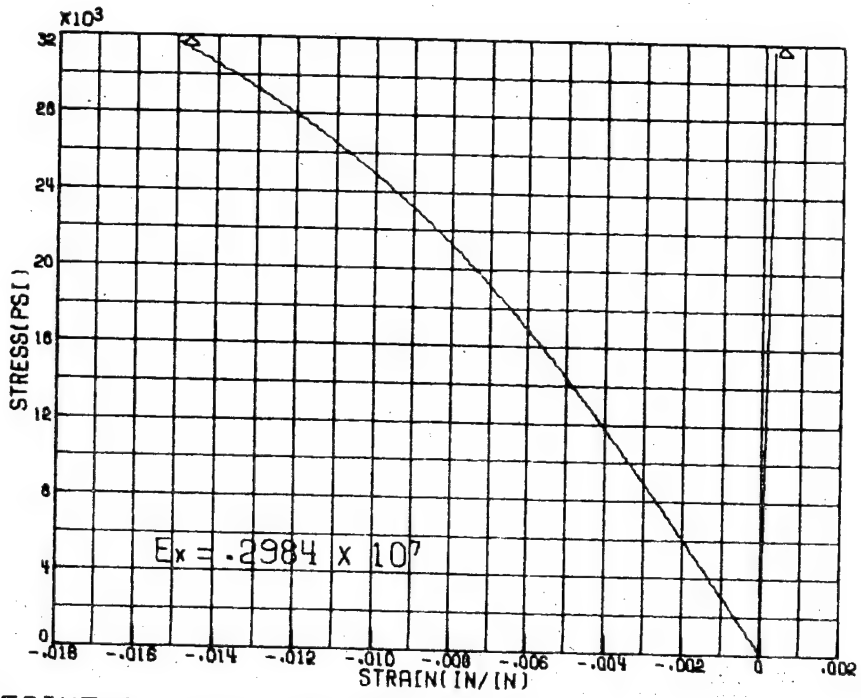

FIGURE 23A:-COMPRESSION RESPONSE OF PLANAR SPECIMENS- B/E LAMINATE- [90]

○ TEST 537 RUN 1 △ BEST FIT
□ TEST 537 RUN 2 A= $-.2947 \times 10^{-6}$
◇ TEST 537 RUN 3 B= $-.4079 \times 10^{-24}$
N= 5

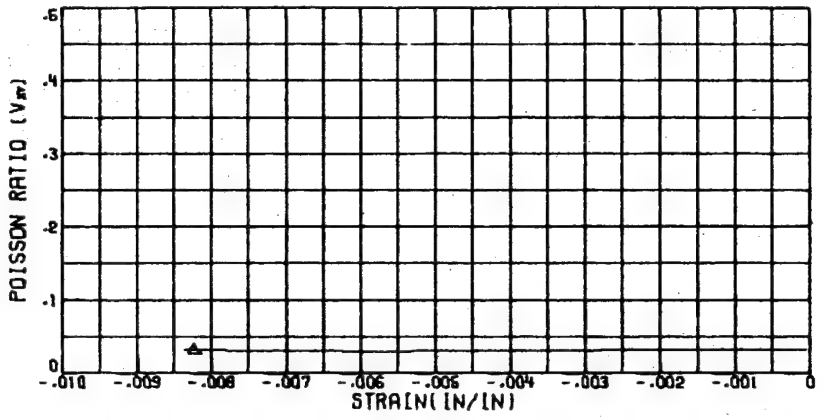

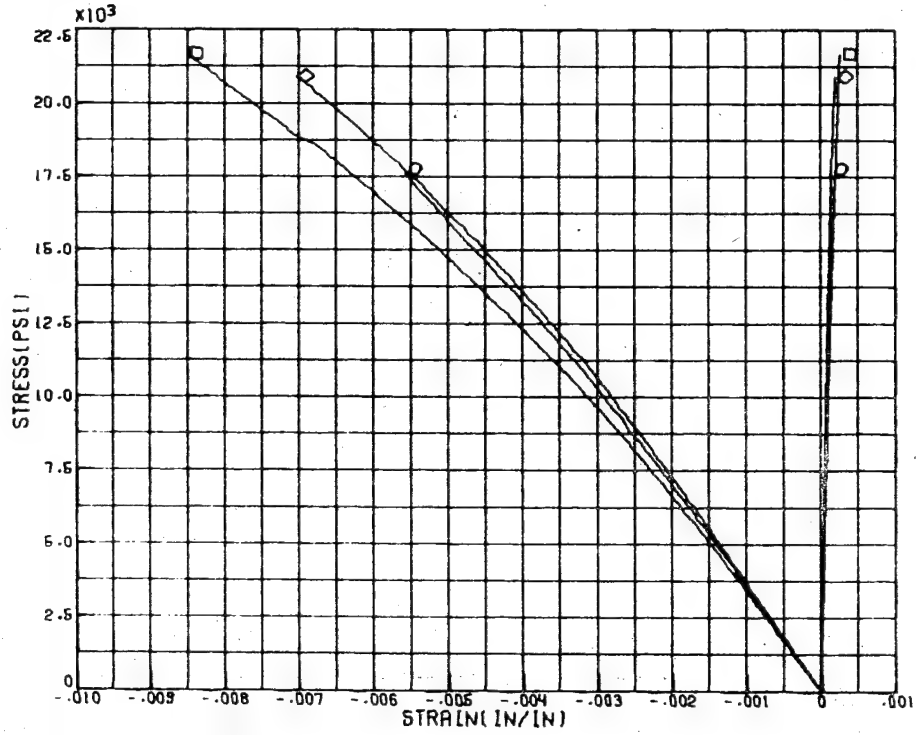

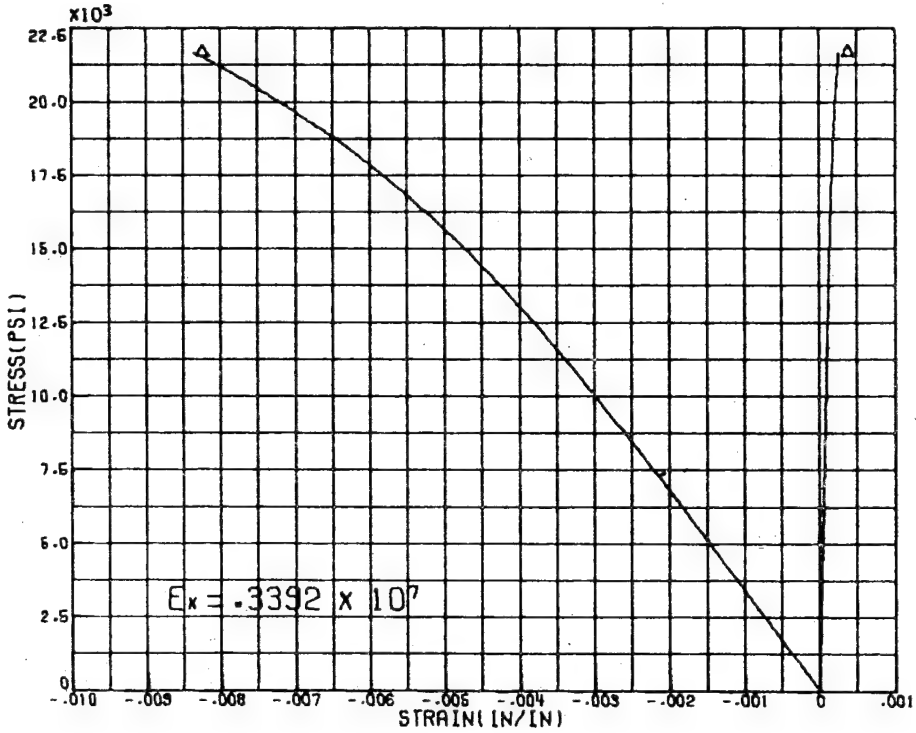

FIGURE **23B**:-COMPRESSION RESPONSE OF TUBULAR SPECIMENS-B/E LAMINATE- [90]

o TEST 502 RUN 16 △ BEST FIT
□ TEST 502 RUN 17 A= $-.5821 \times 10^{-7}$
◇ TEST 502 RUN 18 B= $-.1246 \times 10^{-110}$
N= 20

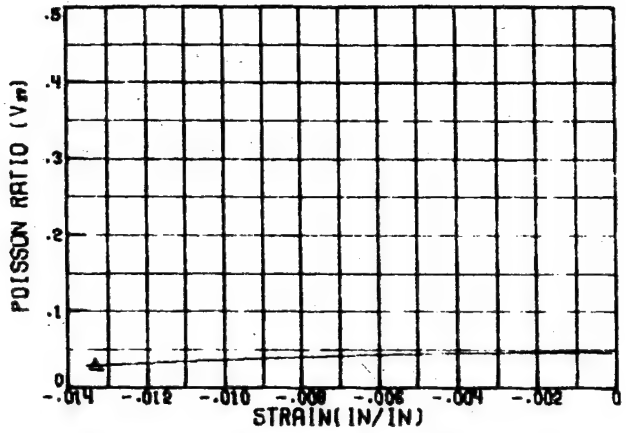

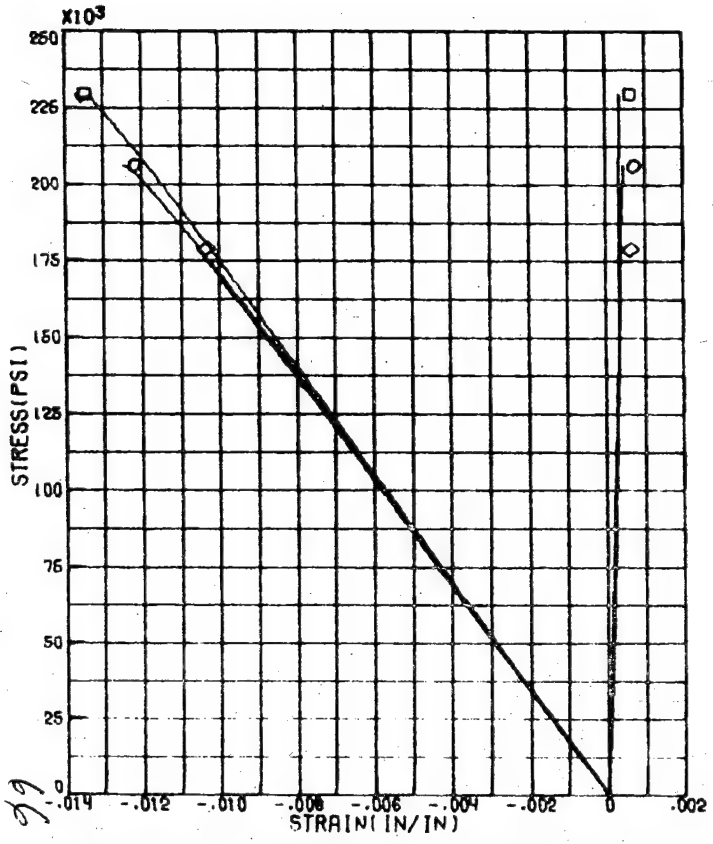

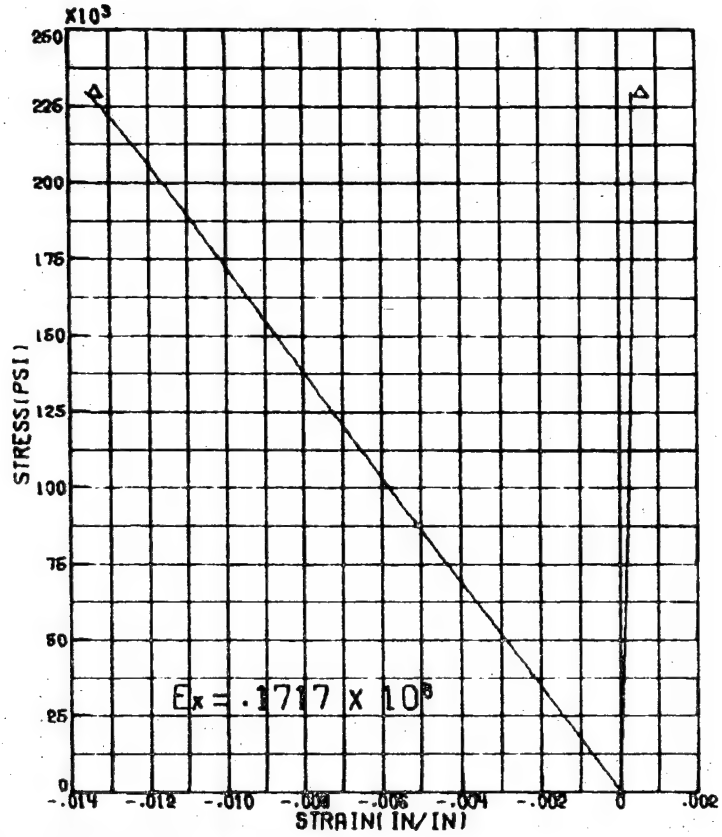

FIGURE 24A;-COMPRESSION RESPONSE OF PLANAR SPECIMENS- B/E LAMINATE- [0/90]

o TEST 609 RUN 11 △ BEST FIT
□ TEST 609 RUN 12 A= -.3945 x 10^{-7}
◇ TEST 609 RUN 14 B= -.8021 x 10^{-89}
△ TEST 609 RUN 15 N= 16

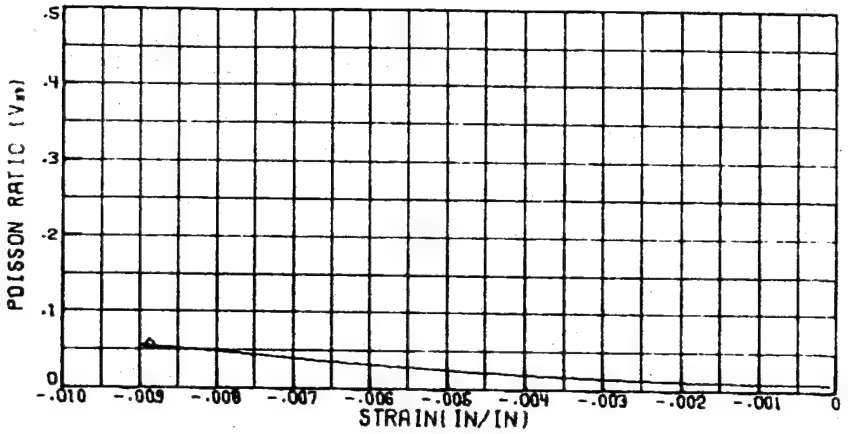

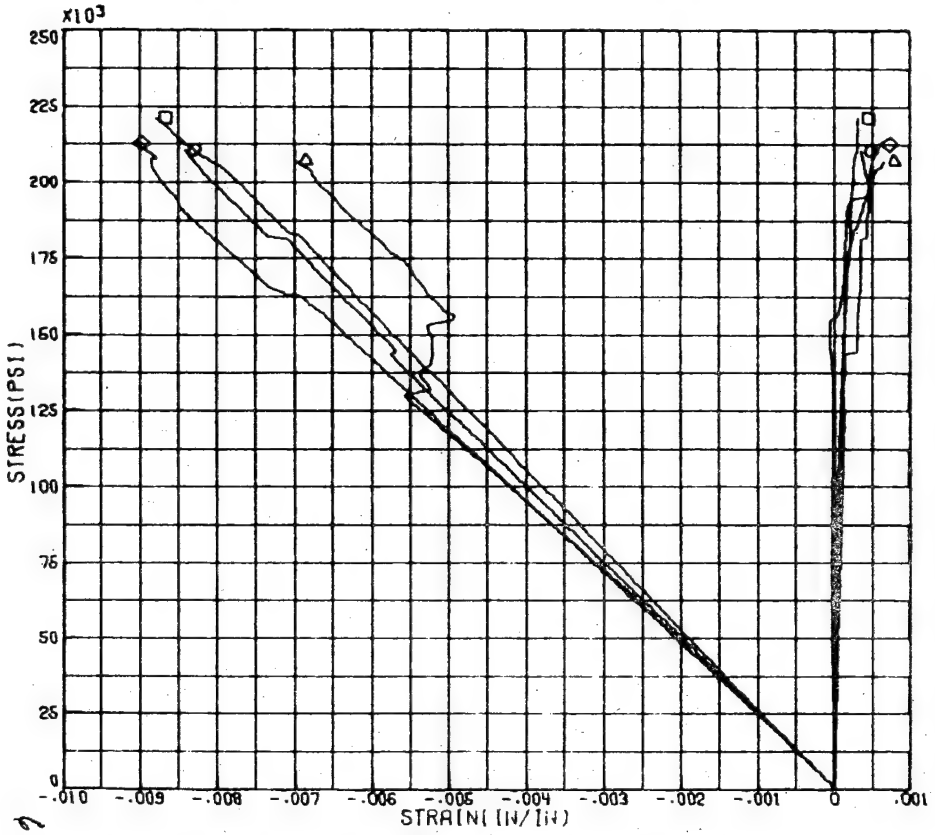

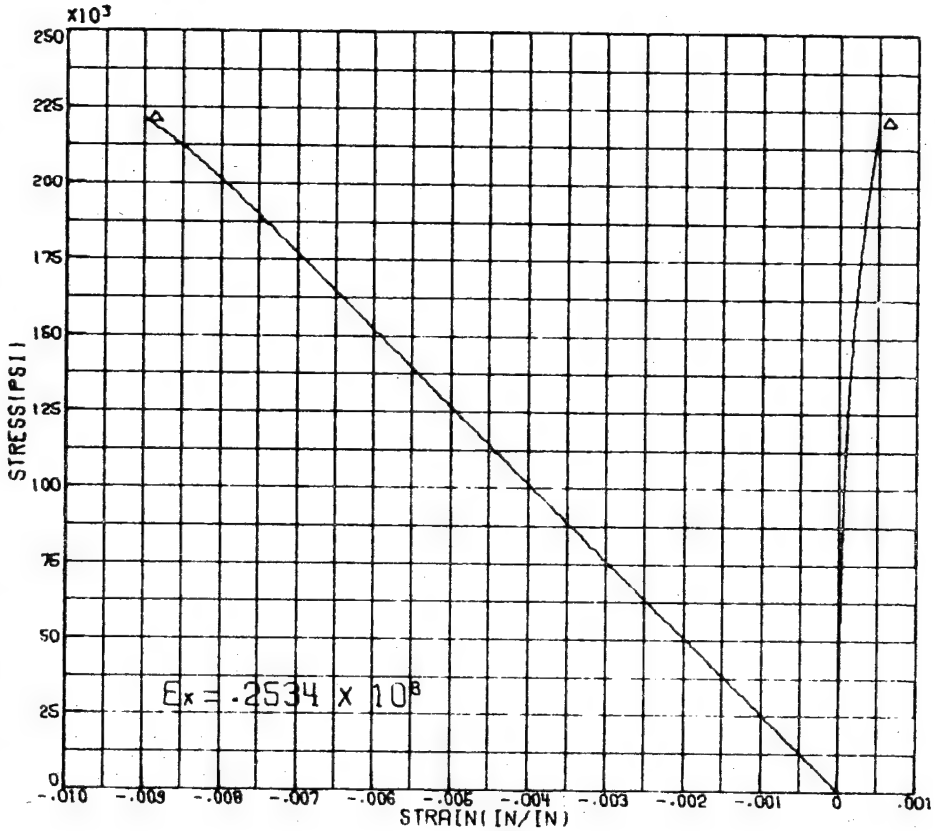

FIGURE **24B**:-COMPRESSION RESPONSE OF TUBULAR SPECIMENS-B/E LAMINATE- [0/90]

o TEST 502 RUN 22 △ BEST FIT
□ TEST 502 RUN 23 A= $-.8714 \times 10^{-7}$
◇ TEST 502 RUN 24 B= $-.3142 \times 10^{-39}$
N= 7

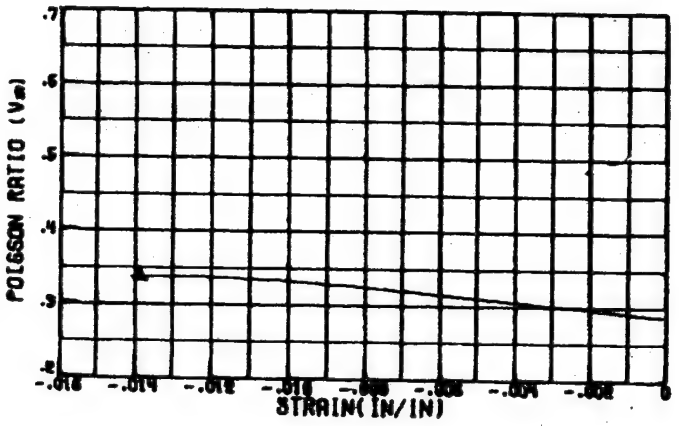

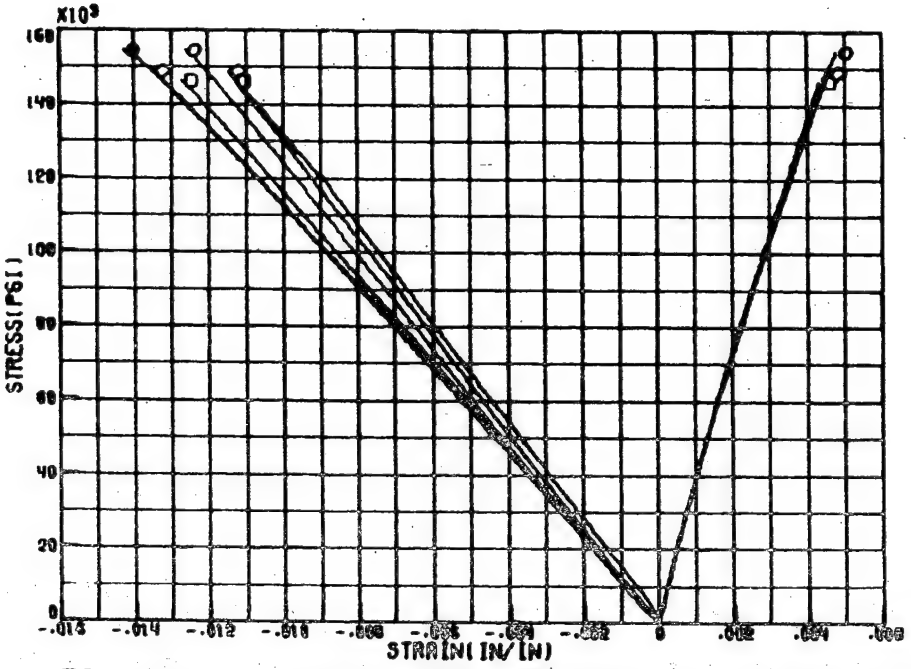

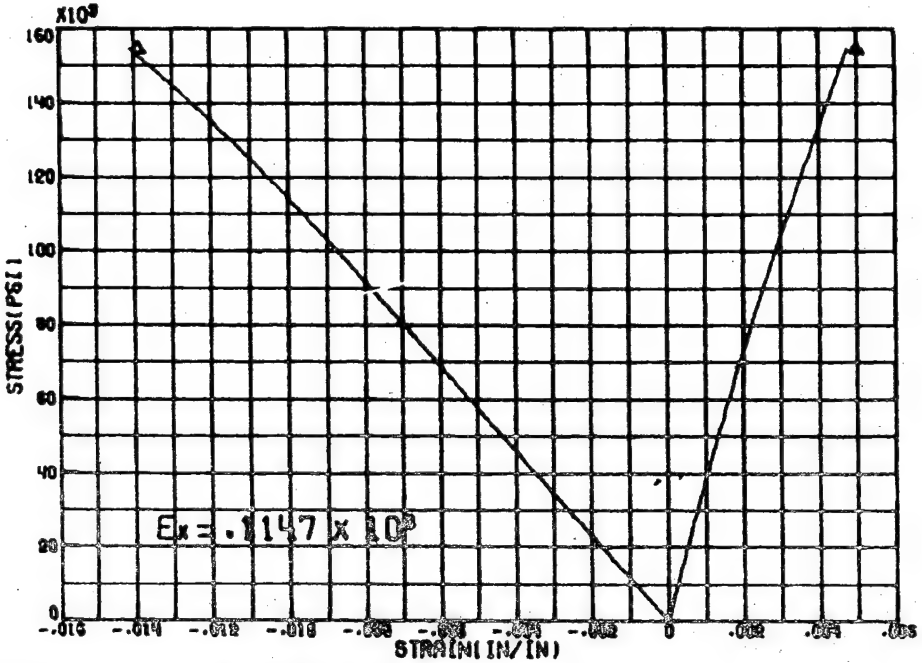

FIGURE 25A:-COMPRESSION RESPONSE OF PLANAR SPECIMENS- B/E LAMINATE- [0/±45/90]

○ TEST 537 RUN 5 △ BEST FIT
□ TEST 537 RUN 6 A= $-.6004 \times 10^{-7}$
◇ TEST 537 RUN 7 B= $-.1892 \times 10^{-49}$
N= 9

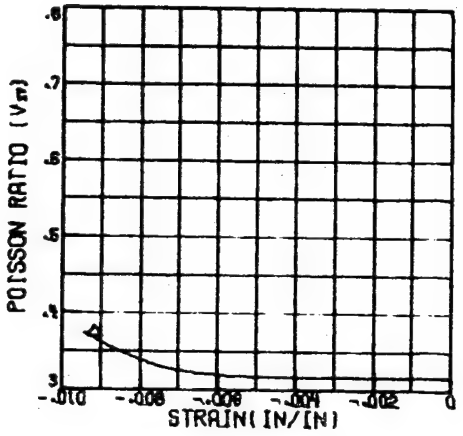

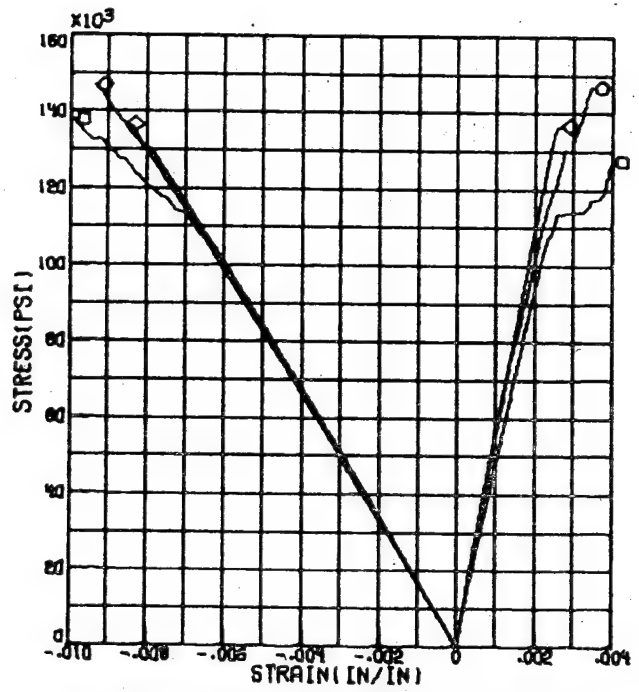

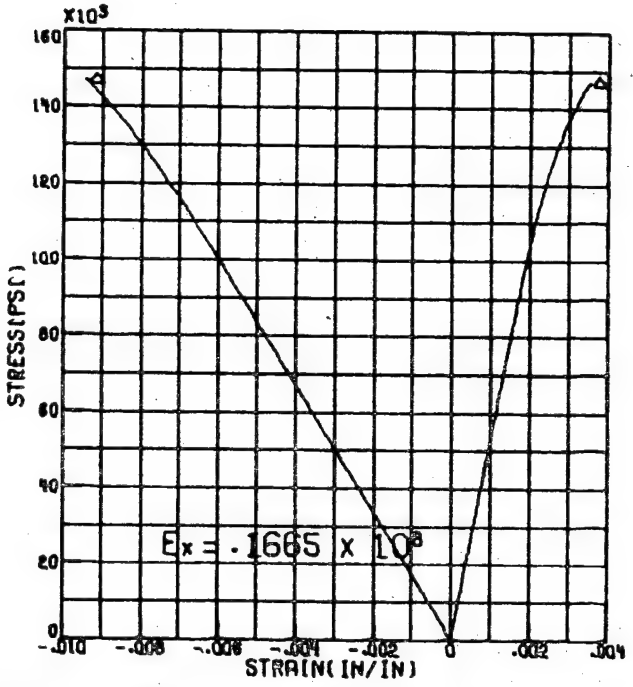

FIGURE 25B:-COMPRESSION RESPONSE OF TUBULAR SPECIMENS-B/E LAMINATE- [0/±45/90]

○ TEST 490 RUN 1 △ BEST FIT
□ TEST 490 RUN 2 A= $-.6092 \times 10^{-7}$
B= $-.2912 \times 10^{-13}$
N= 2

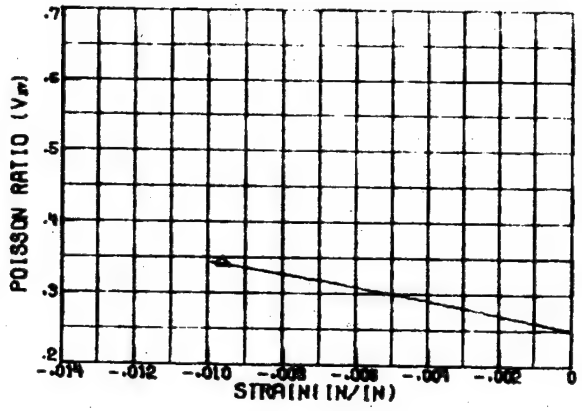

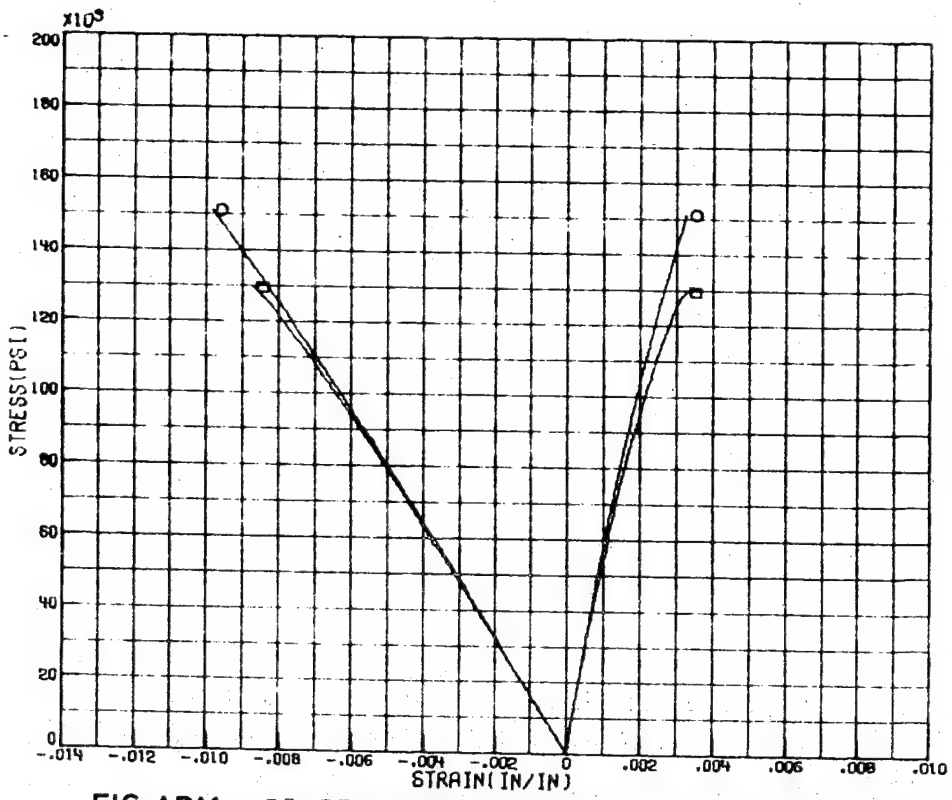

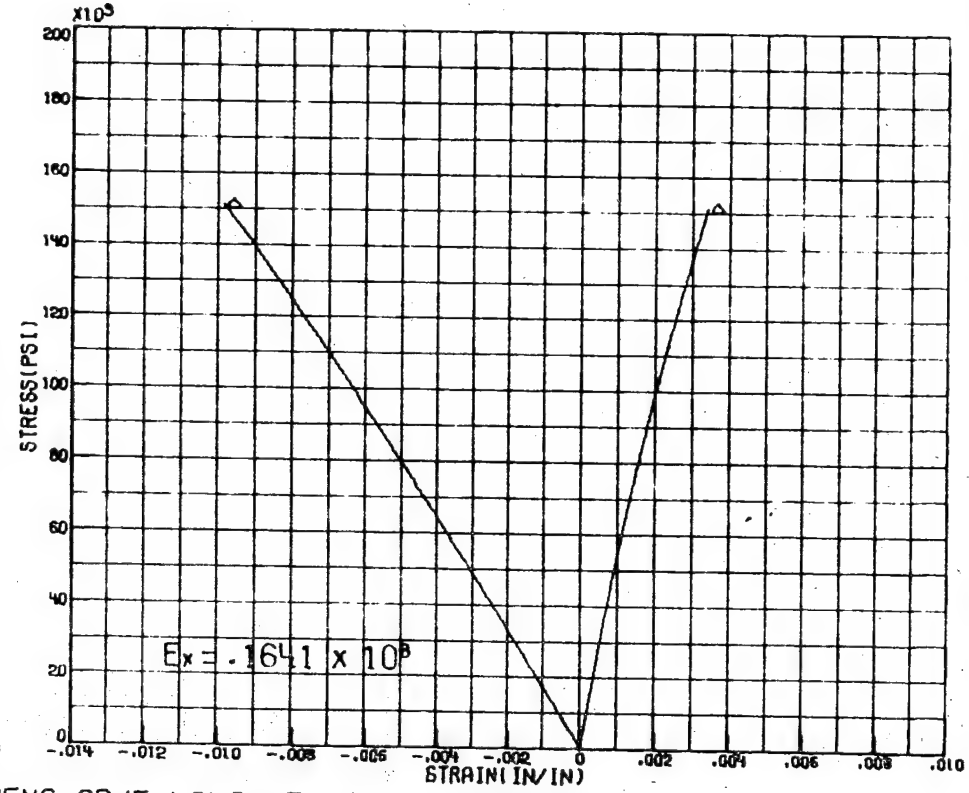

FIG. APA1 ;-COMPRESSION RESPONSE OF PLANAR SPECIMENS-GR/E LAMINATE-[0] (DAMAGED)

o TEST 490 RUN 3 △ BEST FIT

□ TEST 490 RUN 9 A= $-.7068 \times 10^{-7}$

B= $-.3694 \times 10^{-18}$

N= 3

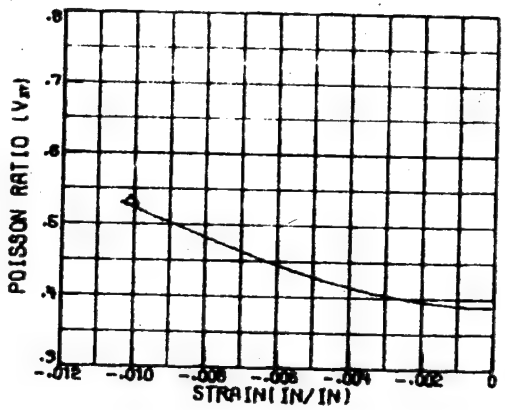

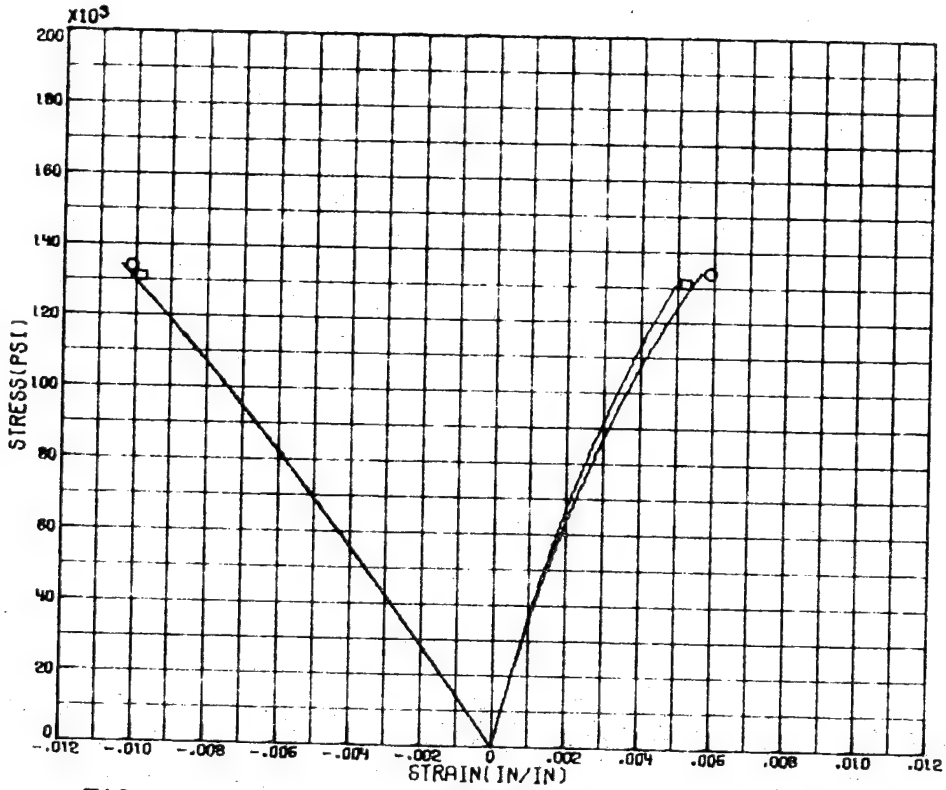

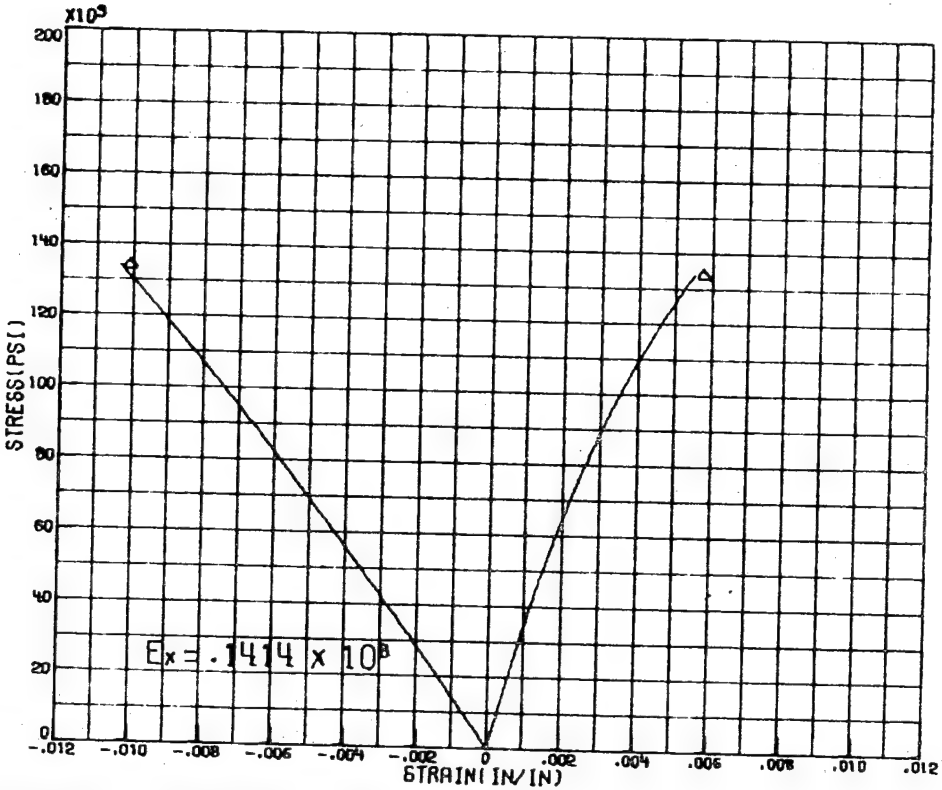

FIG. APA 2:-COMPRESSION RESPONSE OF PLANAR SPECIMENS-GR/E LAMINATE-[±15] (DAMAGED)

14

o TEST 490 RUN 4 △ BEST FIT

□ TEST 490 RUN 11 A= $-.1276 \times 10^{-6}$

B= $-.4956 \times 10^{-17}$

N= 3

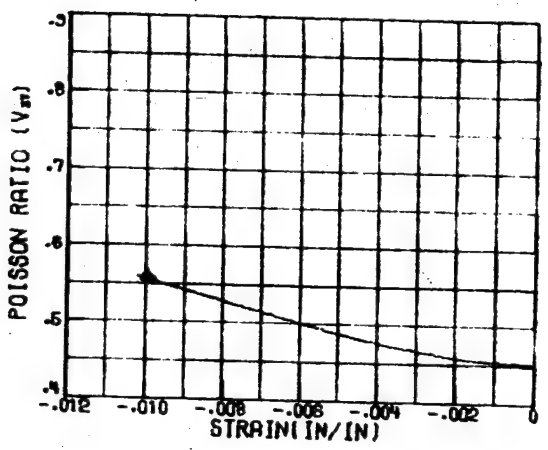

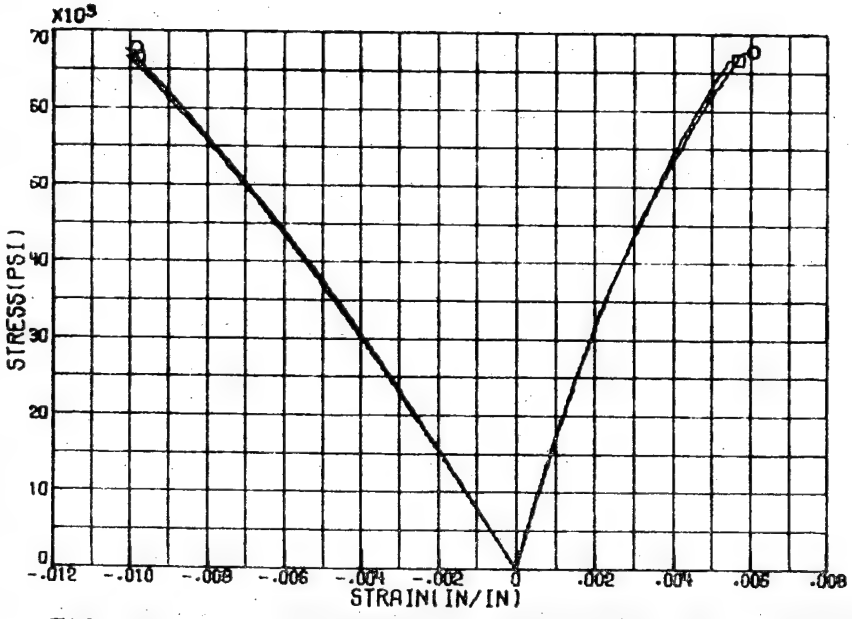

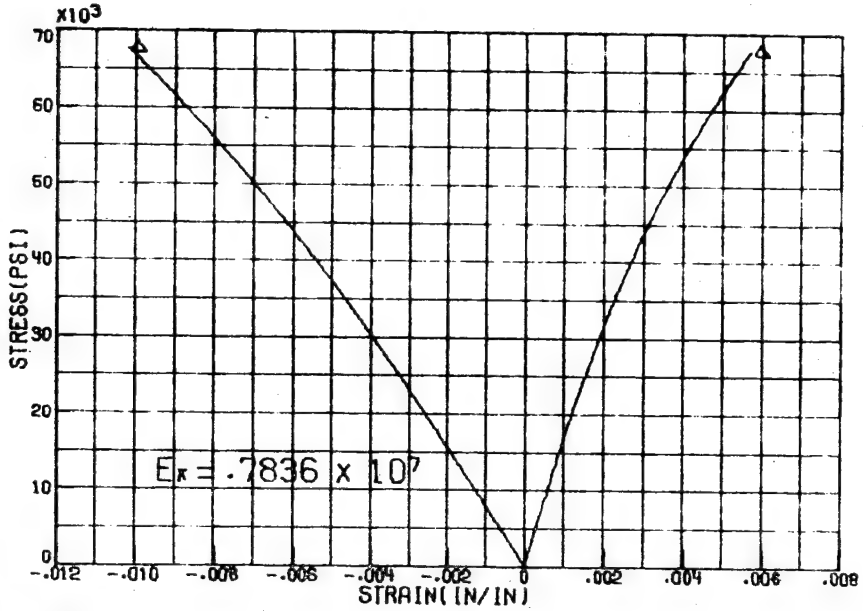

FIG. APA3 ;-COMPRESSION RESPONSE OF PLANAR SPECIMENS-GR/E LAMINATE-[±30] (DAMAGED)

○ TEST 490 RUN 15

□ TEST 490 RUN 16

△ BEST FIT

A= $-.3325 \times 10^{-6}$

B= $-.2344 \times 10^{-15}$

N= 3

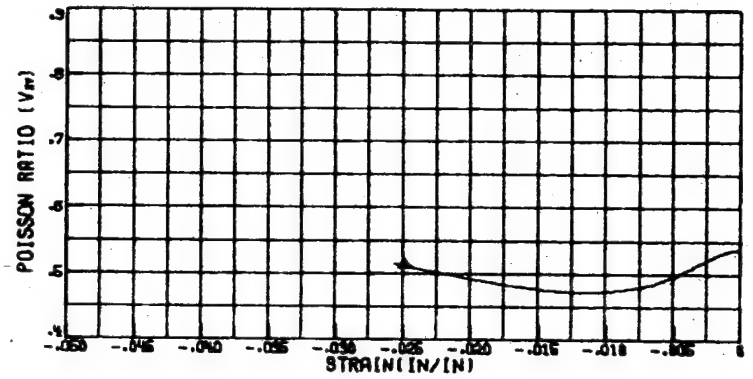

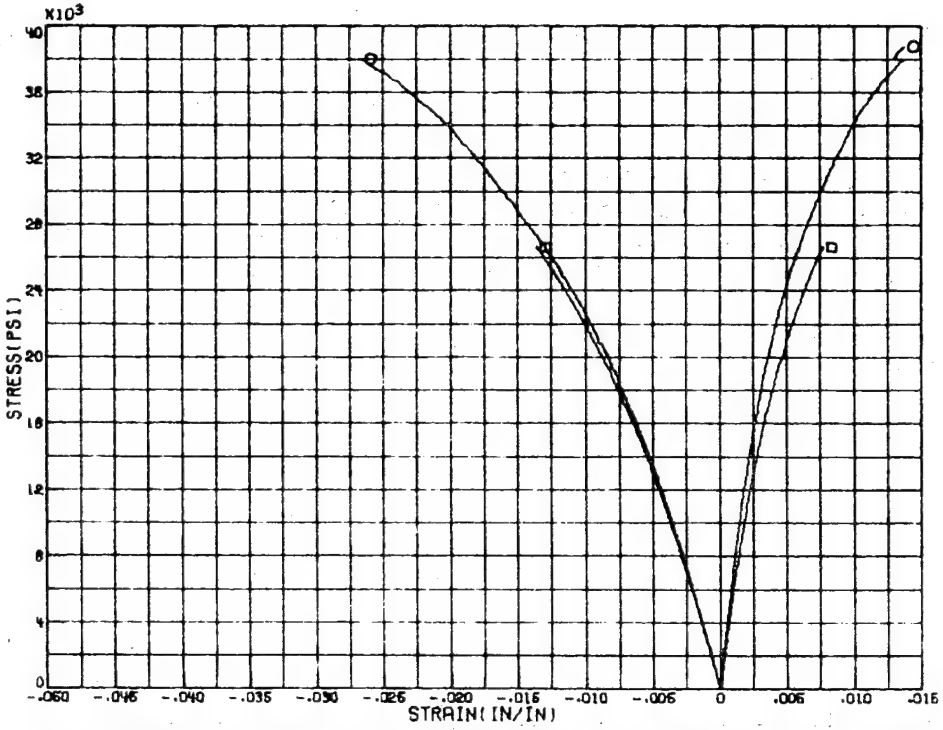

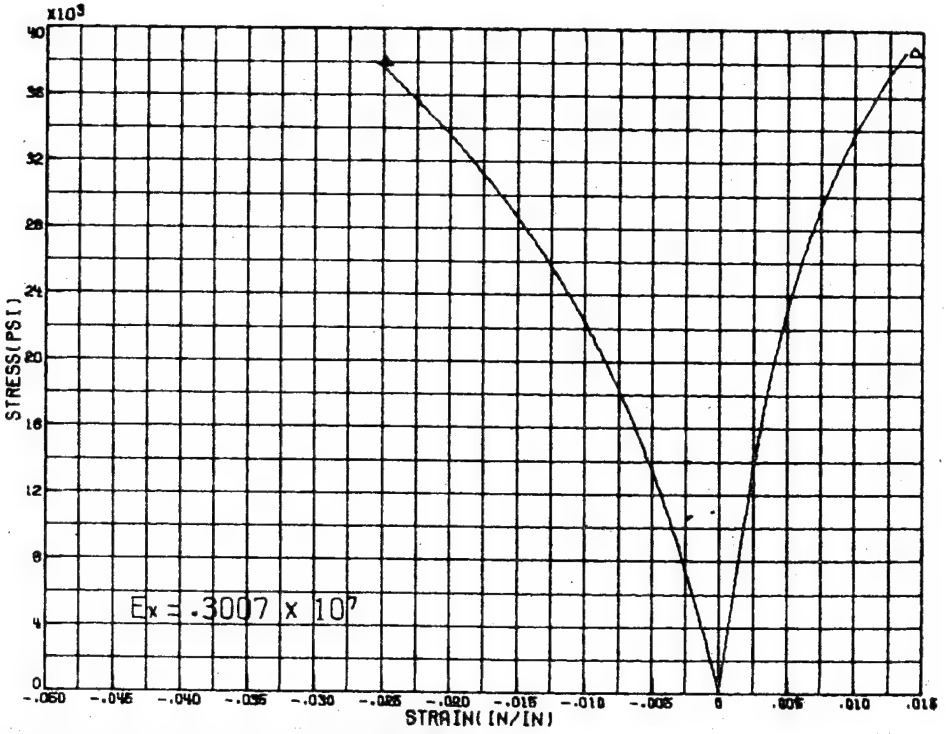

FIG. APA4 :-COMPRESSION RESPONSE OF PLANAR SPECIMENS-GR/E LAMINATE-[±45] (DAMAGED)

43

○ TEST 490 RUN 5 △ BEST FIT
□ TEST 490 RUN 12 A= $-.5852 \times 10^{-6}$
B= $-.7207 \times 10^{-15}$
N= 3

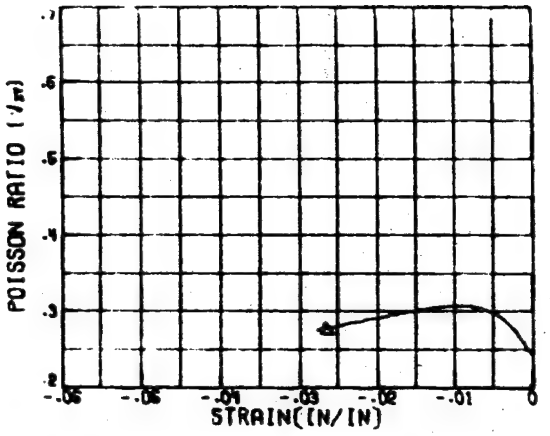

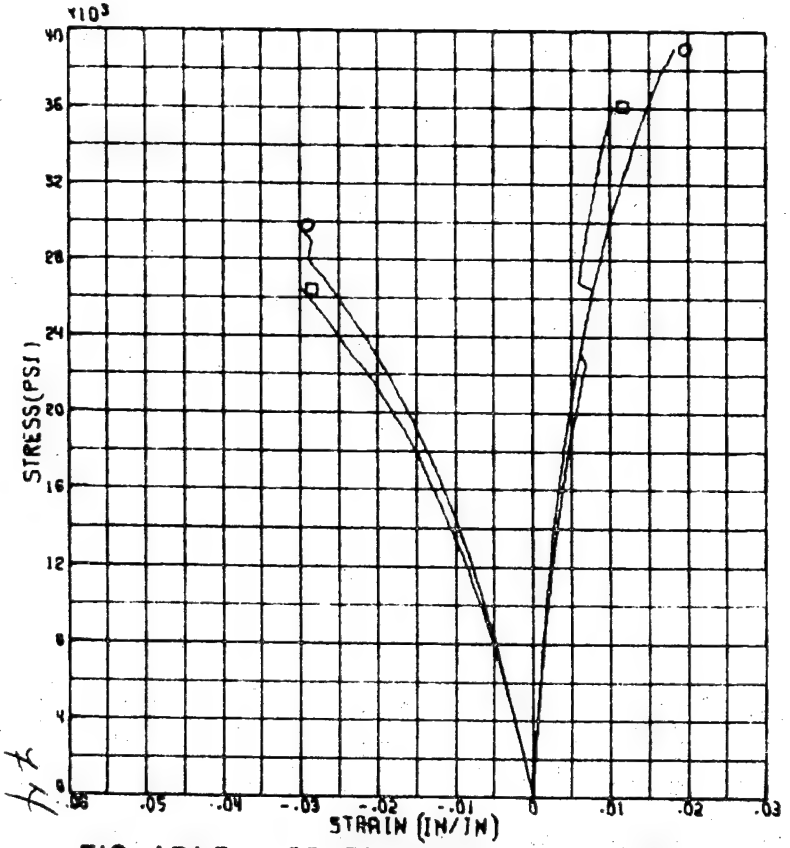

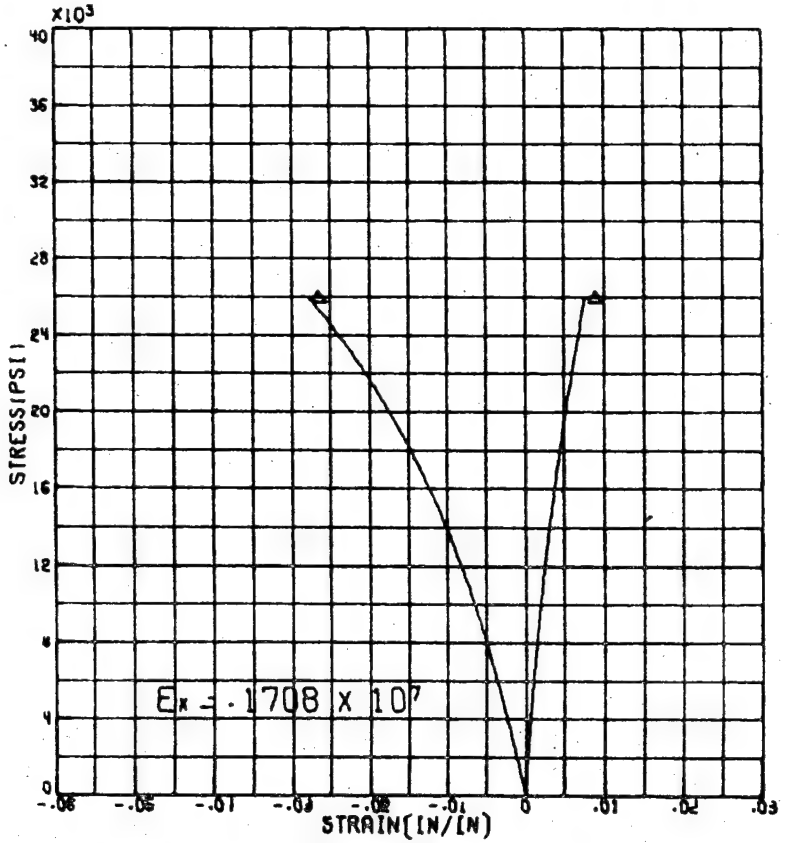

FIG. APA5 :-COMPRESSION RESPONSE OF PLANAR SPECIMENS-GR/E LAMINATE-[±60] (DAMAGED)

○ TEST 490 RUN 6 △ BEST FIT
□ TEST 490 RUN 7 A= $-.4852 \times 10^{-6}$
B= $-.1375 \times 10^{-10}$
N= 2

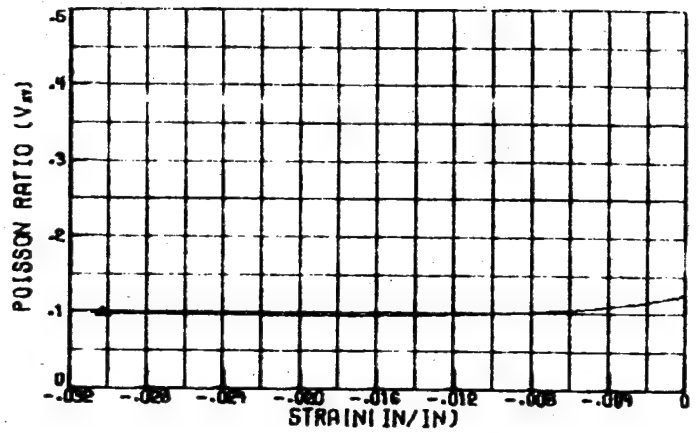

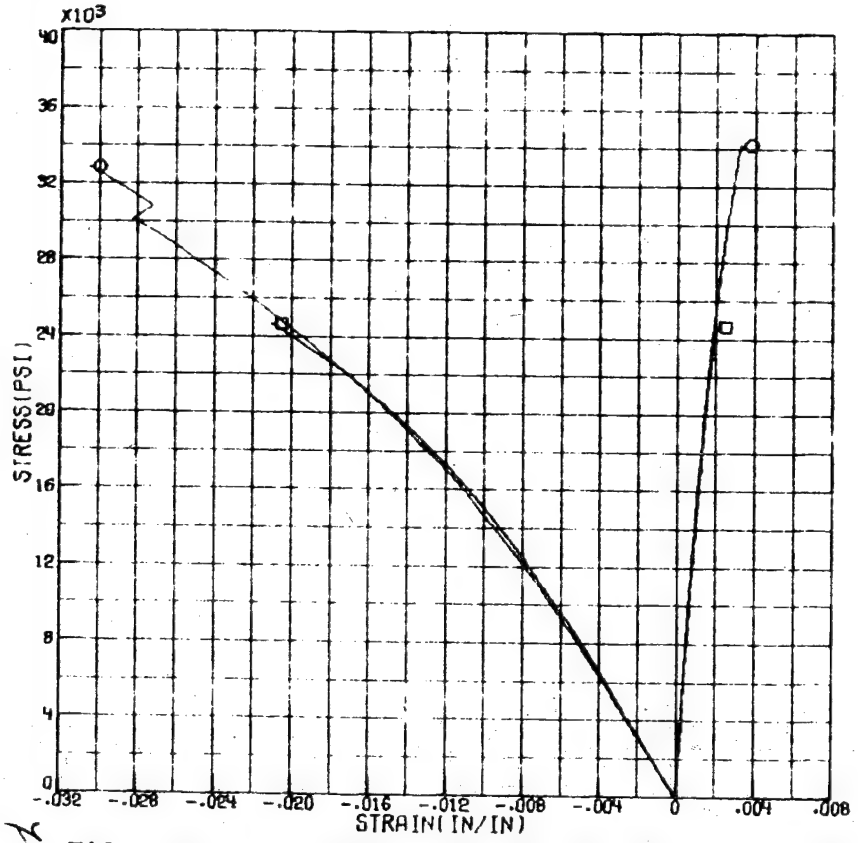

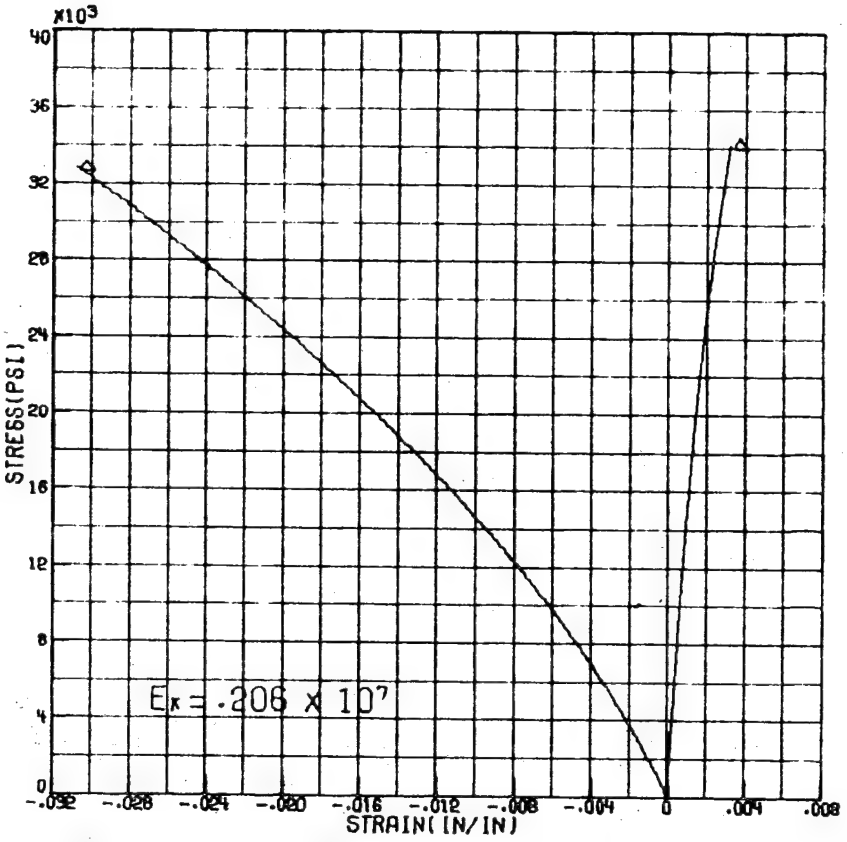

FIG. APA 6 :-COMPRESSION RESPONSE OF PLANAR SPECIMENS-GR/E LAMINATE-[±75] (DAMAGED)

○ TEST 490 RUN 8 △ BEST FIT
□ TEST 490 RUN 13 A= $-.5595 \times 10^{-6}$
B= $-.4186 \times 10^{-11}$
N= 2

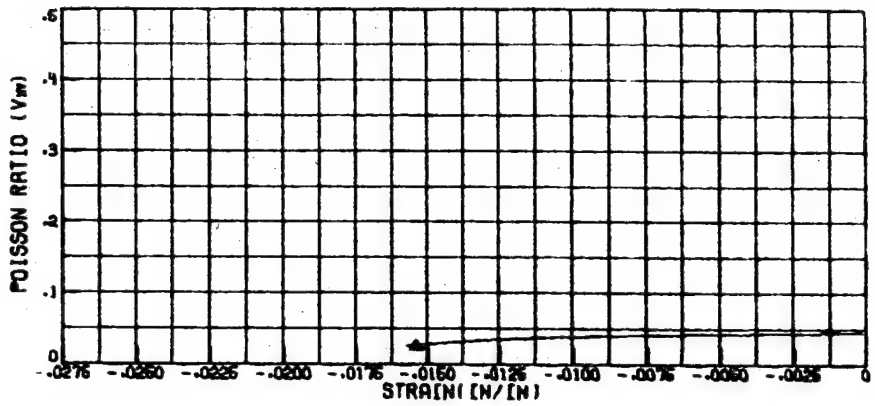

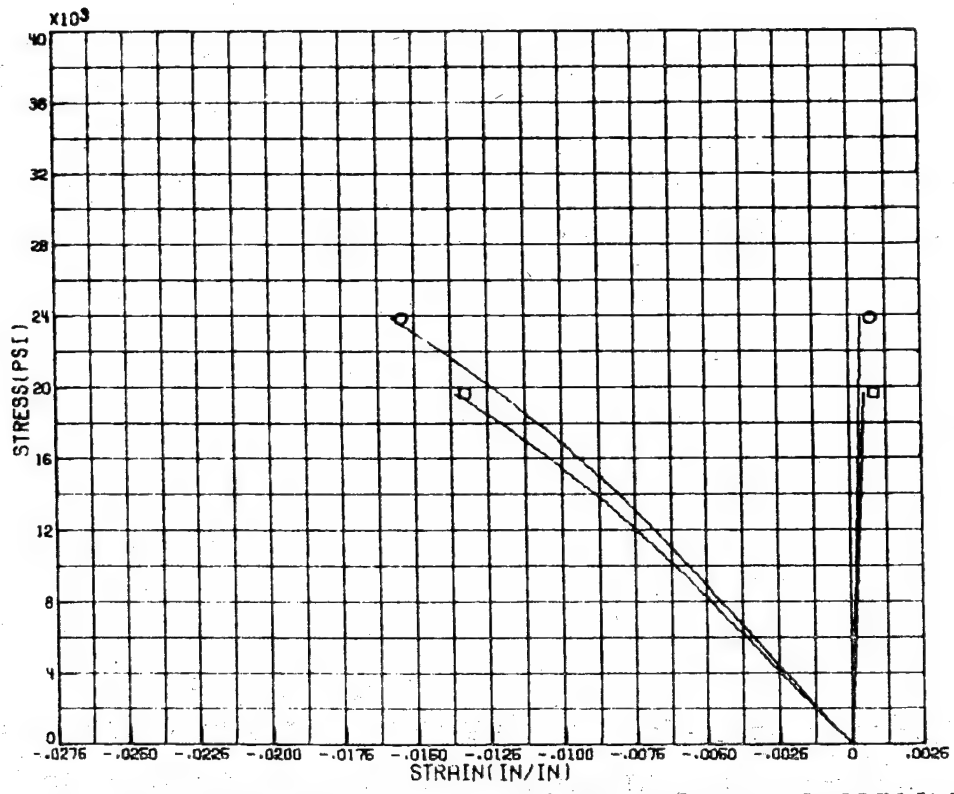

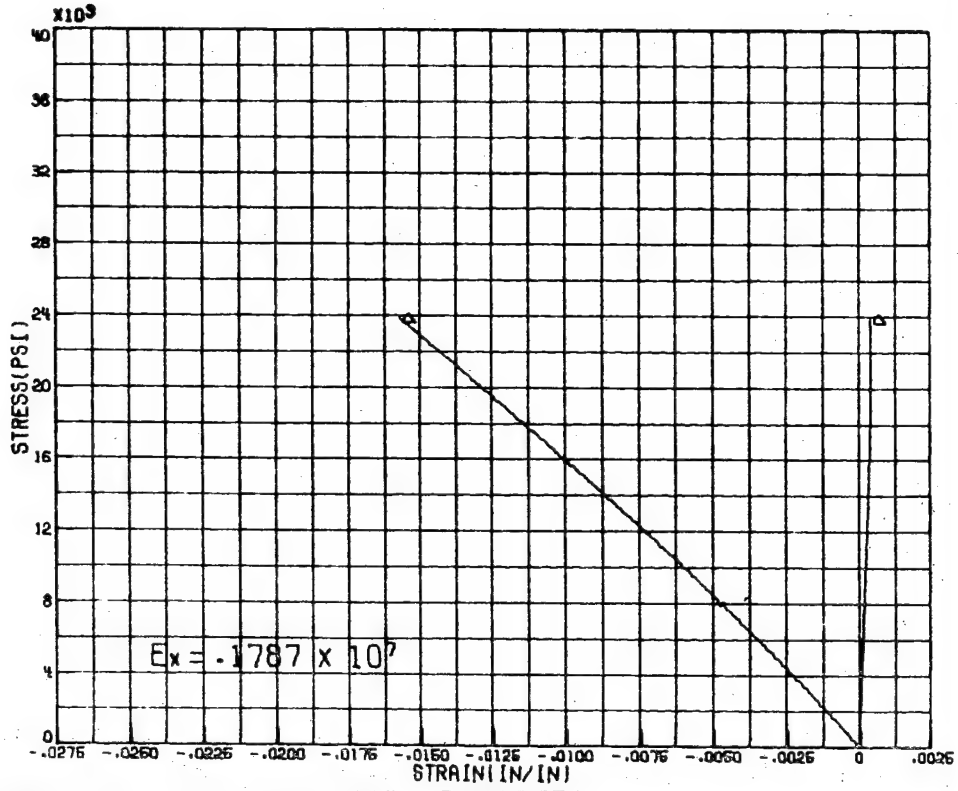

FIG. APA7 :-COMPRESSION RESPONSE OF PLANAR SPECIMENS-GR/E LAMINATE-[90] (DAMAGED)

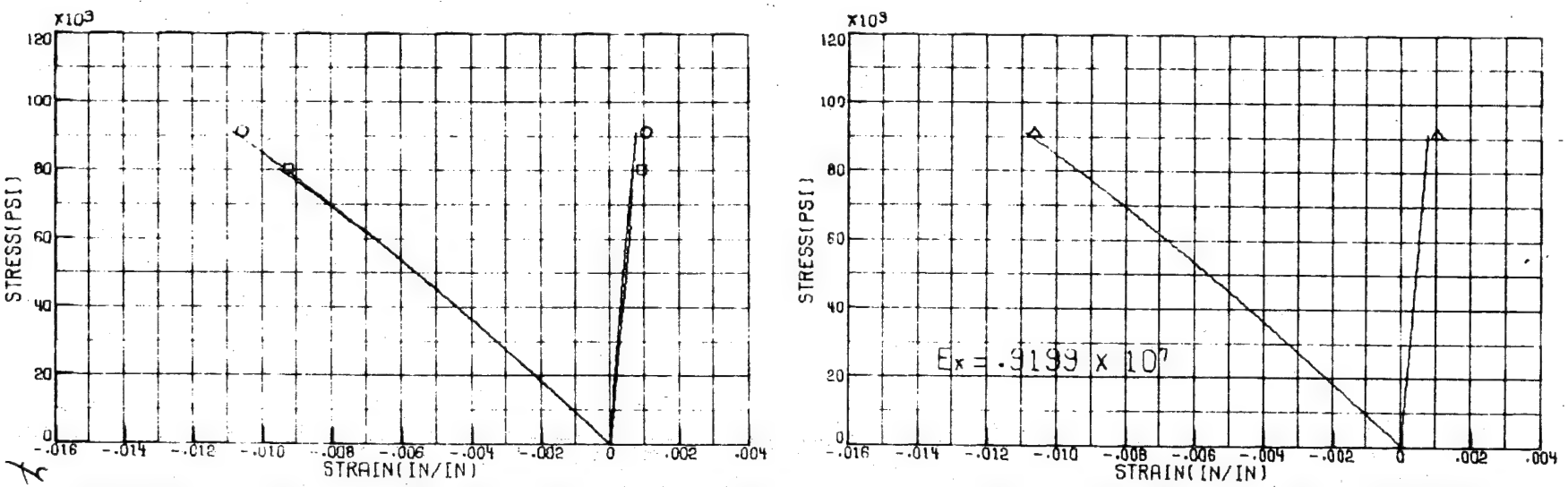

FIG. APA 8 :-COMPRESSION RESPONSE OF PLANAR SPECIMENS-GR/E LAMINATE-[0/90] (DAMAGED)

○ TEST 490 RUN 27 △ BEST FIT
□ TEST 490 RUN 28 A= -.4166 x 10^{-7}
B= -.1456 x 10^{-14}
N= 2

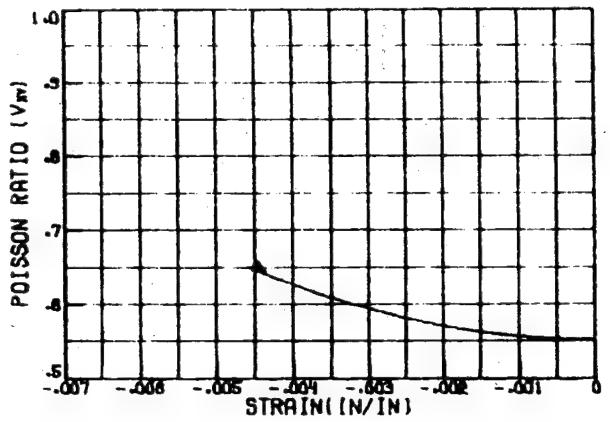

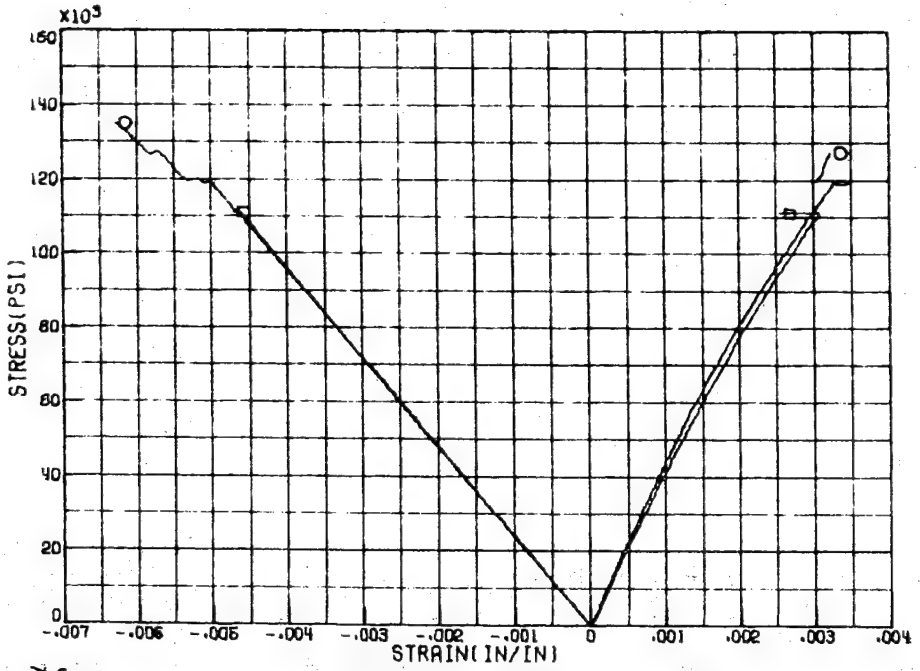

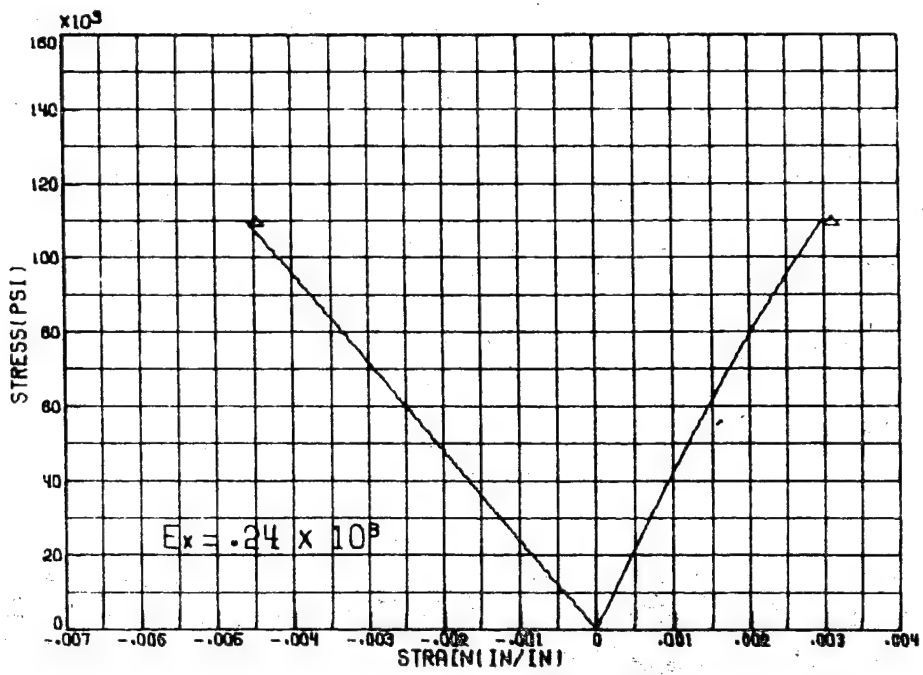

FIG. APA 9 :-COMPRESSION RESPONSE OF PLANAR SPECIMENS- B/E LAMINATE- [±15] (DAMAGED)

o TEST 495 RUN 2 △ BEST FIT

□ TEST 495 RUN 3 A= $-.8278 \times 10^{-7}$

B= $-.1402 \times 10^{-33}$

N= 7

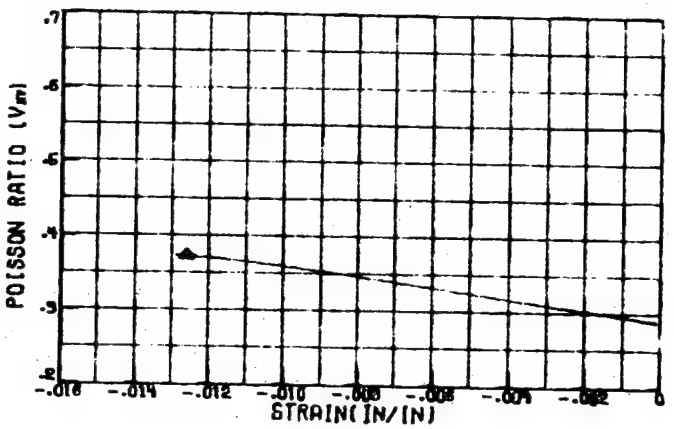

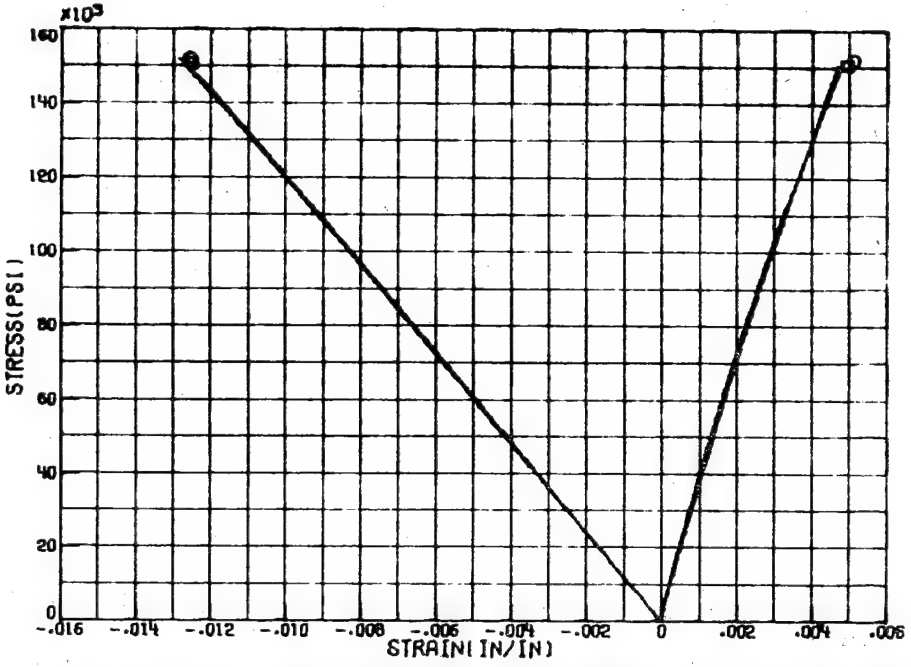

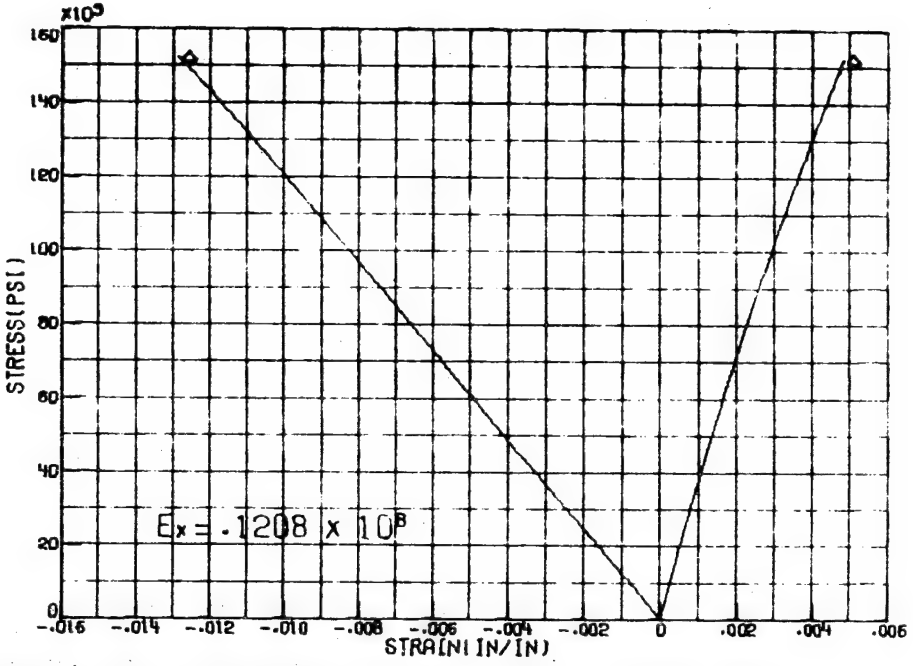

FIG. APA 10 :-COMPRESSION RESPONSE OF PLANAR SPECIMENS- B/E LAMINATE- [0/±45/90] (DAMAGED)

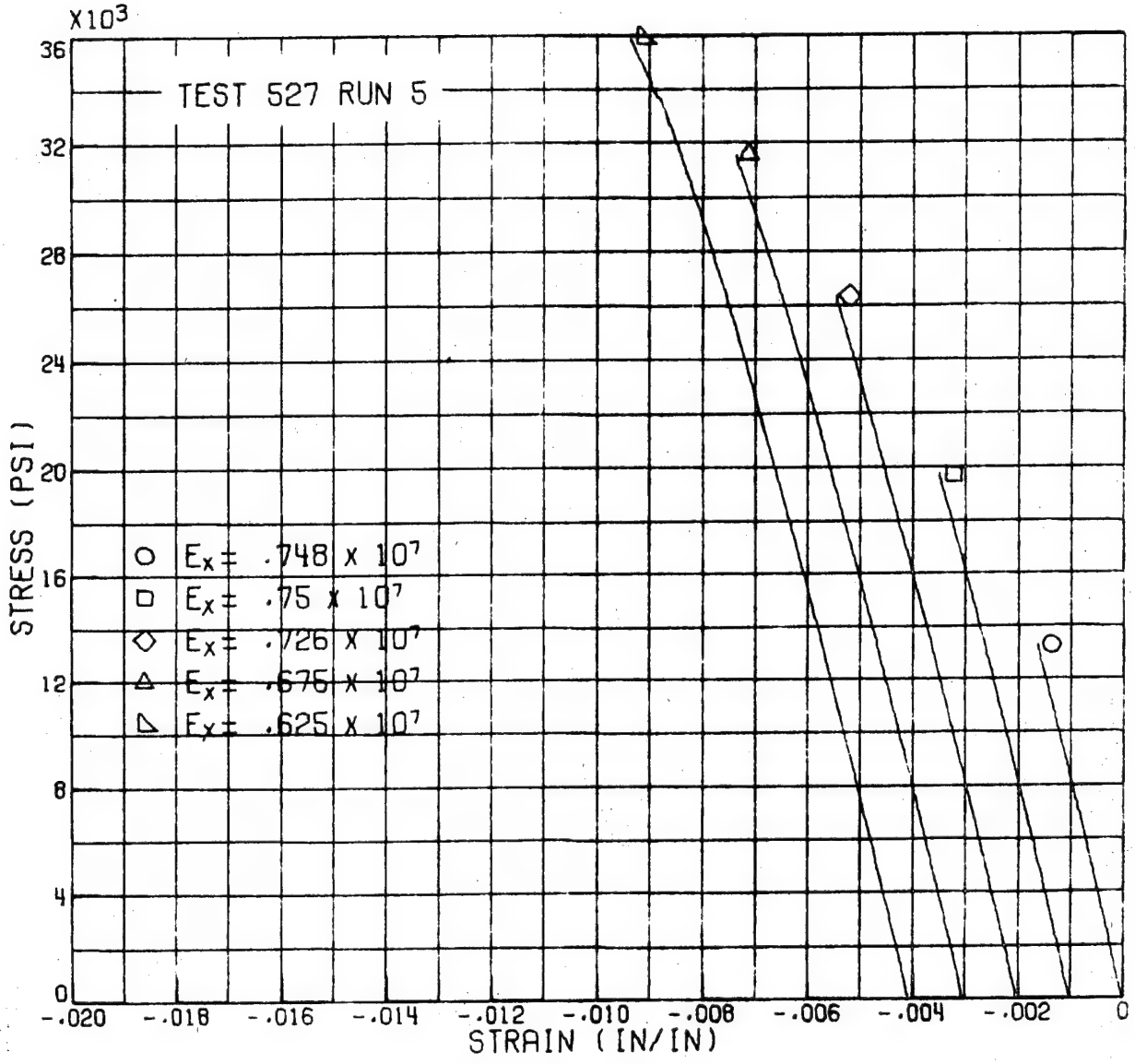

FIG. APB 1 ;-INFLUENCE OF LOADING AND UNLOADING ON RESPONSE OF COMPRESSION TUBES- [±30] GR/E

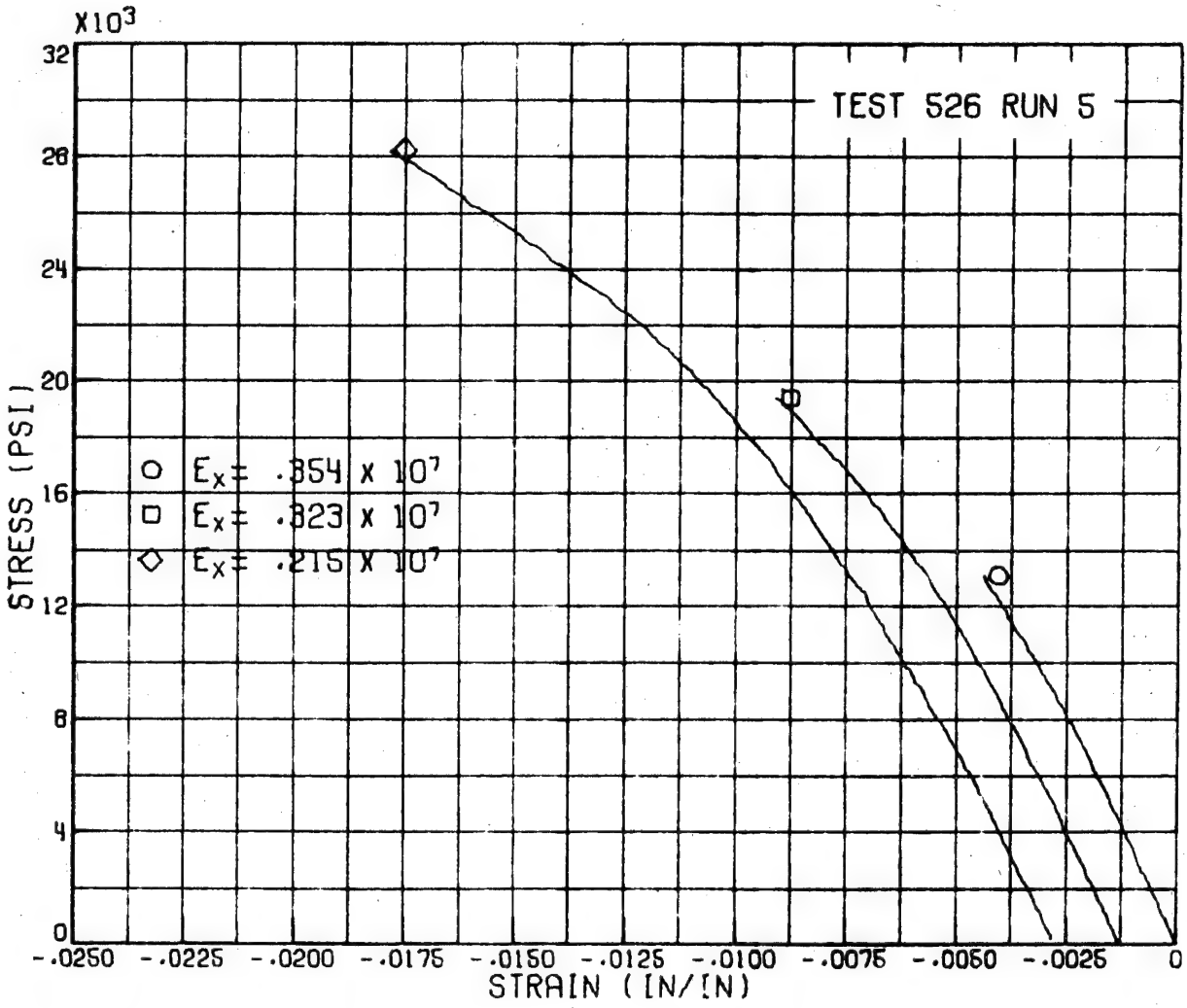

FIG. APB 2 ;-INFLUENCE OF LOADING AND UNLOADING ON RESPONSE OF COMPRESSION TUBES- [±45] GR/E

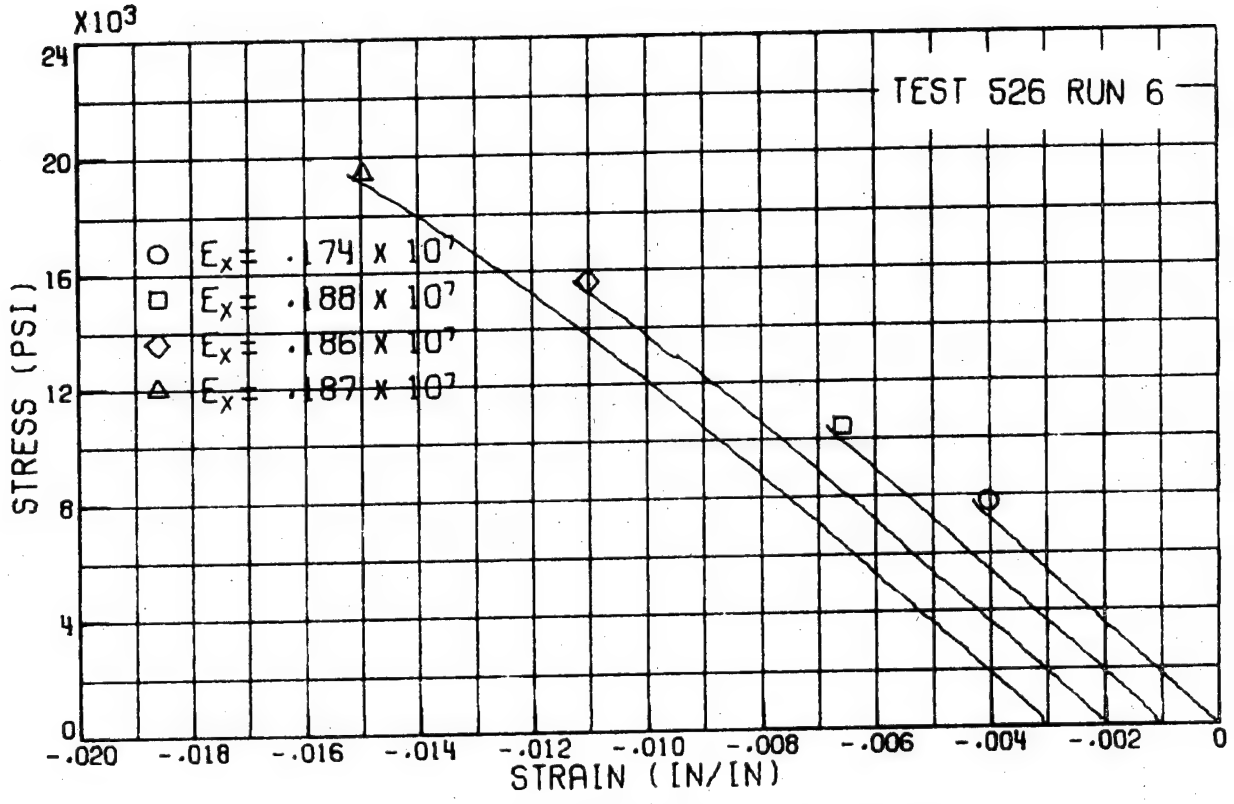

FIG. APB 3I ;- INFLUENCE OF LOADING AND UNLOADING ON RESPONSE OF COMPRESSION TUBES- [±75] GR/E

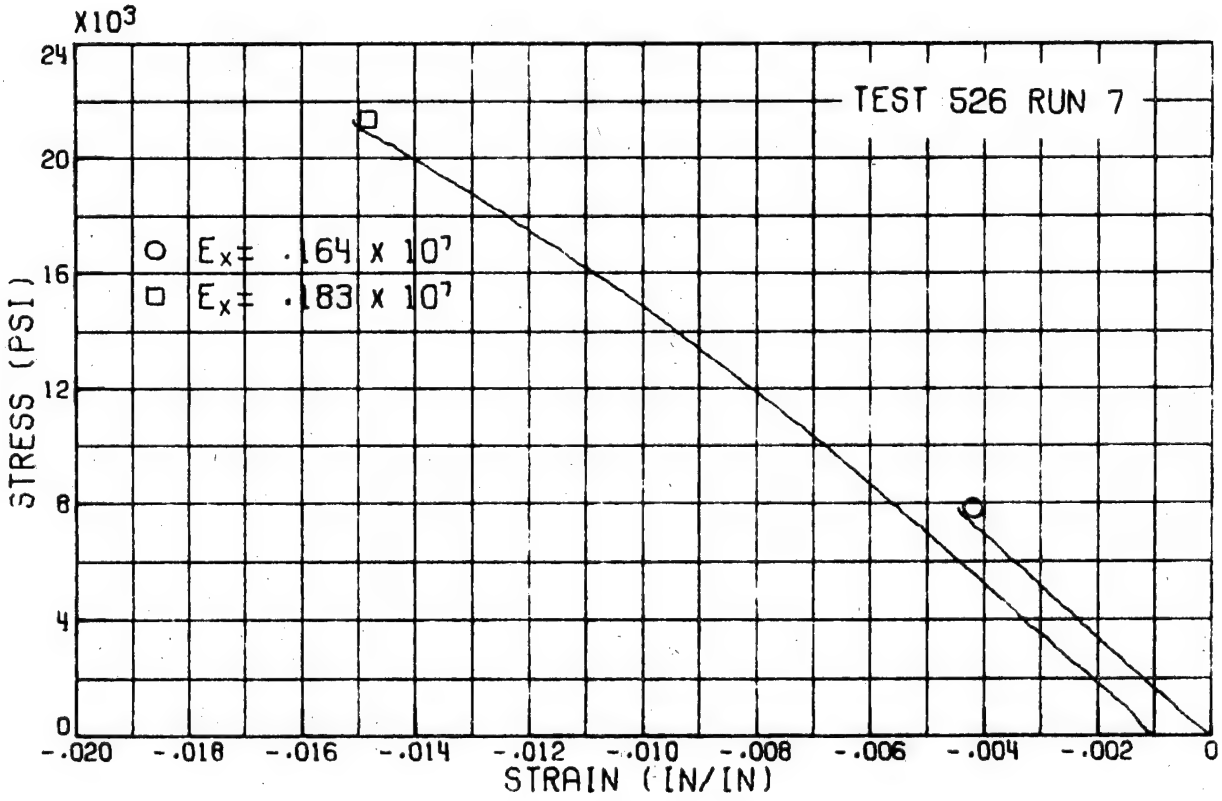

FIG. APB 3II :- INFLUENCE OF LOADING AND UNLOADING ON RESPONSE OF COMPRESSION TUBES- [±75] GR/E

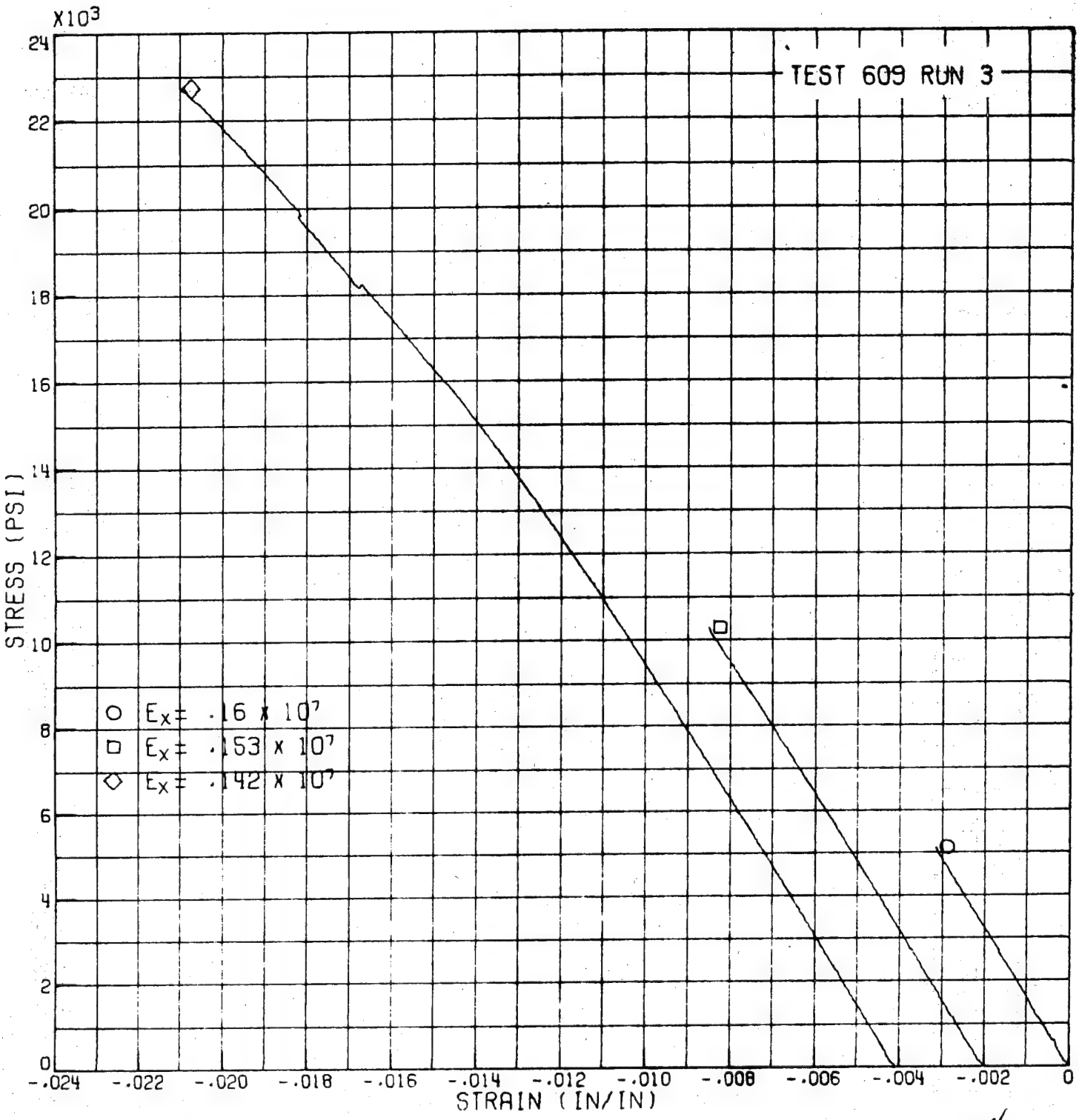

FIG. APB 41 :- INFLUENCE OF LOADING AND UNLOADING ON RESPONSE OF COMPRESSION TUBES- [90] GR/E

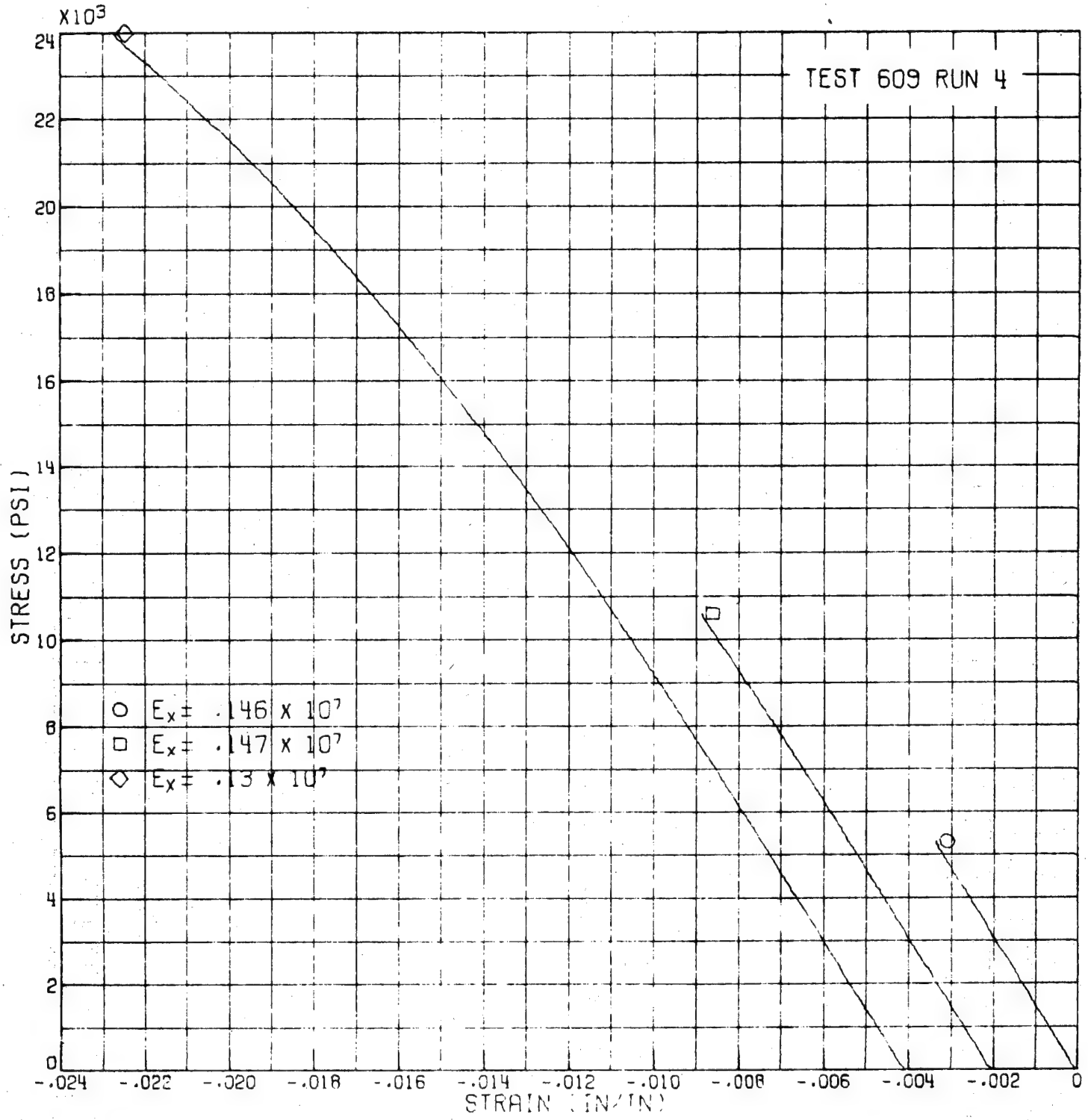

FIG. APB 4II ;- INFLUENCE OF LOADING AND UNLOADING ON RESPONSE OF COMPRESSION TUBES- [90] GR/E

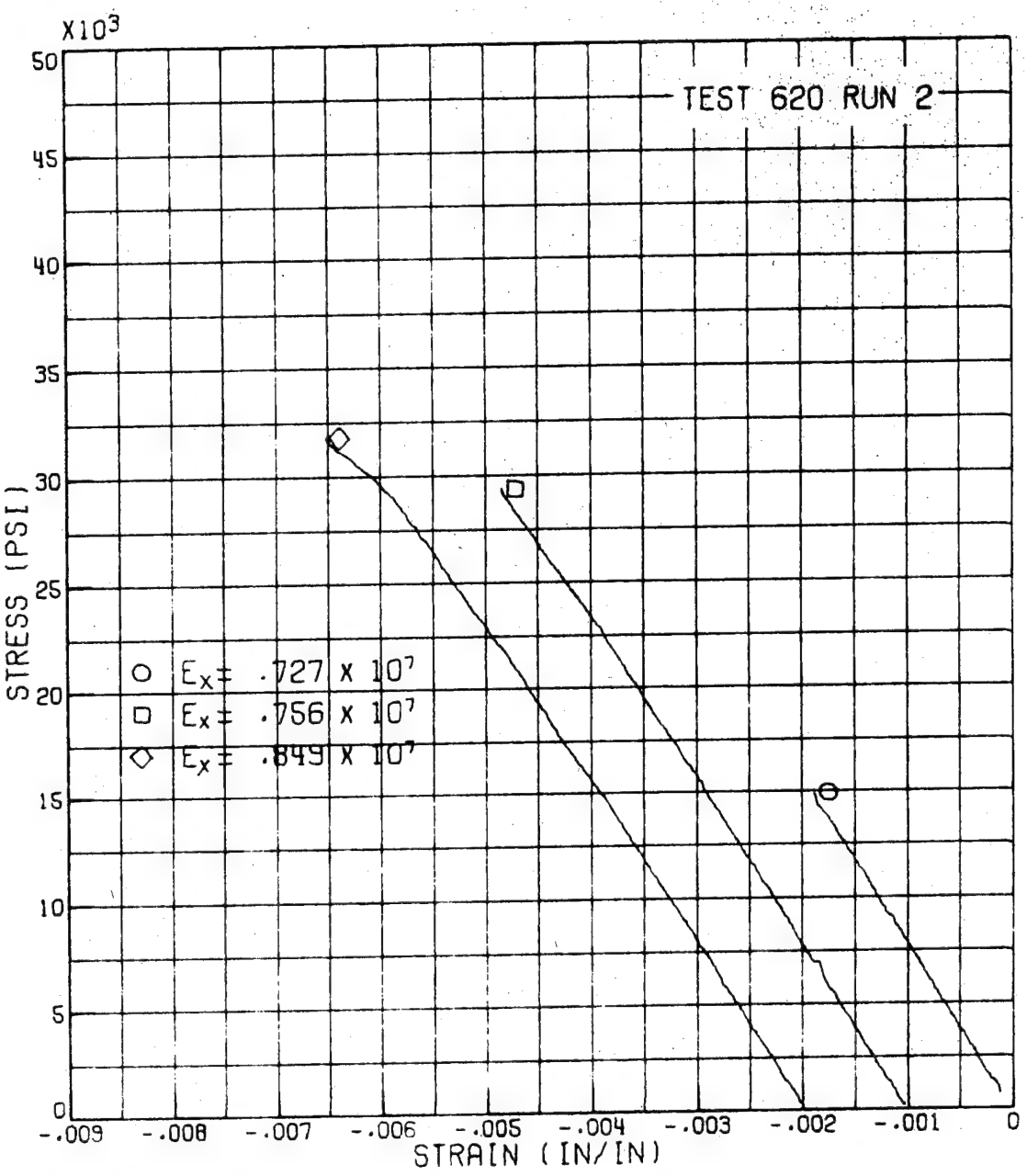

FIG. APB 5 ;-INFLUENCE OF LOADING AND UNLOADING ON RESPONSE OF COMPRESSION TUBES- [0/90] GR/E

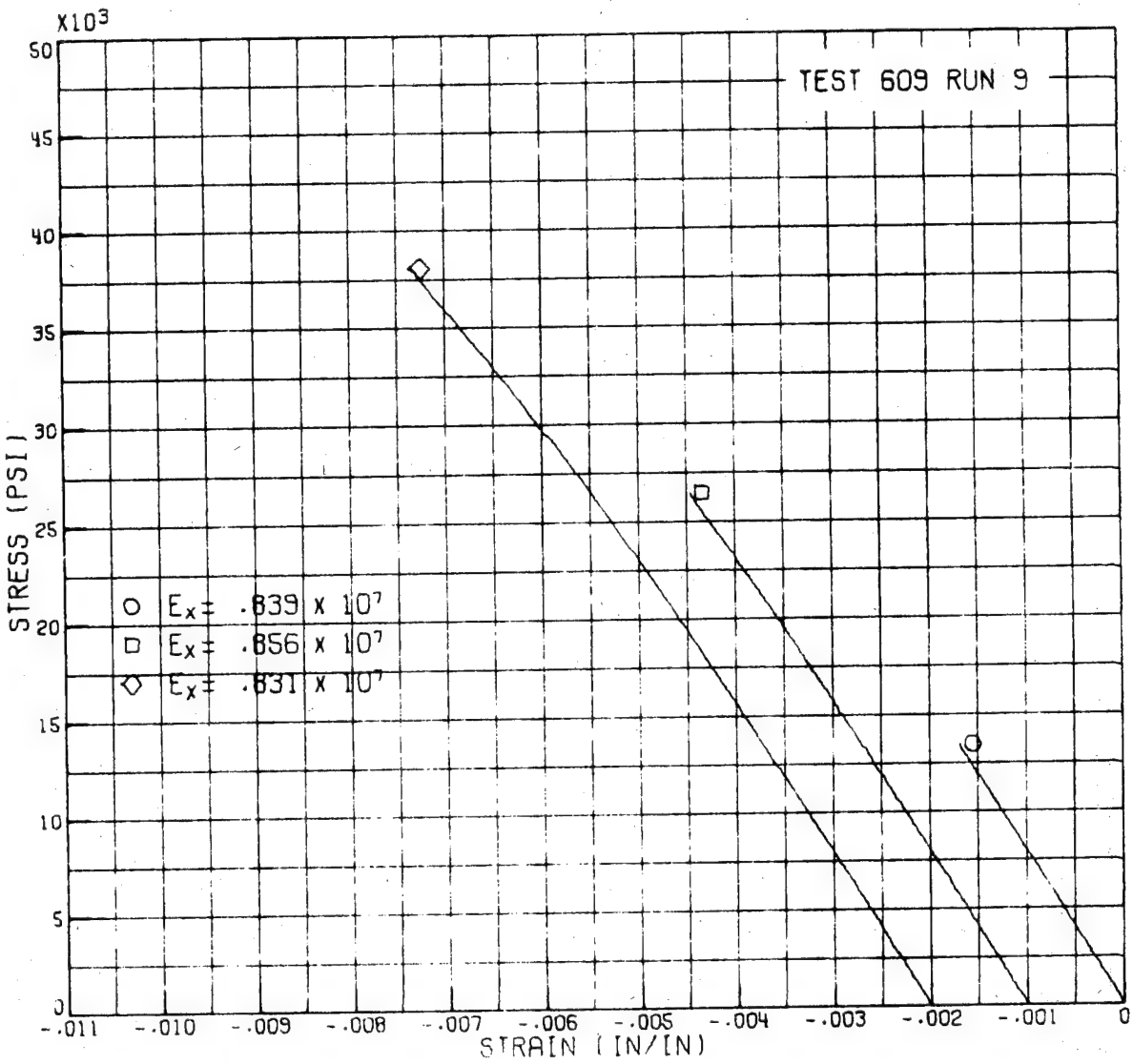

FIG. APB 61:-INFLUENCE OF LOADING AND UNLOADING ON RESPONSE OF COMPRESSION TUBES-[0/±45/90] GR/E

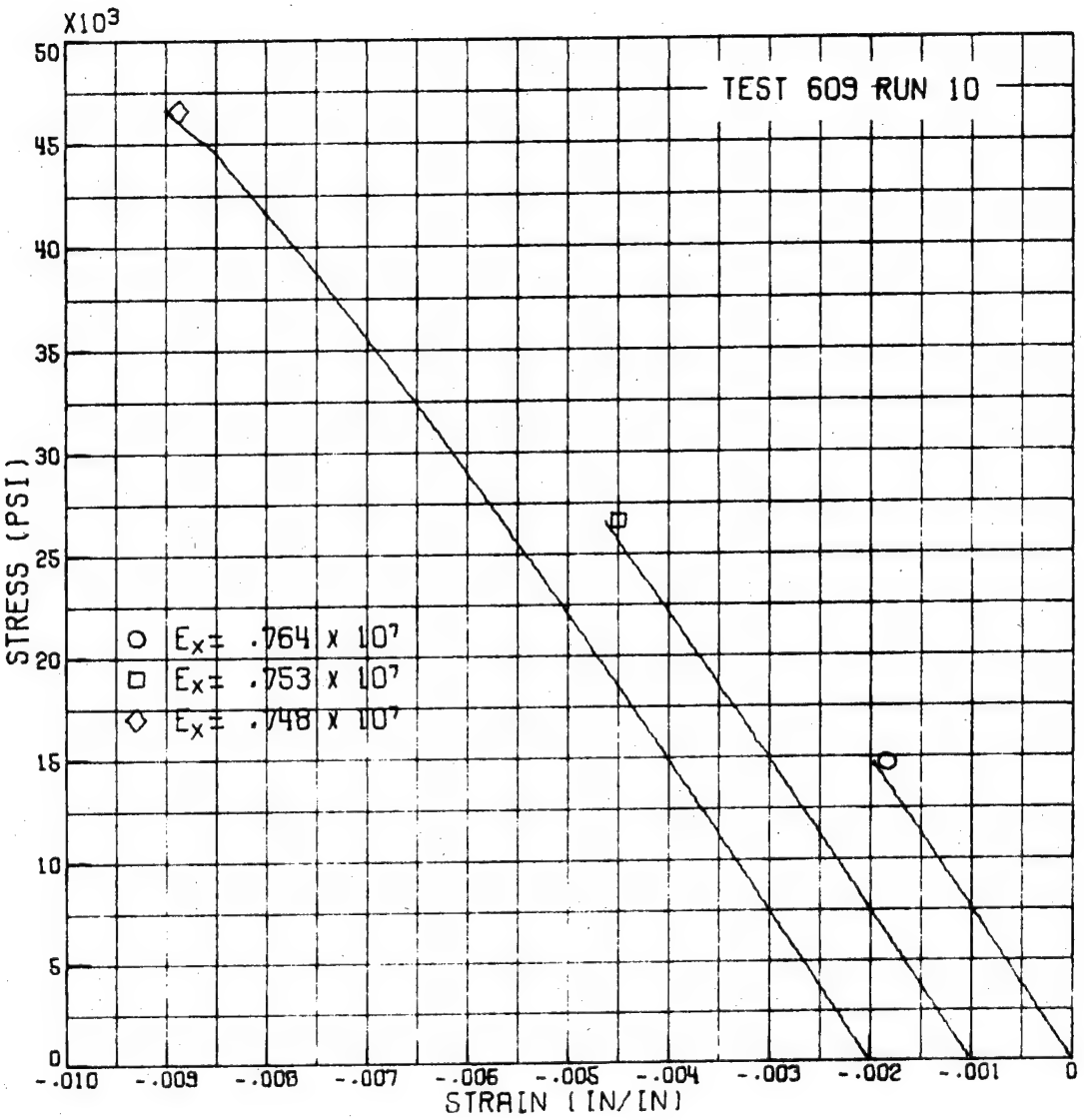

FIG. APB 6II:- INFLUENCE OF LOADING AND UNLOADING ON RESPONSE OF COMPRESSION TUBES- [0/±45/90] GR/E

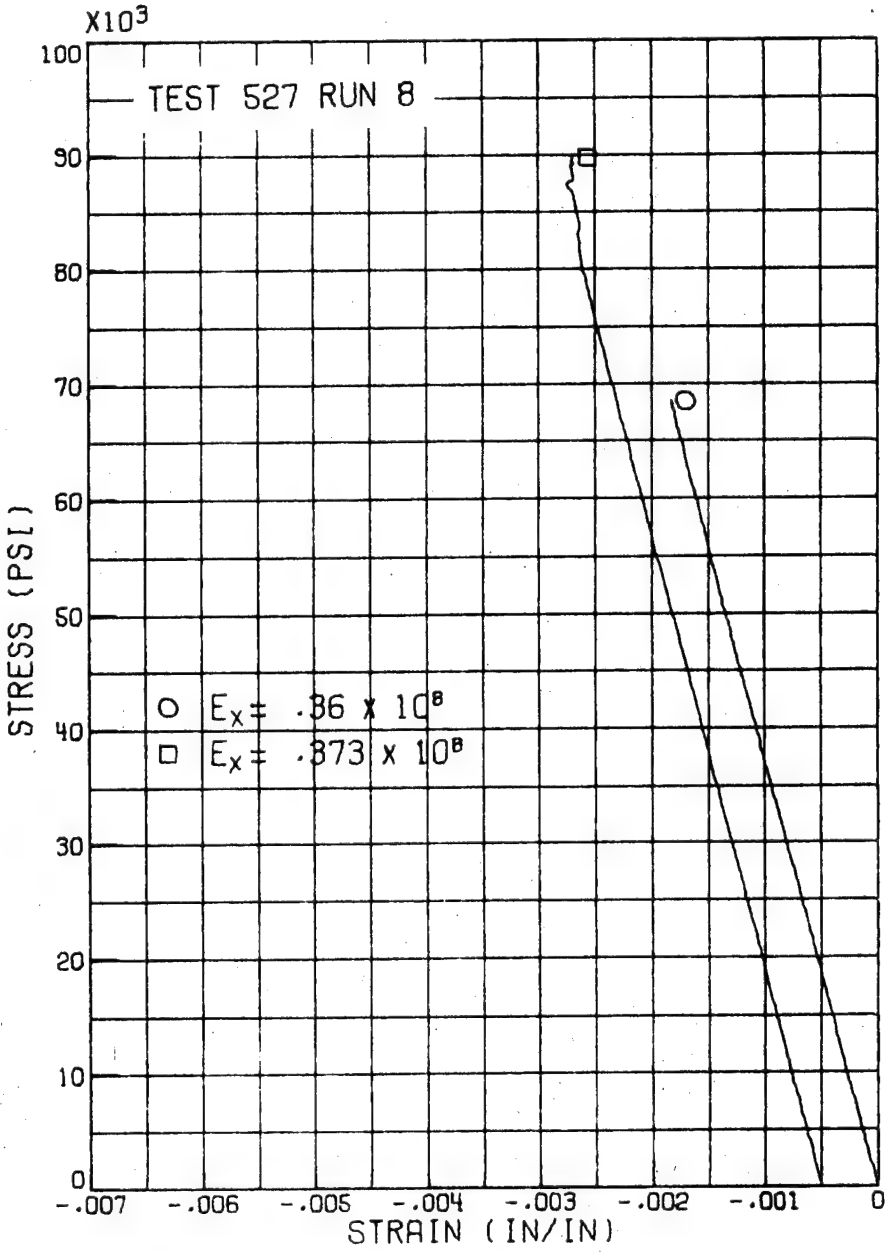

FIG. APB 71 :- INFLUENCE OF LOADING AND UNLOADING ON RESPONSE OF COMPRESSION TUBES- [±15] B/E

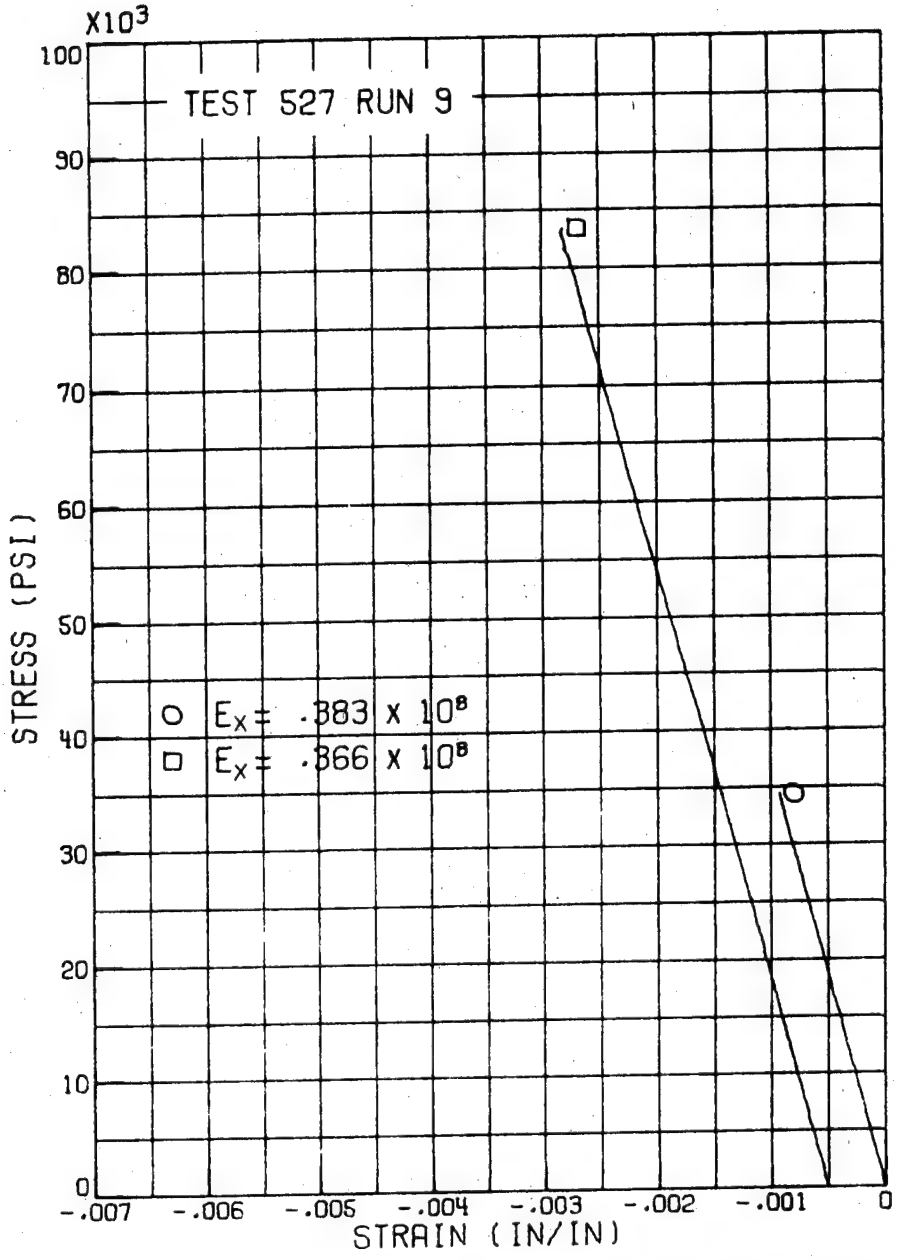

FIG. APB 7II :- INFLUENCE OF LOADING AND UNLOADING ON RESPONSE OF COMPRESSION TUBES- [±15] B/E

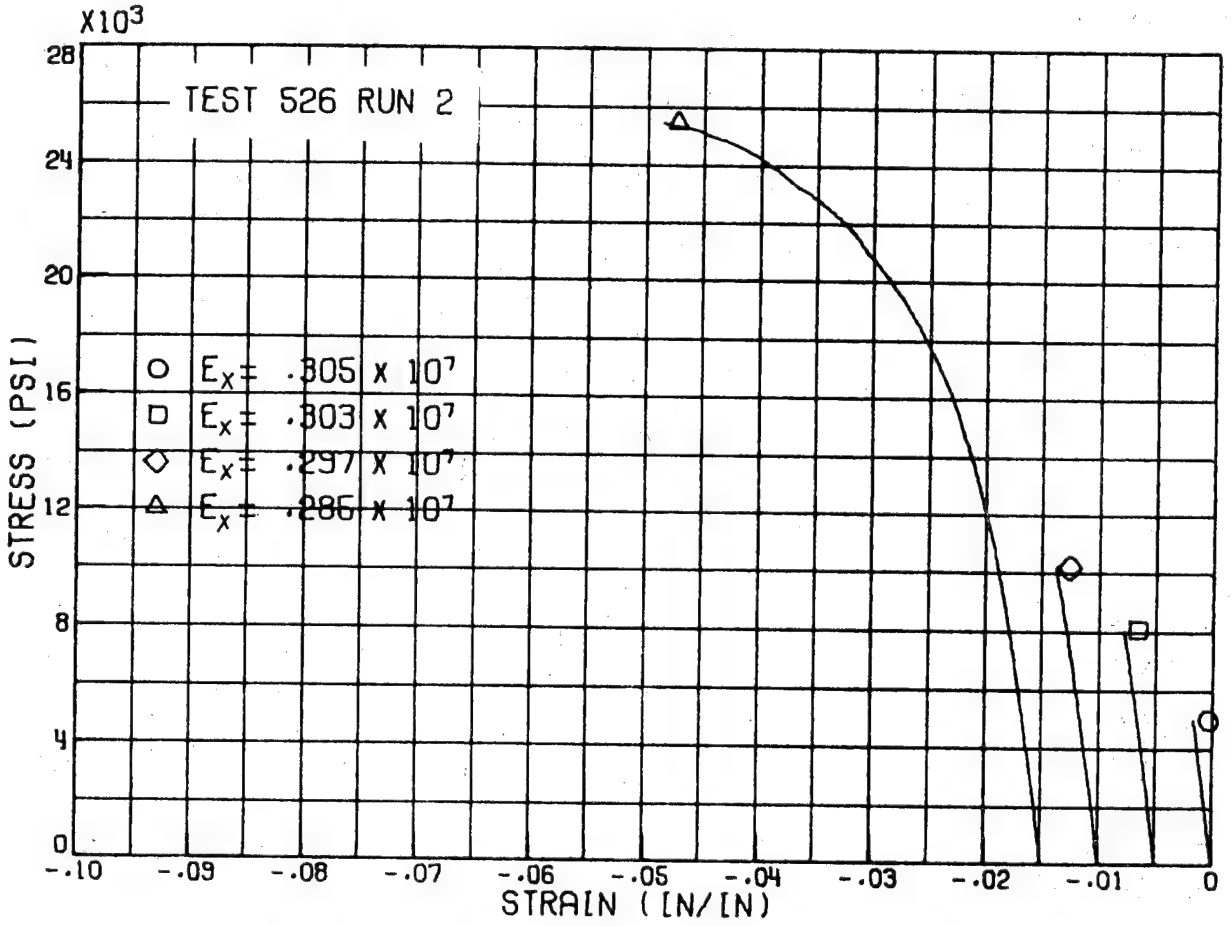

FIG. APB 8 ;- INFLUENCE OF LOADING AND UNLOADING ON RESPONSE OF COMPRESSION TUBES- [±45] B/E

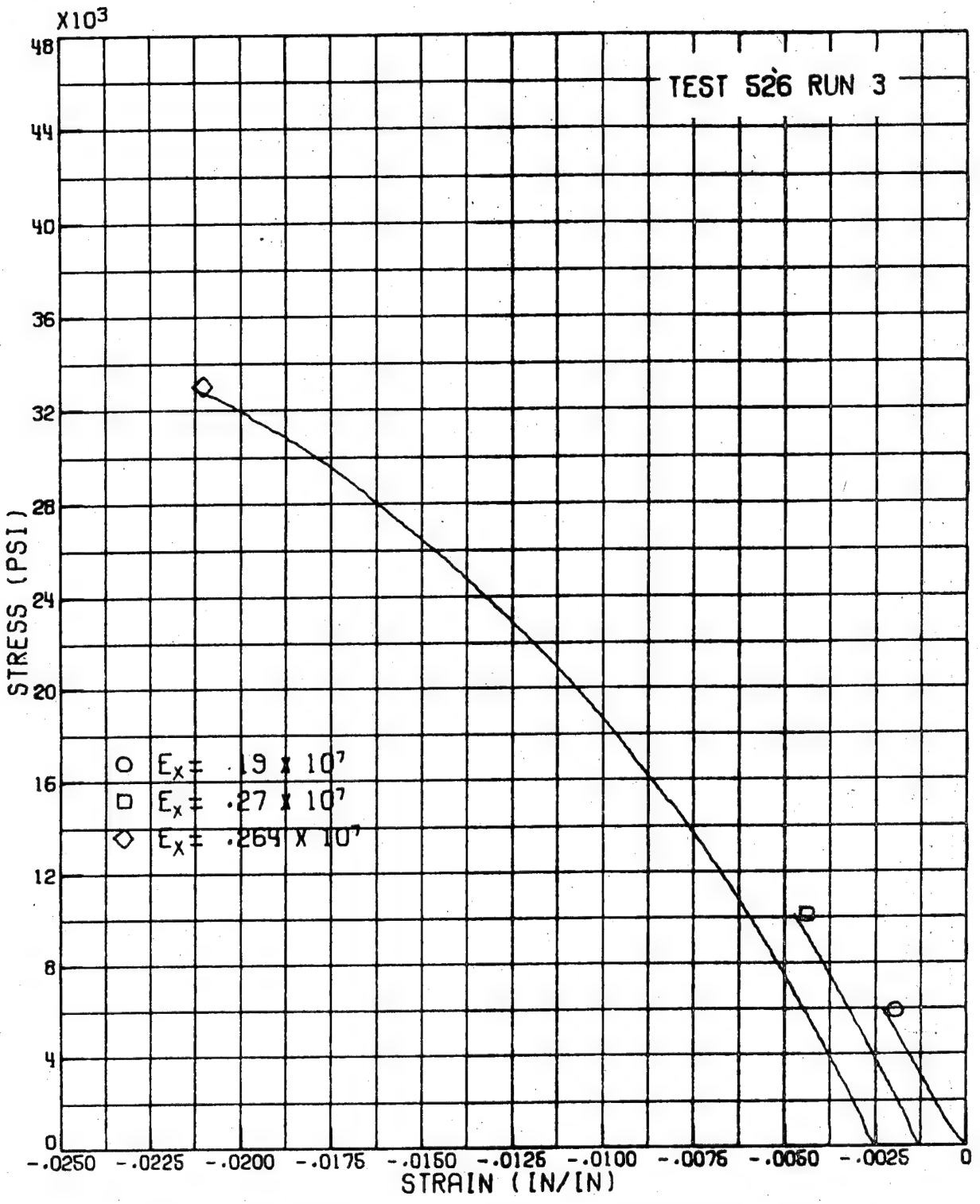

FIG. APB 9I ;- INFLUENCE OF LOADING AND UNLOADING ON RESPONSE OF COMPRESSION TUBES- [±60] B/E

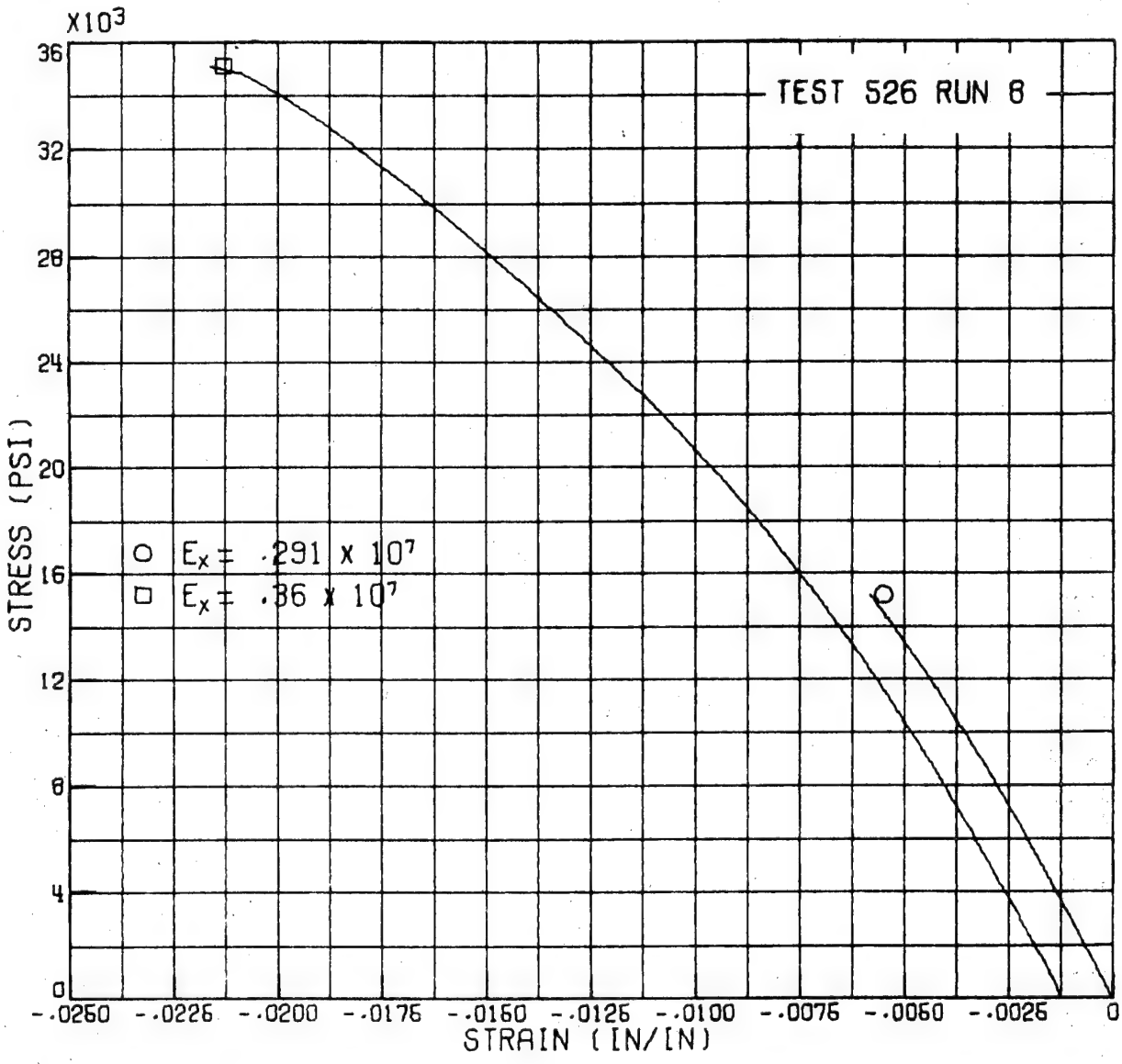

FIG. APB 9 II :- INFLUENCE OF LOADING AND UNLOADING ON RESPONSE OF COMPRESSION TUBES- [±60] B/E

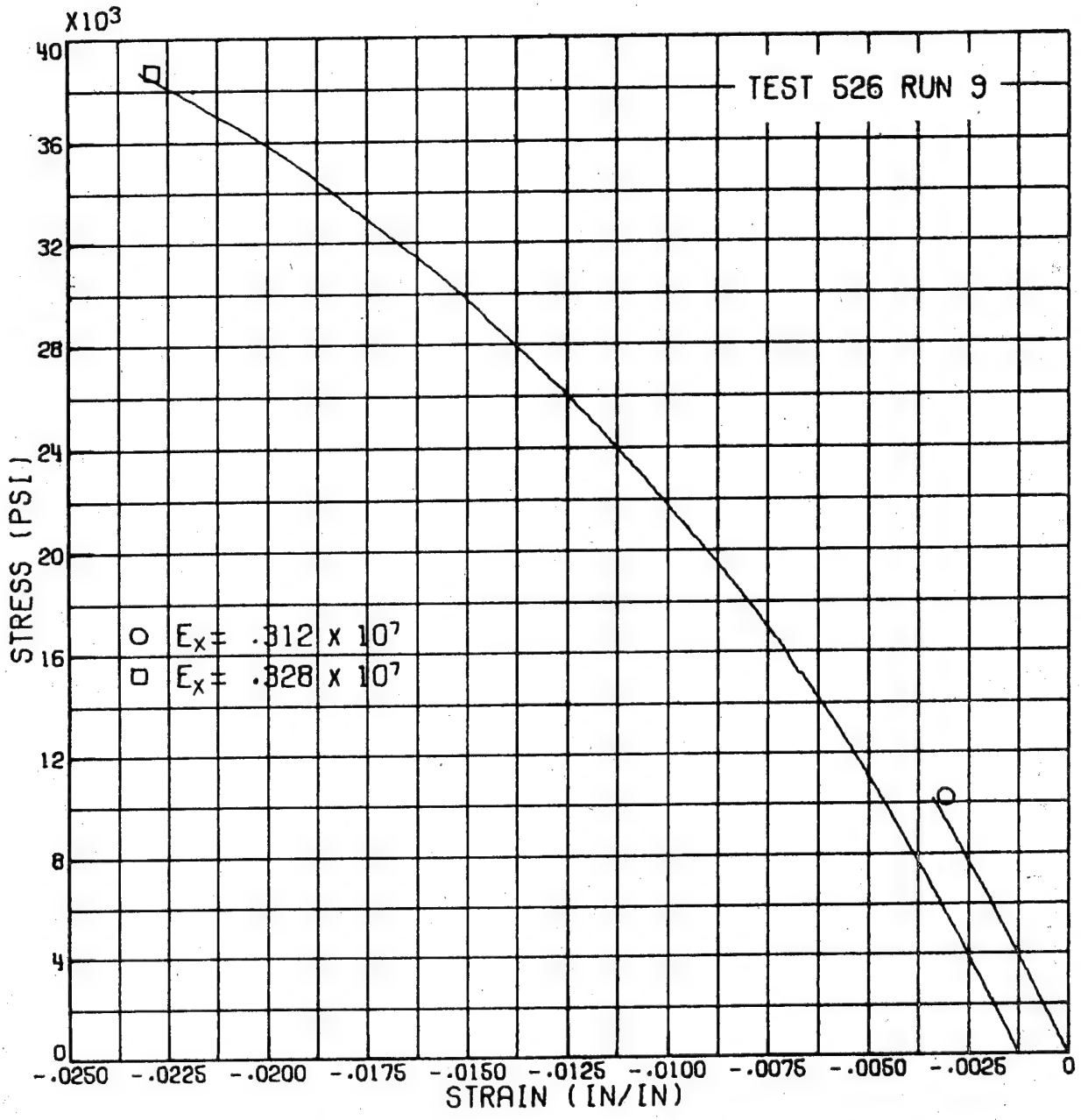

FIG. APB 9 III ;- INFLUENCE OF LOADING AND UNLOADING ON RESPONSE OF COMPRESSION TUBES- [±60] B/E

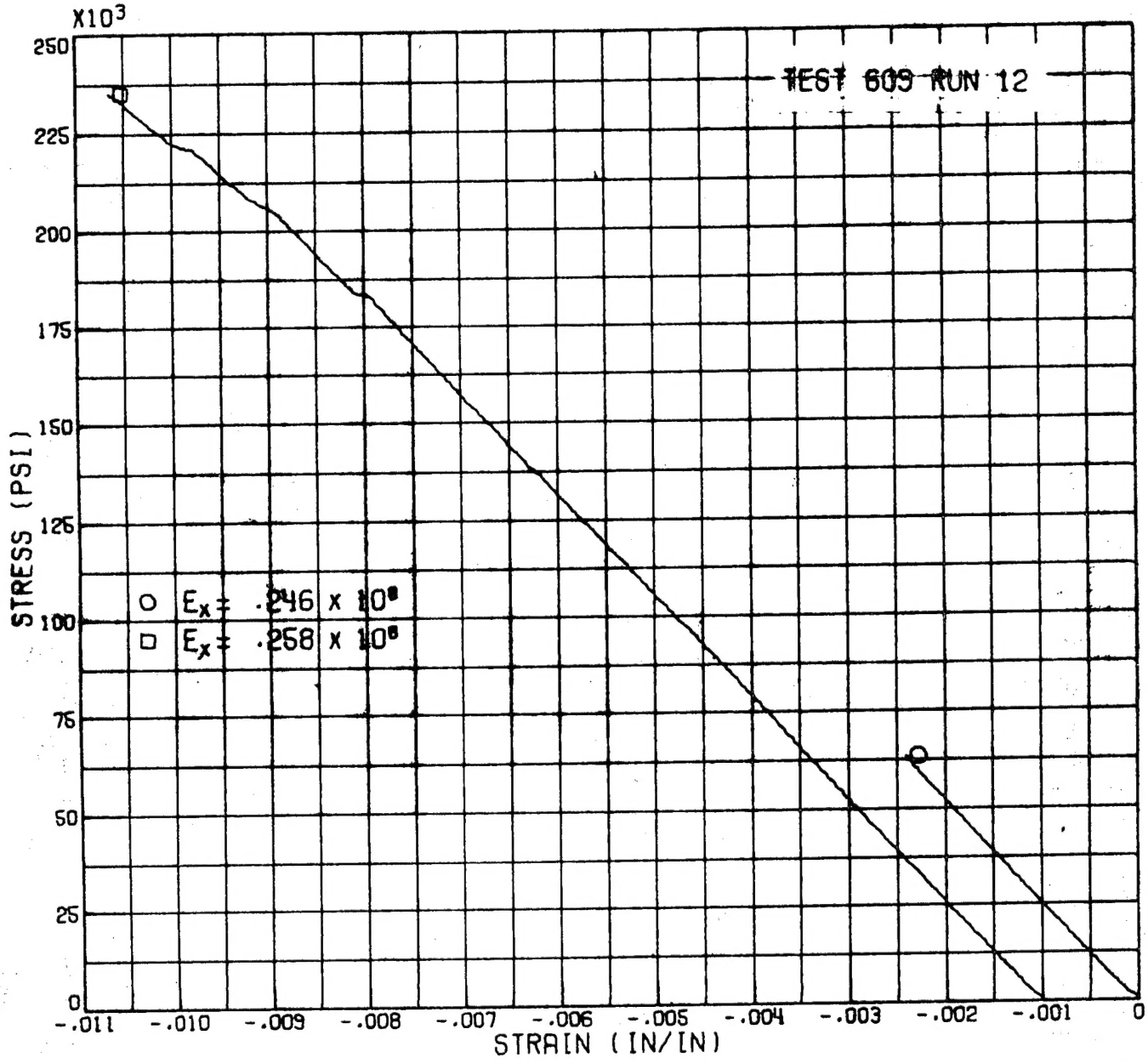

FIG. APB 101 :- INFLUENCE OF LOADING AND UNLOADING ON RESPONSE OF COMPRESSION TUBES- [0/90] B/E

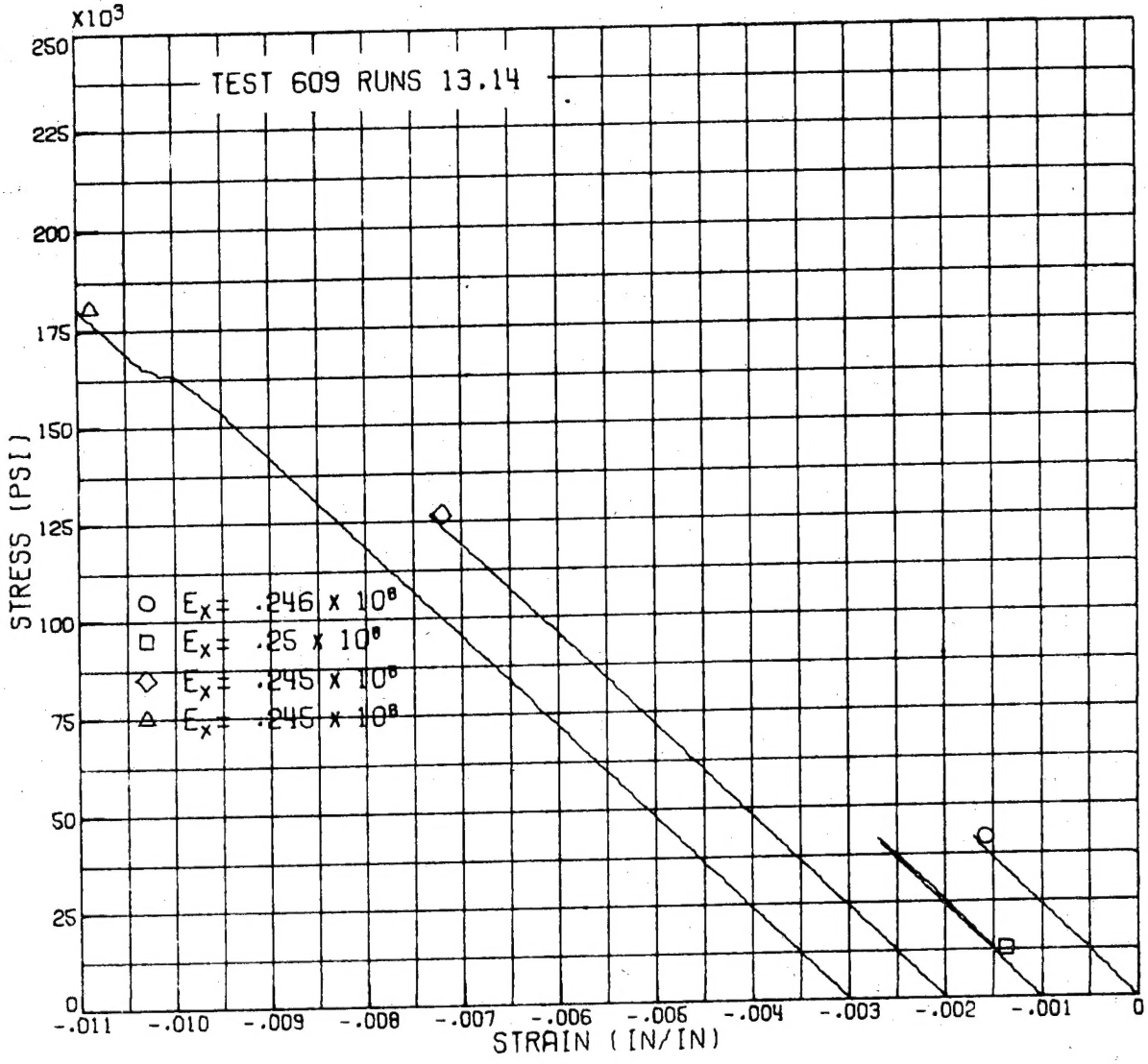

FIG. APB 10 II :- INFLUENCE OF LOADING AND UNLOADING ON RESPONSE OF COMPRESSION TUBES- [0/90] B/E

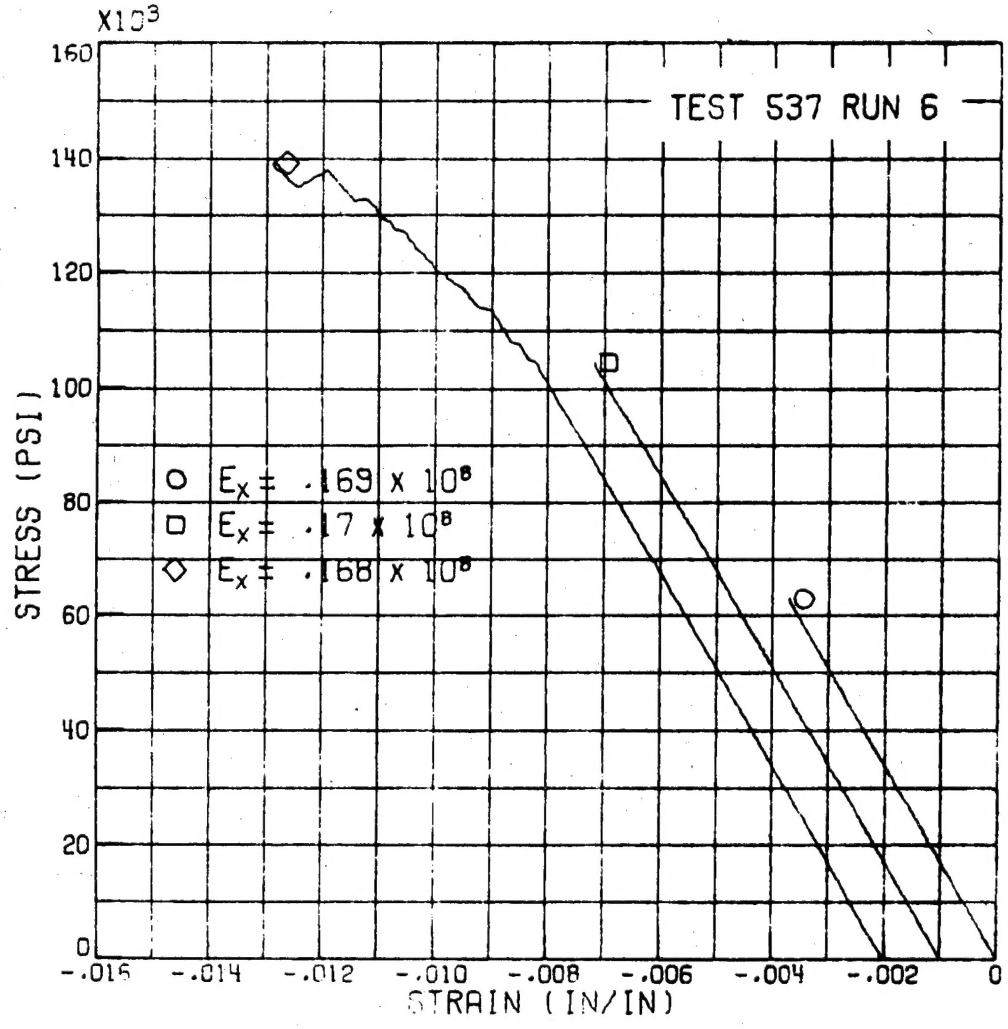

FIG. APB 111 :- INFLUENCE OF LOADING AND UNLOADING ON RESPONSE OF COMPRESSION TUBES- [0/±45/90] B/E

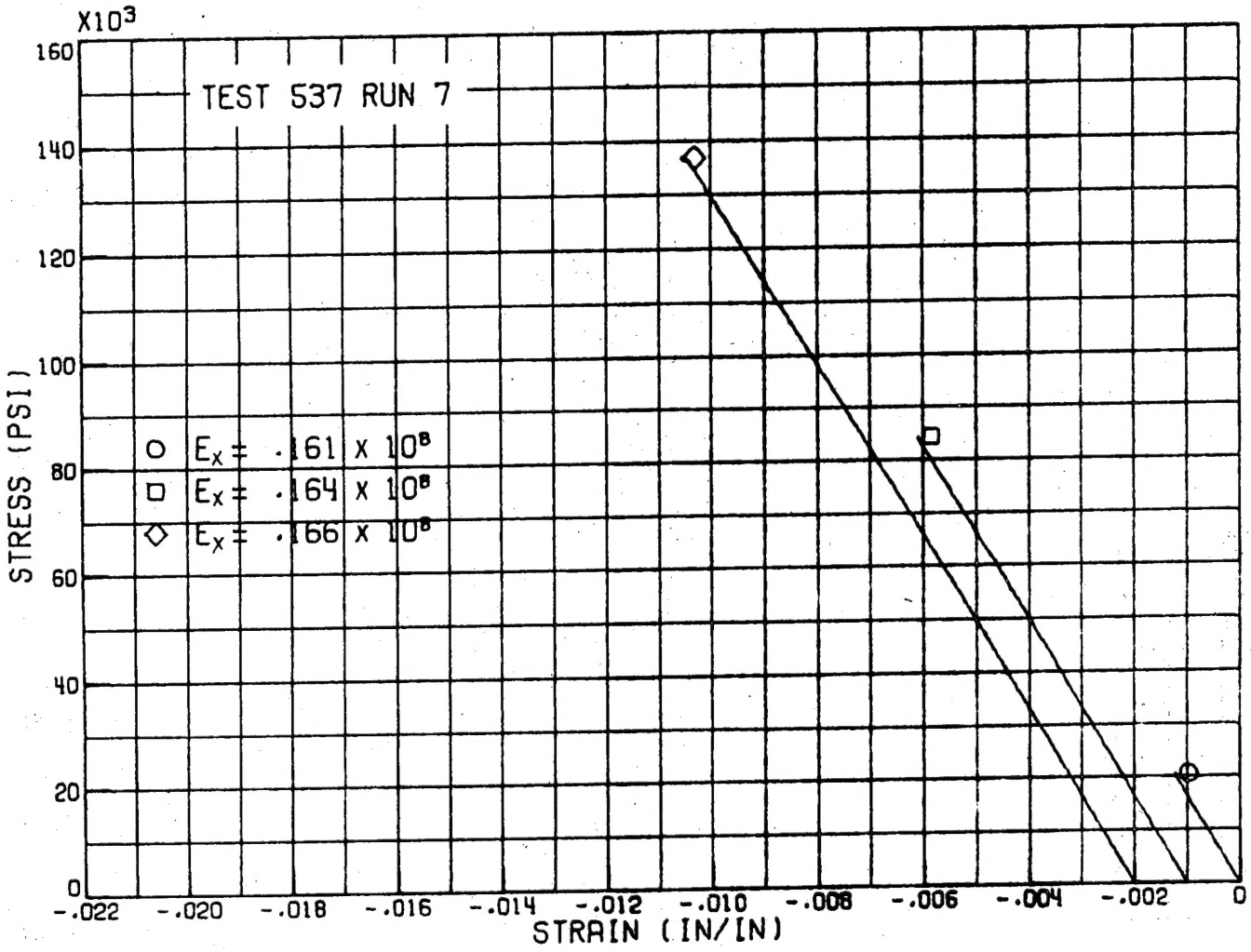

FIG. APB 11 II :- INFLUENCE OF LOADING AND UNLOADING ON RESPONSE OF COMPRESSION TUBES- [0/±45/90] B/E